

2020 4 12 4 68

Volume 12 Number 4 April 2020

A B C

A O B 15 C 30

P431

O 15 30 x50

Figure P431 The result of immortalized lymphocyte cell line transformation on day 0 day15 and day 30 x50

ISSN 1674-6929



9 771674 692204



IMMUNOL

DNA and Cell Biology

2004

2008

J CLIN

30
Clinical Immunology
Physiol

3

2

3

5

3

3

6

3

60

J Cell Mol Med

7

1

SCI
Cancer
Front

分子诊断与治疗杂志

JOURNAL OF MOLECULAR DIAGNOSTICS AND THERAPY

2020 4 12 4 68 Bimonthly Volume 12 Number 4 April 2020

179 11 510620

020 32290789-206 32290789-201

jmdt vip.163.com

ISSN 1674-6929

CN 44-1656/R

46-283

440100190057

2020 4 18

RMB 15.00

Responsible Institution	Sun Yat sen University
Sponsor	China Family Doctors Magazine Publisher Co. Ltd.
Organizer	Da An Gene Co., Ltd. of SunYat sen University
Consultant	SHEN Ziyu
Editor in Chief	LI Ming
Managing Director	JIANG Xiwen
Associate Editor	LIU Yue
Editorial Office	<JOURNAL OF MOLECULAR DIAGNOSTICS AND THERAPY> Editorial Office
Editors	LI Xiaolan LI Caizhen
Editing	China Family Doctors Magazine Publisher Co. Ltd.
Add	11 Fl., Xianglong Building, 179# Tian he bei Lu, Guangzhou, China 510620
Tel	020 32290789-206 32290789-201
E-mail	jmdt@vip.163.com
CSSN	ISSN 1674-6929 CN 44-1656/R
Printing	TianYi Yofus Technology Co., Ltd.
Publish Date	2020.4.18
Price	RMB 15.00

分子诊断与治疗杂志

2020 4 12 4

	RNA GAS5	401
	
	-	
	RT PCR	406
	
	2019	410
	
15	COVID 19 CT	414
	
	HCV RNA	419
	
	2 Glu504Lys 2	423
	
	6	428
	
	miR 21 miR 155	433
	
	PCR	437
56	
	441
2	hs CRP UAER	445
	
	OPG TNF α	450
	
	CRP sCD14 ST	454
	
17 β	rBMSCs Wnt	459
	
	OSAHS MIF	464
	
	PCT NT proBNP	469
	

分子诊断与治疗杂志

2020 4 12 4

4	9	473
	Survivin	478
	LP a OPN IRF 4	483
	LBP HSP70 DcR3	487
	IgM	492
SAA sTREM 1 CRP/PAB SP		497
TSP 1 PDGF		502
	TNF α PCT IL 1 β	507
	β hCG	511
CysC α 1 MG β 2 MG		516
AML	COX 2 VEGF p53	520
CD40 CD40L	BAFF ITP	525
	1	529
COPD	CysC VEGF IL 17 ACTA	533
14 3 3 ζ		538
		542

JOURNAL OF MOLECULAR DIAGNOSTICS AND THERAPY

Monthly Volume 12 Number 4 April 2020

CONTENTS

- The Role Of Long Non Coding RNA GAS5 In The Occurrence And Development Of Atherosclerosis And Atherosclerosis related Diseases
WEI Guijiang YANG Jun WEI Yesheng (401)
- Nucleic Acid Detection of Different Specimen Types of SARS CoV 2 Base on Real time Fluorescent RT PCR
ZHOU Gang LI Chao ZHENG Guodong LIU Hongtao ZHOU Rongrong WANG Hongtao WANG Gangping..... (406)
- The effect of 2 different inactivation methods on the results of viral nucleic acid in 2019 new coronavirus throat swab specimens
JIANG Lei ZHANG Liyuan LIU Daning (410)
- Analysis of the clinical manifestations and computed tomography characteristics of patients with coronavirus disease 2019 COVID 19
CHEN Shaojin WANG Xiaoxia WANG Licheng CHEN Hai ZHANG Meng..... (414)
- Application of high sensitivity HCV RNA detection in preoperative screening
HE Yuting CHEN Xuefang CHEN Peisong HUANG Hao YU Xuegao HUANG Bin (419)
- Distribution characteristics of Glu504Lys polymorphism of acetaldehyde dehydrogenase 2 gene in Type 2 Diabetes Mellitus in Han Nationality
AN Hongliang JIANG Haiyan ZHANG Jinfeng LI Weixuan SU Rong HE Xian LV Weifeng (423)
- Establishment of immortalized lymphocyte cell lines with mutation of the glucose 6 phosphate dehydrogenase gene
JIA Zheng ZHANG Yanyan SUN Nan ZHANG Wenxin GAO Fei SUN Jing, HUANG Jie QU Shoufang (428)
- Correlation between changes of miR 21 miR 155 and inflammatory cytokines and cardiac dysfunction in patients with sepsis
JIA Qiming ZHANG Tao HE Nana WEI Lei..... (433)
- Establishment of nested fluorescent quantitative PCR for rapid detection of *Burkholderia cepacia*
LIN Liying DENG Suiyan GUO Xuguang (437)
- Preliminary study on the effect of 56 °C heat inactivation on the detection of influenza virus nucleic acids
ZHOU Bailing YANG Guangneng CHEN Junling FENG Xingxing XU Bin KUI Liyue DU Tingyi (441)
- Correlation between carotid intima thickness and hs CRP UAER in patients with type 2 diabetes mellitus
XIE Jun SUN Yuanyuan YU Qigui..... (445)
- Diagnostic analysis of serum OPG TNF α and adiponectin in gestational diabetes mellitus
WEN Jie LIU Ping GUO Rui (450)
- Nosocomial infection factors and prediction of CRP and sCD14 ST in patients with rheumatoid arthritis
MENG Qingfang GUO Dongfang DANG ZB

JOURNAL OF MOLECULAR DIAGNOSTICS AND THERAPY

Monthly Volume 12 Number 4 April 2020

CONTENTS

The application value of human epididymis protein 4 and chemokine ligand 9 in the diagnosis and prognosis of lupus nephritis <i>WEI Hua ZHANG Caifeng WANG Jiali</i>	(473)
The expression of Survivin in cervical phosphorous carcinoma and its relationship with clinicopathological features <i>Eerdemutu JIA Yuling QIN Xiaoling NIU Li rong BAO Ying na YU Zhilong</i>	(478)
Expressions and clinical significance of serum LP a OPN IRF 4 in patients with degenerative heart valve disease <i>WANG Junhua CUI Qintao HAN Peili LIU Xiaochen</i>	(483)
The value of serum LBP HSP70 DcR3 levels in predicting the outcome of patients with acute respiratory distress syndrome <i>MA Lingling YANG Qiuwei KONG Bianduo</i>	(487)
Detection characteristics and epidemiological trend analysis of different pathogenic antigens and IgM antibodies in children with severe pneumonia <i>TAO Shan</i>	(492)
Significance of SAA sTREM1 CRP/PAB in pulmonary infection after general anesthesia in SP patients <i>SUN Yuan WANG Xin WANG Li</i>	(497)
Clinical value of serum TSP 1 and PDGF in evaluating short term prognosis in patients with intracerebral hemorrhage <i>GAO Yangyang LI Jiteng</i>	(502)
Changes and Significance of Serum TNF alpha PCT and IL 1beta Levels in Patients with Postoperative Infection after Cesarean Section <i>WU Xiaofeng WANG Ran LI Wanling</i>	(507)
Correlation of serum hCG and progesterone expression with thyroid function and motilin in patients with hyperemesis gravidarum <i>LI Feng LU Haifeng CUI Bingyi QIN Chunyi</i>	(511)
The detection and significance of CysC 1 MG 2 MG of early kidney injure in patients with chronic obstructive pulmonary disease <i>LI Haiyan</i>	(516)
Expressions of COX 2 VEGF and p53 in elderly AML patients treated with decitabine and their prognosis <i>WANG Zhanfang ZHANG Fangfang YANG Hai CHEN Chaohua</i>	(520)
The predictive value of peripheral blood CD40 CD40L expression and serum BAFF level on the efficacy of patients with immune thrombocytopenic purpura <i>YIN Fenglei YIN Juan ZHAO Fang ZHANG Rui LIU Jing ZHANG Wei LI Shuchen WANG Juan</i>	(525)
Solid variant of papillary renal cell carcinoma a case report and literature review <i>WANG Fang XIANG Longquan LI Qian WANG Haiqing CHENG Jun LIN Fanzhong</i>	(529)
Changes of serum Cys C VEGF IL 17 and ACTA levels in elderly patients with COPD and severe respiratory failure <i>CAO Tingting WAN Jun FENG Yonghai CHU Heying</i>	(533)
14 3 3 and breast cancer <i>DONG Zhengyuan YANG Qingling CHEN Changjie</i>	(538)
Molecular subgroups and treatment progress of pediatric medulloblastoma <i>LI Qiu WANG Xiaojiang ZHU Jiandong ZHANG Yong XIE Mingxiang</i>	(542)

RNA GAS5

1 2 3 1 1

RNA LncRNA 200 nt

RNA LncRNA GAS5 LncRNA 1

2 5 4 087 nt 12 LncRNA GAS5

LncRNA GAS5

The Role Of LongNon - Coding RNA GAS5 In The Occurrence And Development Of Atherosclerosis And Atherosclerosis-related Diseases

WEI Guijiang^{1 2 3} YANG Jun¹ WEI Yesheng¹

1. Department of Medical Laboratory Affiliated Hospital of Guilin Medical University Guilin Guangxi China 541000 2 Medical College of Guangxi University Nanning Guangxi China 530000 3 Department of Medical Laboratory Affiliated Hospital of Youjiang Medical University for Nationalities Baise Guangxi China 533000

ABSTRACT LongNon Coding RNA LncRNA is a type of RNA that is located in the nucleus or cytoplasm and is longer than 200 nt. LncRNA GAS5 is a member of the LncRNA family that has attracted attention in recent years. The encoding gene is in the q25 regio of human chromosome 1, has a total length of 4 087 nt and consists of 12 exons. Several studies have shown that LncRNA GAS5 is involved in inflammation mediates vascular endothelial cell damage and plays an important role in the development of atherosclerosis and related diseases. This article reviews the role of LncRNA GAS5 in the occurrence and development of atherosclerosis and atherosclerosis related diseases.

KEY WORDS LncRNA GAS5 Atherosclerosis Coronary heart disease Diabetes

RNA long non coding RNA

LncRNA

200 nt

RNA ¹

LncRNAs

2018GXNSFAA138120 81560552 2018AB58018

1. 541000

2. 530000

3. 533000

E-mail wyshi22@163.com

5
 LncRNAs
 LncRNAs LncRNA GAS5
 LncRNA GAS5
 GAS5 LncRNA
 LncRNA GAS5
 68 LncRNA GAS5 1
 1q25.1 LncRNA GAS5
 RNAs 12 11
 9 LncRNA GAS5
 Mourtada T
 17 18
 19 20 21 22
 LncRNA GAS5
 Mourtada 10 LncRNA GAS5
 LncRNA GAS5 Liu 23
 GAS5 LncRNA LncRNA GAS5 PDGF bb
 LncRNA GAS5 PDGF bb
 Mourtada 11 Tang 24
 LncRNA GAS5 LncRNA GAS5
 LncRNA GAS5 LncRNA GAS5 p53 Ln
 cRNA GAS5 p53
 LncRNA GAS5 LncRNA p53 p300 p53
 GAS5 LncRNA p300 p53
 Tang
 Liu LncRNA GAS5 Sun
 1 LncRNA GAS5 MTT Liu Tang
 Transwell
 qRT PCR Ln
 cRNA GAS5 miR 137 IGFBP 5 mRNA
 Western blot IGFBP 5
 PDGF bb LncRNA GAS5 IGFBP 5
 12 13 Chen 14 LncRNA miR 137
 GAS5 LncRNA GAS5 PDGF bb

IGFBP 5
miR 137 LncRNA GAS5 2 LncRNA GAS5
Liu
Tang
LncRNA GAS5 ^{28,29} LncRNA GAS5
LncRNA GAS5
Shen ²⁵ LncRNA qRT PCR
GAS5 LncRNA GAS5
Western blot Western blot mTOR mTOR
oxLDL THP 1 APO E PPAR α GAS5 mTOR LncRNA
CPT1 LncRNA GAS5 miR 135a LncRNA GAS5
LncRNA GAS5 LncRNA GAS5
oxLDL THP 1 LncRNA GAS5 mTOR
LncRNA GAS5 LncRNA GAS5
oxLDL THP 1 LncRNA GAS5 mTOR
miR 135a miR 135a mTOR LncRNA GAS5 mTOR
oxLDL THP 1 LncRNA GAS5
miR 135a LncRNA GAS5 LncRNA GAS5
²⁶ THP 1 LncRNA GAS5 Li ³¹ 102
LncRNA GAS5 oxLDL THP 1 98 LncRNA
LncRNA GAS5 LncRNA GAS5
oxLDL THP 1 THP 1 catenin Wnt/ α
Caspases THP 1 GAS5 LncRNA
²⁷ LncRNA GAS5 LncRNA GAS5
THP 1 catenin Wnt/ α
LncRNA GAS5 Yin Li
GAS5 LncRNA
LncRNA GAS5 LncRNA GAS5
LncRNA GAS5
LncRNA GAS5
LncRNA GAS5

3 LncRNA GAS5

qRT PCR 96
LncRNA GAS5
LncRNA GAS5 2
LncRNA GAS5 12

qRT PCR 0.81 LncRNA GAS5
2 85.1% 67.3%
2

LncRNA GAS5
³⁴

LncRNA GAS5 2
Shi ³⁵ 2
LncRNA GAS5 LncRNA GAS5

LncRNA GAS5
B
2
o
LncRNA GAS5

&

- 16 Yao Jiamei Shi Zanhua Ma Xinhua Xu Daomiao Ming Guangfeng. LncRNA GAS5/miR 223/NAMPT Axis Modulates the Cell Proliferation and Senescence of Endothelial Progenitor Cells through PI3K/AKT Signaling J . J Cell Biochem 2019 120 9 14518 14530.
- 17 Silva Telma Jager Willi Neuss Radu Maria Sequeira Adelia. Modeling of the Early Stage of Atherosclerosis with Emphasis on the Regulation of the Endothelial Permeability J . J Theor Bio 2020 1 e110229.
- 18 Zheng Bin Yin Weina Suzuki Toru Zhang Xinhua Zhang Yu Song Lili et al. Exosome Mediated miR 155 Transfer from Smooth Muscle Cells to Endothelial Cells Induces Endothelial Injury and Promotes Atherosclerosis J . Mol Ther 2017 25 6 1279 1294.
- 19 Peng Yinyang Li Yundun Pang Chengchun. The Role of MicroRNAs in the Involvement of Vascular Smooth Muscle Cells in the Development of Atherosclerosis J . Cell Bio In 2019 43 10 1102 1112.
- 20 Li Yihui Qin Ranran Yan Hongdan Wang Feng Huang & Meng Zhang Yun et al. Inhibition of Vascular Smooth Muscle Cells Premature Senescence with Rutin Attenuates and Stabilizes Diabetic Atherosclerosis J . J Nutr Biochem 2018 51 91 98.
- 21 Zhang Qinghai Hu Jie Wu Yan Luo Hairong Meng Wen Xiao Bo et al. RHEB Ras Homolog Enriched in Brain 1 Deficiency in Mature Macrophages Prevents Atherosclerosis by Repressing Macrophage Proliferation Inflammation and Lipid Uptake J . Arterioscler Thromb Vas Biol 2019 39 9 1787 1801.
- 22 Zhang Xianfeng Yang Yang Yang Xinyu Tong Qian. miR 188 3p Upregulation Results in the Inhibition of Macrophage Proinflammatory Activities and Atherosclerosis in Apoe Deficient Mice J . Thromb Res 2018 171 1 55 61.
- 23 Liu Kefeng Liu Chen Zhang Zhengyu. LncRNA GAS5 Acts as a ceRNA for miR 21 in Suppressing PDGF bb Induced Proliferation and Migration in Vascular Smooth Muscle Cells J . J Cell Biochem 2019 120 9 15233 15240.
- 24 Tang Rui Mei Xiaohan Wang Yungchun Cui Xiaobing Zhang Gui Li Wenjing et al. LncRNA GAS5 Regulates Vascular Smooth Muscle Cell Cycle Arrest and Apoptosis Via P53 Pathway J . Biochim Biophys Acta Mol Basis Dis 2019 1865 9 2516 2525.
- 25 Sun Yuechen Xu Lan Tan Ying. Long Non Coding RNA GAS5 Promotes PDGF bb Induced Proliferation and Migration of Vascular Smooth Muscle Cells Via Regulating miR 137/GFBP 5 J . Immunol J 2018 34 10 856 862.
- 26 Shen Songhe Zheng Xiaoli Zhu Zhixiang Zhao Sen Zhou Qing Song Zhiming et al. Silencing of GAS5 Represses the Malignant Progression of Atherosclerosis through Upregulation of miR 135 J . Biomed and Pharmacother 2019 118 1 e109302.
- 27 Chen Lei Yang Wenjin Guo Yijun Chen Wei Zheng Ping Zeng Jinsong et al. Exosomal LncRNA GAS5 Regulates the Apoptosis of Macrophages and Vascular Endothelial Cells in Atherosclerosis. PLoS One 2017 12 9 e0185406.
- 28 Polak Joseph Ouyang Pamela Vaidya Dhananjay. Total Brachial Artery Reactivity and First Time Incident Coronary Heart Disease Events in a Longitudinal Cohort Study The Multi Ethnic Study of Atherosclerosis J . PLoS One 2019 14 4 e0211726.
- 29 Jiang Dan Sun Min You Linna Lu Kai Gao Lei Hu Chunxiao et al. DNA Methylation and Hydroxymethylation Are Associated with the Degree of Coronary Atherosclerosis in Elderly Patients with Coronary Heart Disease J . Life Sci 2019 224 1 241U: 1 P M `` 0 0 J B MÖY F 1 Å ÷ •g=UÅ UÅ \$DP ð ó

COVID 19

RT PCR

1 1 1 1 1 1 2

SARS CoV 2
2020 1 2020 2 2 258 SARS

CoV 2 3 284

RT PCR PCR SPSS 19.0 3 284

79 13 7 P<0.05

P<0.05

RT PCR

RT PCR

Nucleic Acid Detection of Different Specimen Types of SARS-CoV-2 Base on Real-time Fluorescent RT-PCR

ZHOU Gang¹ LI Chao¹ ZHENG Guodong¹ LIU Hongtao¹ ZHOU Rongrong¹ WANG Hongtao¹ WANG Gangping²

1. Department of Microbiological Laboratory Rizhao Center for Disease Control and Prevention Rizhao Shangdong, China 276826 2 Central Laboratory & Clinical Molecular Diagnosis Center Rizhao clinical molecular medicine research center Rizhao key laboratory of precision medicine Rizhao People's Hospital Rizhao Shangdong, China 276800

ABSTRACT Objective To investigate the positive detection rate of Severe Acute Respiratory Syndrome Coronavirus 2 SARS CoV 2 in different samples in order to provide guidance and suggestions for the prevention and control of epidemic. Methods A total of 3 284 throat swabs nasopharyngeal swabs sputum specimens and fecal specimens were collected from 2 258 SARS CoV 2 suspected patients who were admitted in our hospital from January 2020 to February 2020. The real time polymerase chain reaction RT PCR method was used for PCR amplification and SPSS19.0 software was used for statistical analysis. Results A total of 79 positive samples were detected among 3 284 samples. A statistical analysis was performed on the positive detection rates of different sample types tested at the same time and the difference

2019KJYF319

1.
2.

276826

276800

E-mail wgprzph93@126.com

was statistically significant $P < 0.05$. There are 13 male suspects and 7 females in this study, respectively no statistically significant difference in gender positive detection rates $P > 0.05$. The results from different sample types showed that the positive detection rate of throat swabs was the lowest nasopharyngeal swabs and sputum samples were higher than throat swabs. Interestingly the positive detection rate of fecal samples was the highest although the sample number in this group was small compared to other types. However there was no significant difference in the positive rate of the same suspected patient with different sample types at the same time. Conclusion The RT-PCR method has different positive detection rates for different sample types which can provide guidance for the selection of samples in laboratory testing and better prevention and control of epidemics.

KEY WORDS Real Time Polymerase Chain Reaction Positive rate SARS-CoV-2 throat swabs

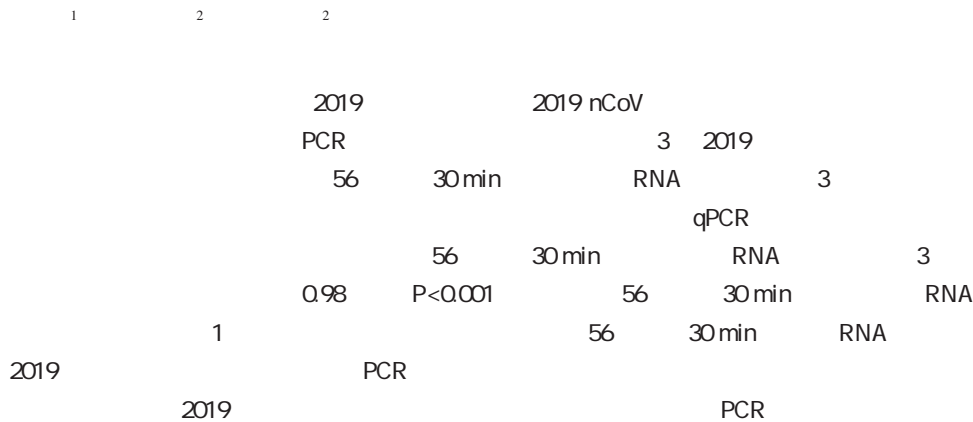
Severe Acute Respiratory Syn
drome Coronavirus 2 SARS-CoV-2

1
2020 3 26 SARS-CoV-2
8
37
2 SARS-CoV-2
SARS-CoV-2 3

2 4.5 \$ E

COVID 19

2019



The effect of 2 different inactivation methods on the results of viral nucleic acid in 2019 new coronavirus throat swab specimens

JIANG Lei¹ ZHANG Liyuan² LIU Daning²

1. Laboratory of Puyang Oilfield General Hospital Puyang Henan China 457001 2. Laboratory of Puyang people sHospital Puyang Henan China 457000

ABSTRACT Objective To investigate the effect of two different pharyngeal swab specimens inactivation methods on the results of 2019 new coronary virus fluorescent quantitative PCR. Method Three cases of 2019 new coronary virus positive specimens were treated by two different inactivation methods the nucleic acids were extracted by manual centrifugation method from three groups of samples which were inactivated at 56 for 30 minutes and inactivated with guanidine salt RNA preservation solution. Simultaneous detection of virus content with two different nucleic acid detection kits the results of qPCR were analyzed statistically. Result The results of two different nucleic acid detection reagents showed that the results of the three groups which were not inactivated inactivated at 56 for 30 minutes and inactivated with guanidine salt RNA preservation solution were significantly correlated and had good consistency. The correlation coefficients among the three groups were all above 0.98 P<0.001 . Conclusion 2019 new coronary virus nucleic acid qPCR results were not affected by the two inactivation methods.

KEY WORDS 2019 new coronary virus Novel coronary virus pneumonia qPCR

2019 2019 novel coronavirus 10 2019 nCoV
 2019 nCoV RNA WHO
 29 903 bp 10 Novel coronavirus pneu

1. 457001
2. 457000

monia NCP

RNA

1.2

1.5

PCR

PCR

3

1.6

Graphpad Prism 8.0

Spearman

Bland Altman

CT

CT

PCR

2

1

2.1 3 qPCR

A

56

30 min

1.1

CT

Spearman

r=

2020 2 1

0.9959 P<0.001

RNA

3

CT

r=0.9958 P<

0.001 56 30 min

RNA

CT

r=0.9966 P<

1.2

2019 nCoV

0.001 1 B

56

30 min CT

Spearman

RNA

r=0.9886 P<0.001

RNA

RT PCR

CT

r=

A

0.9967 P<0.001 56 30 min

RNA

B RNA

CT

r=

0.9915 P<0.001 2

A

B

PCR ABI7500 Life Technologies NY

min 5 F 30 #2 56 30

USA

1.3

3

3

2-3 mL

140 L

280 L

56

30 min

280 L

280 L

RNA

1.4

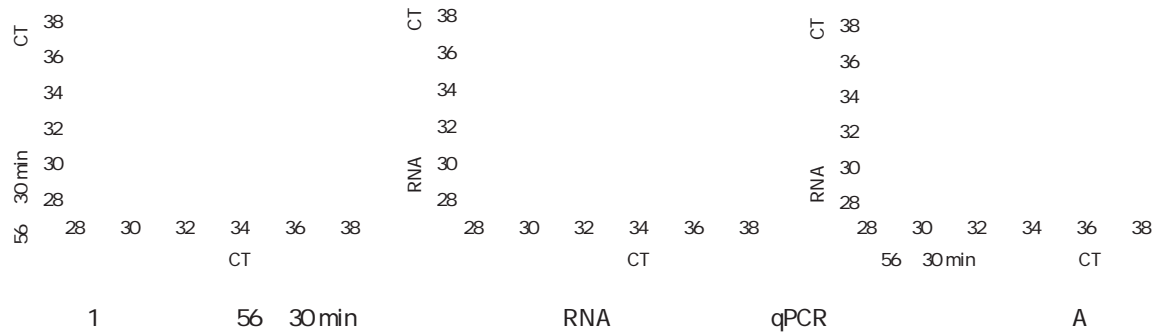


Figure 1 Correlation analysis of qPCR results among the un inactivated group the inactivated group heated at 56 for 30 minutes and the guanidine inactivation group detection kit A

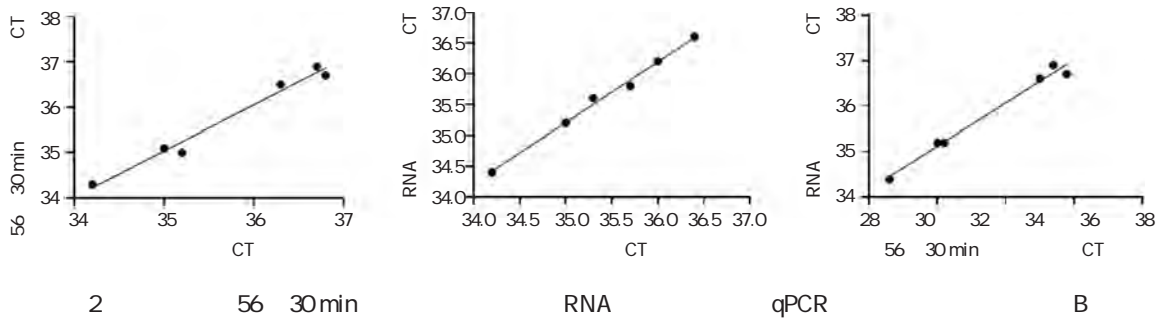


Figure 1 Correlation analysis of qPCR results among the un inactivated group the inactivated group heated at 56 for 30 minutes and the guanidine inactivation group detection kit B

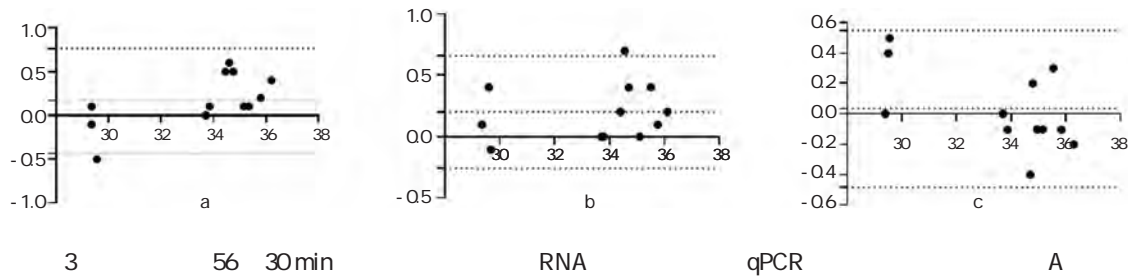


Figure 3 Consistency analysis of qPCR results among the un inactivated group the inactivated group heated at 56 for 30 minutes and the guanidine inactivated group detection kit A

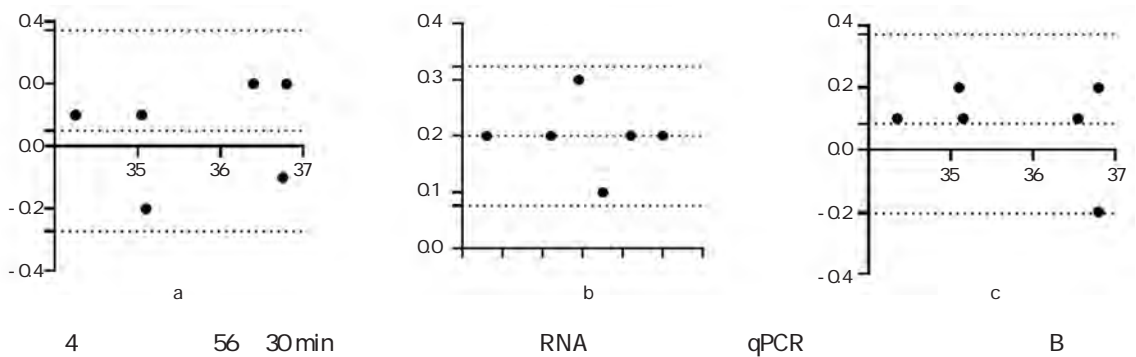


Figure 4 Consistency analysis of qPCR results among the un inactivated group the inactivated group heated at 56 for 30 minutes and the guanidine inactivated group detection kit B

56 30 min RNA
qPCR
2.3

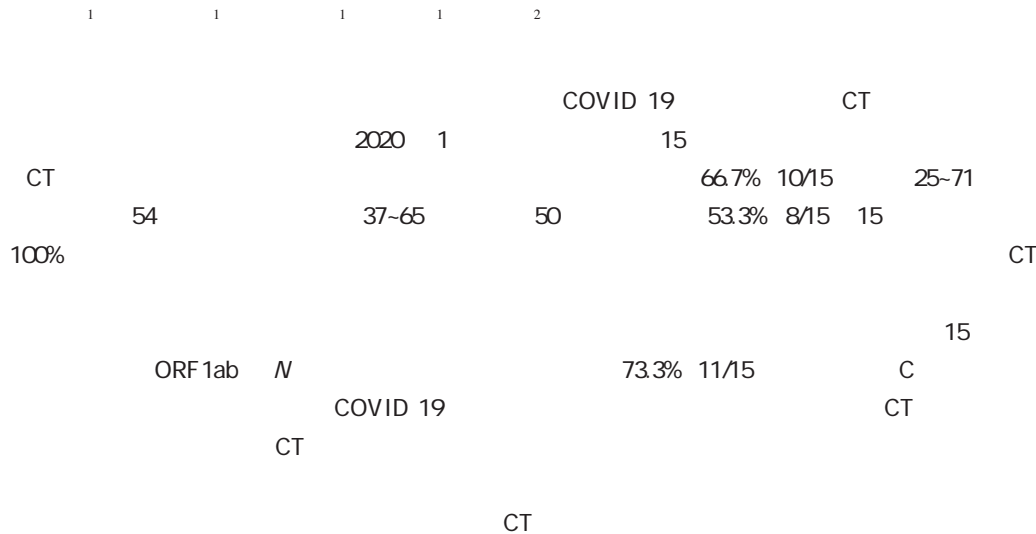
A B CT
=1.031 5 Bland Altman
qPCR

COVID 19

15

COVID 19

CT



Analysis of the clinical manifestations and computed tomography characteristics of patients with coronavirus disease-2019 COVID-19

CHEN Shaojin¹ WANG Xiaoxia¹ WANG Licheng¹ CHEN Hai¹ ZHANG Meng²

1. Clinical Laboratory of Sanya People sHospital Sanya Hainan China 572000 2. Radiology department of Sanya People sHospital Sanya Hainan China 572000

ABSTRACT Objective To analyze the clinical presentations and computed tomography characteristics of coronavirus disease 2019 COVID 19 and to further improve the understanding of the disease. Methods A retrospective analysis and summary of the clinical manifestations and CT imaging features were performed based on 15 patients with COVID 19 diagnosed in our hospital since January 2020. Results Most patients diagnosed in this study were men 67% 10/15 aged 25 to 71 years with a median age of 54 years in tertile range of 37 to 65 . Most of them were over 50 years old 53.3% 8/15 . All 15 cases had a history of contact with the affected area 100% . The clinical manifestations are fever cough dry cough or sputum with white mucus some accompanied by chest tightness shortness of breath and fatigue. Most patients were in early or advanced disease stages according to the chest imaging manifestations. They have a ground glass patchy shadow in bilateral pulmonary multi lobular lesions predominantly in the subpleural regions blurred lesion margins. They were also accompanied by thickening of blood vessels thickening of the pleura bronchial inflation and increased lymph nodes in the mediastinum in some cases. 15 patients have positive nucleic acid tests for the

ZDYF2019149 ZDYF2017163

1. 572000
2. 572000

E-mail zanmon@163.com

novel coronavirus ORF1ab and N genes. In addition 93% 14/15 of patients have high level of hypersensitivity C reactive protein. Conclusion COVID 19 patients have fever and cough at the early stage and there are abnormal chest CT examinations. The combination of epidemiological investigations clinical manifestations chest CT imaging characteristics analysis and nucleic acid detection and other laboratory test results will help early screening prevention and control of COVID 19.

KEY WORDS Coronavirus disease 2019 Clinical manifestations Computed tomography characteristics

2019 12

1.2

PCR 1.2.1

β Sarbecovirus T310 04/T320 04

orthocoronavirinae¹ 5 mL

2019 novel coronavirus 2019 nCoV 2 se DA0633 2019 nCoV

vere acute respiratory syndrome 2 SARS CoV 2

WHO DA0930

coronavirus disease 2019 COVID 19 DA3200

ABI 7500

2019 nCoV BC 5390

4 19 84 237 LC M 5LEO I M 5LEO II M 53LH

77 895 4 642 M 53P C CRP

/ COVID 19 7600 020 CT GE Light

² WHO 2020 2 1 COVID 19 Speed 16

³ 1.2.2

15 EDTA K₂ 3 mL

CT 1.2.3

1 56 30 min

1.1 1 mL

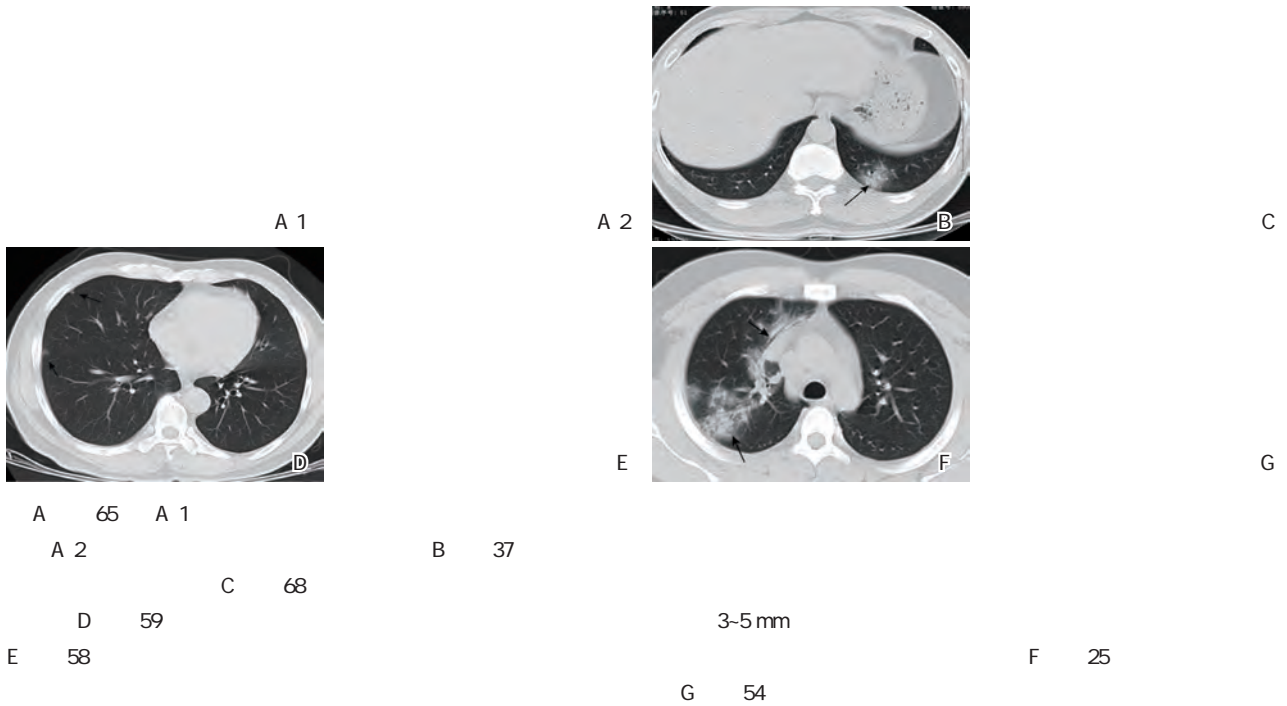
2020 1 25 15 COVID 19 2019

RT PCR nCoV

15 1.2.4

CT GE LightSpeed 16 CT

CT	120 kV	2.2			
200 mA	1.375 1	5 mm	7	8	62.5% 5/
5 mm	512x512		8	25% 2/8	
	L 500HU W 1 500		12.5% 1/8		
HU	L 50HU W 300HU		66.7% 10/15		
1.2.5			13.3% 2/15	86.7% 13/15	
	C	2.3 CT			
1.3		1			14
	SPSS 20.0				9
	$\bar{x} \pm s$	64.3%			2
M	IQR	14.3%	3	21.4%	
n %			1		
2		6	42.9%		
		3	21.4%	1	7.1%
2.1		4	28.6%		8
	66.7% 10/15	33.3% 5/15	57.1%		
	25-71	54			
	37-65	50			
30-40	33.3% 5/15	20-30	13.4%	1	2
2/15	15				1
100%					



1 COVID 19 CT
 Figure 1 The chest CT imaging of partial COVID 19 patients

2.4

ORF1ab N 4.5% 69.9%
 33.3% 5/15 25.5% 25.2%
 13.3% 2/15 13.3% 2/15 15
 73.3% 11/15 C 73.3% C
 60.0% 9/15

3

COVID 19
 2019 nCoV MERS CoV SARS CoV
 nCoV SARS CoV 2019
 80%^{1 4} SARS CoV 75% ~
 86.9%¹ SARS CoV 16 CT
 COVID 19
 2019 nCoV 99%
 2019 nCoV COVID 19
 5 6 CT
 2019 nCoV SARS CoV 2019 nCoV
 2 ACE2
 ACE2
 7 8
 86 2019 nCoV
 9
 COVID 19

10 11 31 44 672
 COVID 19 30-
 79

7.3¹² 30-71
 86.7% 2 1

SARS
 SARS
 COVID 19¹³ MERS 35%
 50 66.6%

MERS 14
 66.7% 10/15

- 1 Zhu N Zhang D Wang W et al. A novel coronavirus from patients with pneumonia in China. 2019 J. N Eng J Med 2020 382 8 727-733.
- 2 Gardner L. 2019n CoV Global Cases. <https://gisanddata.maps.arcgis.com/apps/opsdashboard/index.html#/bda7594740fd40299423467b48e9ecf6> 2 February 2020 date last accessed .
- 3 Chaolin H Yeming W Xingwang L et al. Clinical features of patients infected with 2019 novel coronavirus in Wuhan, China. J. Lancet 2020 395 10223 .
- 4 Hui DS I Azhar E Madani TA et al. The continuing COVID 19 epidemic threat of novel coronaviruses to global health: The latest 2019 novel coronavirus outbreak in Wuhan, China. J. Int J Infect Dis 2020 91 264-266.
- 5 Lam TT Y Shum MH H Zhu H C et al. Identification of 2019 nCoV related coronaviruses in Malayan pangolins in southern China. J. bioRxiv. 2020.2002.2013.945485.

- 6 Liu P Jiang J Z Wan X F et al. Are pangolins the intermediate host of the 2019 novel coronavirus 2019 nCoV J . bioRxiv. 2020.2002.2018.954628. DOI: 10.1101/2020.02.17.357102. <https://doi.org/10.1101/2020.02.17.357102>
- 7 Xu X Chen P Wang J et al. Evolution of the novel coronavirus from the ongoing Wuhan outbreak and modeling of its spike protein for risk of human transmission J . Sci China Life Sci 1 4 2020 02 27 . <http://kns.cnki.net/kcms/detail/11.5841.q.20200204.1852.046.html>. DOI: 10.1007/s11427-020-1852-0
- 8 Yushun W Jian S Rachel G et al. Receptor recognition by novel coronavirus from Wuhan: An analysis based on decade long structural studies of SARS J . J virol 2020. DOI: 10.1128/JVI.01198-20. <https://doi.org/10.1128/JVI.01198-20>
- 9 Phan T. Genetic diversity and evolution of SARS CoV 2 J . Infection Genet Evol 2020 81 104260. DOI: 10.1016/j.ymge.2020.104260
- 10 World Health Organization. Question and answer on coronavirus. <https://www.who.int/news-room/q-a-detail/q-a-coronavirus>. 11 February 2020.
- 11 Zhu H Wang L Fang C et al. Clinical analysis of 10 neonates born to mother with 2019 nCoV pneumonia. *Translational Pediatrics* 2020 DOI: 10.21037/tp.2020.02.06 published Online First 2020/02/10 . DOI: 10.21037/tp.2020.02.06
- 12 Leung GM Hedley AJ Ho LM et al. The epidemiology of severe acute respiratory syndrome in the 2003 Hong Kong epidemic: an analysis of all 1755 patients J . Ann Intern Med 2004 141 662 73. DOI: 10.7326/0000-9876-141-6-200403160-00001
- 14 Rivers CM Majumder MS

HCV RNA

1 2 1 1 1 1

10 HCV RNA 1 005 2019 1
 PCR HCV HCV RNA HCV CMIA
 HCV RNA HCV S/CO
 1 005 HCV 228 22.7% HCV
 HCV RNA HCV PCR HCV
 RNA 83 36.4% HCV S/CO HCV RNA
 HCV S/CO 10.7 92.59%
 77.93% HCV HCV RNA

HCV RNA

Application of high-sensitivity HCV RNA detection in preoperative screening

HE Yuting¹ CHEN Xuefang² CHEN Peisong¹ HUANG Hao¹ YU Xuegao¹ HUANG Bin¹

1. Department of Laboratory Medicine The First Affiliated Hospital Sun Yat sen University Guangzhou Guangdong China 510080 2 Nanfang College of Sun Yat sen University Guangzhou Guangdong China 510970

ABSTRACT Objective To investigate the application of high sensitivity HCV RNA detection in preoperative screening. Methods A total of 1 005 serum samples were collected from the preoperative screening patients in the Hospital Sun Yat sen University from January to October 2019. HCV antibodies and HCV RNA were detected using chemiluminescence microparticle immunoassay CMIA and fluorescence quantitative polymerase chain reaction FQ PCR . The comparison and correlation analysis between the S/CO value of HCV antibody and the high sensitivity HCV RNA test results were performed. The predictive efficacy of HCV antibody S/CO value for hepatitis C viremia was evaluated. Results Among the 1 005 serum samples 228 were positive for HCV antibody and the positive rate was 22.7%. HCV RNA were not detected from HCV antibody negative specimens. High sensitivity FQ PCR method detected 83 HCV RNA positive cases and the positive rate was 36.4%. There was no correlation between the HCV antibody S/CO value and the HCV RNA quantitative value. Using the critical S/CO value 10.7 with a sensitivity and specificity of 92.59% and 77.93% respectively can reduce the false positive rate for predicting hepatitis C viremia. Conclusion High sensitivity HCV RNA quantitative detection is applied for the preoperative screening of patients with hepatitis C which can accurately reflect the virus replication and infectivity in patients. Compared with the

2014A030313143

1. 510080

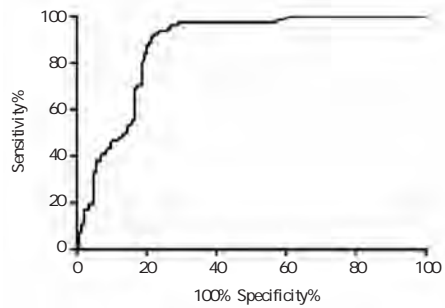
2. 510970

E-mail hb906@163.com

traditional preoperative screening method. FQ-PCR can distinguish the current infection from the previous infection and has the advantages of rapid

HCV RNA 1
 HCV RNA HCV CMIA
 HCV HCV
 100% 78.3%
 36.4% 100% 85.6%
 2.2 HCV S/CO HCV RNA
 HCV S/CO
 1 S/CO
 S/CO HCV RNA
 1 Y=0.06
 617X + 4.259 Spearman r²=0.002 P=
 0.69 HCV S/CO HCV RNA

cut off
 Youden s index 0.705 2
 92.59% 77.93% S/CO 1
 HCV 228 HCV
 HCV RNA 36.4% 83/228 2



2 HCV S/CO
 ROC

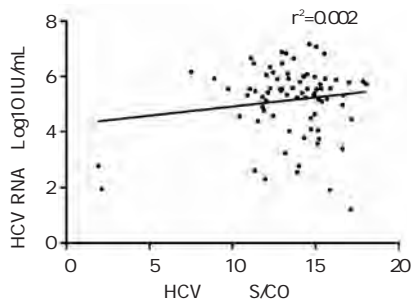
Figure 2 ROC curve of HCV antibody S/CO value for predicting hepatitis C viremia

1 HCV S/CO HCV RNA
 n %

Table 1 Distribution of HCV antibody S/CO value and high sensitivity HCV RNA detection results n %

S/CO	n	HCV RNA	
4>S/CO 1	87	1 1.1	86 98.8
8>S/CO>4	21	2 9.5	19 90.5
12>S/CO>8	29	15 51.7	14 48.3
16>S/CO>12	79	56 70.9	23 29.1
S/CO>16	12	9 75.0	3 25.0
	228	83 36.4	145 63.6

3



1 HCV S/CO HCV RNA

Figure 1 Scatter plot of HCV antibody S/CO value against high sensitivity HCV RNA quantitative detection results

2.3 HCV S/CO

HCV S/CO ROC
 area under the curve AUC 0.872 4
 ROC S/CO 10.7 HCV

HCV

HCV

HCV HCV 4
 HCV 2

HCV 5 HCV

PCR

PCR

Baleriola C 6 - 20

- 70 HCV RNA - 20
 1.2 - 70 9 HCV RNA

- 80 1 HCV RNA
 HCV RNA 228 HCV

36.4%

HCV HCV

HCV RNA

HCV RNA

S/CO HCV RNA

S/CO

Spearman

HCV S/CO HCV RNA

S/CO HCV

ROC S/CO cut

off 10.7

S/CO 1 cut off

HCV HCV RNA

HCV

Pan J Kao HH Ranjbar Kermani F 79

HCV

S/CO 1 cut

off HCV HCV

RNA HCV HCV RNA

HCV HCV

HCV RNA 15 IU/mL

HCV

11

Ha J 12 HCV RNA 32 127

Architect anti HCV HCV

8 0.02% 8/32 127 HCV

RNA 13 148 590 ELISA

HCV HCV RNA 298

0.2% 14 307 440

ELISA HCV

1 HCV RNA 0.000 325%

HCV

15 HCV HCV RNA

HCV RNA

HCV HCV

- 1 Blach S Zeuzem S Manns M et al. Global prevalence and genotype distribution of hepatitis C virus infection in 2015 a modelling study J . Lancet Gastroenterol Hepatol 2017 2 3 161 176.
- 2 Jacobson IM Lim JK Fried MW. American Gastroenterological Association Institute Clinical Practice Update Expert Review Care of Patients Who Have Achieved a Sustained Virologic Response After Antiviral Therapy for Chronic Hepatitis C Infection J . Gastroenterology 2017 152 6 1578 1587.
- 3 J . 2017 17 9 1275 1278.
- 4 J . 2019 37 4 553 556.
- 5 HCV RNA J . 2019 11 5 379 382.
- 6 Baleriola C Johal H Jacka B et al. Stability of hepatitis C virus HIV and hepatitis B virus nucleic acids in plasma samples after long term storage at 20 degrees C and 70 degrees C J . J Clin Microbiol 2011 49 9 3163 3167.
- 7 Kao HH Chen KS Lin CL et al. Utilization of Signal to Cutoff Ratio of Hepatitis C Virus Antibody Assay in Predicting HCV Viremia among Hemodialysis Patients J . Nephron 2015 130 2 127 133.
- 8 Pan J Li X He G et al. Reflex threshold of signal to cut off ratios of the Elecsys anti HCV II assay for hepatitis C virus infection J . J Infect Dev Ctries 2016 10 9 1031 1034.
- 9 Ranjbar Kermani F Sharifi Z Ferdowsian F et al. The Usefulness of Anti HCV Signal to Cut off Ratio in Predicting Viremia in Anti HCV in Patients With Hepatitis C Virus Infection J . Jundishapur J Microb 2015 8 4 e17841.
- 10 2019 J . 2019 13 1 1 18.
- 11 European Association for the Study of the Liver. EASL Recommendations on Treatment of Hepatitis C 2016 J . J Hepatol 2017 66 1 153 194.
- 12 Ha J Park Y Kim HS. Signal to cutoff ratios of current anti HCV assays and a suggestion of new algorithm of supplementary testing J . Clin Chim Acta 2019 498 11 11 15.
- 13 J . HCV HCV RNA 2016 18 4 374 376.
- 14 J . 2012 25 Suppl.1 91.
- 15 J . 2016 26 20 2970 2971.

2 Glu504Lys 2

1 2 1 2 1 1 1

2 T2DM 2 ALDH2 Glu504Lys

ALDH2 504 HbA_{1c}

2016 4 2017 12 629

402 2 227 ALDH2

ALDH2 HbA_{1c} 2 GL LL

37.9% 7.0% 30.8% 3.2% P<0.05 629

GG 390 GL 210 LL 29 ALDH2 2

GG 32.1% 125/390 GL 41.0% 86/210 LL

55.2% 16/29 ALDH2 2 OR =1.578 95% 1.131~

2.202 ALDH2 HbA_{1c} P>0.05 ALDH2 ALDH2

P>0.05 2 ALDH2 HOMA 1 IR

QUICKI ISI P>0.05 2

ALDH2 504 Glu504Lys 2

HbA_{1c}

2 2

Distribution characteristics of Glu504Lys polymorphism of acetaldehyde dehydrogenase 2 gene in Type 2 Diabetes Mellitus in Han Nationality

AN Hongliang¹ JIANG Haiyan² ZHANG Jinfeng¹ LI Weixuan² SU Rong¹ HE Xian¹ LV Weifeng¹

1. Department of Clinical Laboratory Foshan Hospital of Traditional Chinese Medicine Foshan Guangdong China 528000 2 Department of Clinical Laboratory The first people s hospital of Foshan Foshan Guangdong China 528000

ABSTRACT Objective To analyze the distribution characteristics of the Glu504Lys polymorphism of the aldehyde dehydrogenase 2 ALDH2 gene in people with type 2 diabetes T2DM and to explore the relationship between ALDH2 gene mutation at position 504 and fasting blood glucose HbA_{1c} level and insulin resistance. Methods A retrospective study was conducted in 629 cases of physical examination and hospitalization in Foshan Traditional Chinese Medicine Hospital from April to December in 2016. There were 402 healthy controls and 227 patients with type 2 diabetes mellitus. The distribution of ALDH2 genotypes in the two groups was analyzed and the distribution levels of HbA_{1c} fasting blood glucose and insulin resistance in ALDH2 genotypes of the two groups were compared. Results The proportions of GL and LL mutation genotypes in type 2 diabetes group were 37.9% and 7.0% respectively which were significantly higher than those in the physical examination control group 30.8% and 3.2% P<0.05 . Among 629 Han subjects 390

1. 528000

2. 528000

E-mail 438320079@qq.com

cases are GG 210GL and 29LL. With the increase in the number of ALDH2 gene mutations the risk of type 2 diabetes increases. The specific data are 32.1% 125/390 without mutation GG type 41.0% 86/210 with heterozygous mutation GL type and homozygous mutation LL Type 55.2% 16/29 . ALDH2 gene mutation is a risk factor for type 2 diabetes OR value = 1.578 95% confidence interval is 1.131-2.202 ALDH2 gene mutation has no effect on the distribution of HbA 1C level P>0.05 . There was no difference in the distribution of ALDH2 genotypes between men and women in the 2 groups P>0.05 . There was no significant difference in the distribution of insulin resistance index HOMA1 IR quantitative insulin sensitivity test index QUICKI and fasting insulin sensitivity index ISI of each type of ALDH2 genotype in type 2 diabetes group P>0.05 . Conclusion The proportion of ALDH2 gene mutation at position 504 in Han type 2 diabetes population is significantly higher than that in normal population. Glu504Lys mutation is a risk factor for type 2 diabetes but it was not significantly related to fasting blood glucose HbA 1C and insulin resistance.

KEY WORDS Aldehyde dehydrogenase 2 Type 2 diabetes mellitus Genotype Polymorphism genetic

2 acetaldehyde dehydrogenase 2 154 73 18-90
 ALDH2 57.78±15.30
 19 402 330
 72 17-87 38.63±9.47
 ALDH2 12q24 G→A ALDH2
 rs671 504 ALDH2
 glutamic acid G lysine L ALDH2
 G L GG GL P>0.05
 LL ALDH2 2 5 1999 WHO
 ALDH2 Glu504Lys 5
 12 2 11.1 mmol/L 7.0 mmol/L 75
 ALDH2 2 11.1 mmol/L
 HbA_{1c} 20-80 2
 3 2 ALDH2 2
 Glu504Lys 47.80%
 22.0% 19.38% 4
 2
 1.2
 ALDH2 ABI 7500
 2 ALDH2 BR 526 24 ALDH2
 Glu504Lys ALDH2 G7
 HbA_{1c} TOSOH
 AU5400
 1 Centaur XP
 1.1
 2016 4 2017 12 1.3
 2 227 2 8 3-4

mL ALDH2 ALDH2
 EDTA 2Na BR 526 24
 2-
 8 3 1.5
 HOMA1 IR SPSS 22.0
 HOMA1 IR HOMA1 IR= × 1 Sample K S Kolmogorov Smirnov
 /22.5 ISI ISI=1/
 × QUICK $\bar{x} \pm s$
 QUICKI ⁶ χ^2 P<0.05
 ALDH2 DNA DNA 2
 2 mL T2DM ALDH2
 DNA ALDH2
 ALDH2 P<0.01 2
 ABI 7500 1
 1 T2DM ALDH2 n %

Table 1 Distribution of ALDH2 genotypes in control group and T2DM group n %

		GG	GL	LL			
T2DM	402	265 65.9	124 30.8	13 3.2	265 65.9	137 34.1	
	227	125 55.1	86 37.9	16 7.0	125 55.1	102 44.9	
	629	390 62.0	210 33.4	29 4.6	390 62.0	239 38.0	
χ^2			9.489			7.255	
P			0.009			0.007	

ALDH2 2 1.578 95% 1.131~2.202
 2
 ALDH2 ALDH2
 2 ALDH2
 P<0.01 P>0.05 2
 L 2 ALDH2
 ALDH2 Glu504Lys L P>0.05
 2 P<0.01 3

Table 2 Proportion of type 2 diabetes mellitus in 629 subjects with ALDH2 genotype n %

		GG	GL	LL			
T2DM	227	125 32.1	86 41.0	16 55.2	102	125	
DM	402	265 67.9	124 59.0	13 44.8	137	265	
	629	390	210	29	239	390	
χ^2			9.256			7.255	
P			0.002			0.007	

3 ALDH2 n %
Table 3 Distribution of ALDH2 genotypes between male and female n %

		GG	GL	LL			
		330	221 67.0	100 30.3	9 2.7	221 67.0	109 33.0
		72	44 61.1	24 33.3	4 5.6	44 61.1	28 38.9
	χ^2			1.946		0.903	
	P			0.378		0.342	
T2DM		154	85 55.2	58 37.7	11 7.1	85 55.2	69 44.8
		73	40 54.8	28 38.4	5 6.8	40 54.8	33 45.2
	χ^2			0.014		0.003	
	P			0.993		0.955	

2

$\chi^2=0.606 P>0.05$

HbA_{1c} Kolmogorov Smirnov Z =1.393 $\chi^2=0.041 P<0.05$
 HbA_{1c} Z =0.763
 GG GL LL HbA_{1c} F =0.291 P=0.748 P>0.05
 GG GL+LL HbA_{1c} F =0.546 P=0.461 P>0.05

4 T2DM

$\bar{x} \pm s$

Table 4 The distribution level of each biochemical serological index in each genotype $\bar{x} \pm s$

	GG	GL	LL		
HbA _{1c}	8.818±2.559	9.023±2.296	8.955±2.788	8.818±2.559	9.014±2.350
mmol/L	8.897±3.546	9.851±4.431	6.946±2.424	8.897±3.546	9.453±4.321
		F =3.690 P=0.027		F =1.035 P=0.310	
mU/L	19.46±16.59	20.57±17.65	17.82±11.31	19.46±16.59	20.15±16.83
		F =0.205 P=0.815			
	7.553±6.979	9.399±9.463	5.392±3.713	7.553±6.979	8.846±8.986
		F =1.949 P=0.145			
	0.302±0.032	0.299±0.035	0.311±0.034	0.302±0.032	0.301±0.035
		F =0.865 P=0.423			
	6.798±6.281	8.459±8.517	4.853±3.341	6.798±6.281	7.9613±8.088
		F =1.949 P=0.145			

2.4.2

5 T2DM

Table 5 The statistical results of FBG levels among genotypes in the T2DM group

		F	I J	P
	GG	9.851		
	GL			
	LL	6.946		
	GG			
	GL			
	LL			
	GG			
	GL+LL			
	GG VS GL	3.690	/	/ 0.027
	GL+LL	1.035	/	/ 0.310
	GG VS GL	/	-0.954	5.626 0.092
	GG VS LL	/	1.951	1.113 0.087
	GL VS LL	/	2.904	1.156 0.013

3

ALDH2
30%~50%
15%~30%⁷
ALDH2 34.1%
⁸ 2
44.9% ALDH2
2
ALDH2 Glu504Lys 2
ALDH2

DNA

¹⁸
ALDH2 Glu504Lys
2
2
9

HbA_{1c} 8-12

ALDH2 HbA_{1c}
¹³ ALDH2
2 HbA_{1c}

ALDH2

6

	1	2	1	1	1	1	1	1
			27	6				
			6				PCR	
DNA					27	6		
	14				6			
						6		
		6						

Establishment of immortalized lymphocyte cell lines with mutation of the glucose -6- phosphate dehydrogenase gene

JIA Zheng¹ ZHANG Yanyan² SUN Nan¹ ZHANG Wenxin¹ GAO Fei¹ SUN Jing¹, HUANG Jie¹ QU Shoufang¹

1. National Institutes for Food and Drug Control Beijing China 100050 2. MGI Tech Co. Ltd Shenzhen China 518083

ABSTRACT Objective To establish immortalized lymphocyte cell lines by collecting 27 clinical peripheral blood samples harboring glucose 6 phosphate dehydrogenase G6PD gene mutations. Methods The glucose 6 phosphate dehydrogenase gene mutation detection kit fluorescence PCR melting curve method was used to screen the mutation type of clinical samples and then peripheral blood was collected for transformation of immortalized lymphocyte lines. The genomic DNA of the successfully established lymphocyte line was extracted and verified by the next generation sequencing method. Results We established 27 immortalized lymphocyte cell lines including 14 different homozygous or heterozygous G6PD mutation types. The genetic mutation types of immortalized lymphocyte lines were the same as those originally indicated in clinical samples. Conclusion The established immortalized lymphocyte cell lines with G6PD mutations in this study have stable genetic information and can be used as a national reference resource to evaluate the performance of the G6PD gene mutation kit.

KEY WORDS Glucose 6 phosphate dehydrogenase Gene mutation Immortalized cell line

2016YFC1000300

1. 100050
2. 518083

E-mail qushoufang@126.com

E-mail jhuang5522@126.com

6 glucose 6 phosphate de PCR
hydrogenase G6PD X DNA
2 8 Xq28 G6PD G6PD

1 2 SLAN 96S PCR
G6PD 2000 MGISEQ
G6PD G6PD 1.2
G6PD X 1.2.1
PCR 6
1.2.2
1.2.2.1 EBV B95 8
RPMI 1640 FBS
2-3
10 37
3 2 000 rpm 10 min
0.2 m

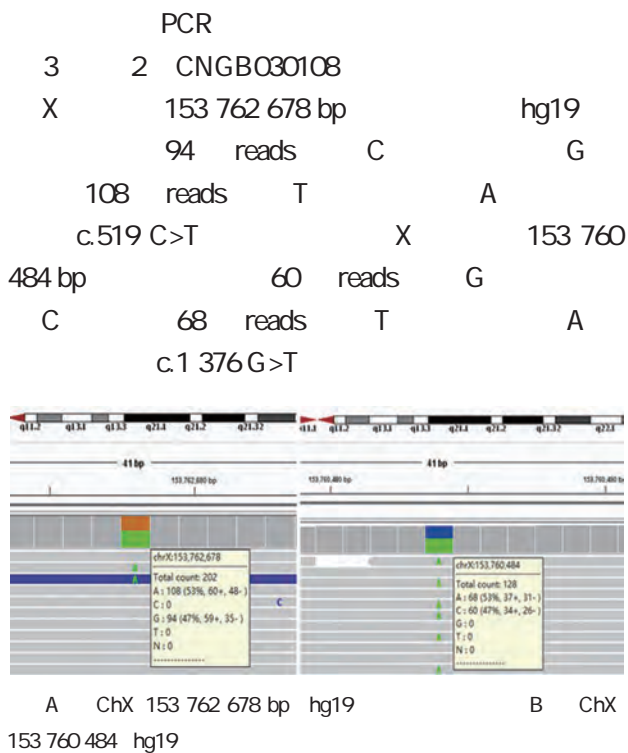
6
6
1.2.2.2 B
5 mL
RPMI 1640
6 2 000 rpm 20 min
8 mL 2 1 500 rpm RPM1640
EBV 10 min
1.5 mL
A 0.4 mL
T25
37 5% CO₂

1
1.1
1.1.1 1.2.2.3 24-
48 h
10 mL 33

1.1.2 1 300 rpm 5
RPMI 1640 FBS 3-6x10⁶ /mL
GIBCO A DMSO 1 300 rpm 5
10% DMSO
6

A O B 15 C 30
2 O 15 30 ×50

Figure 2 The result of immortalized lymphocyte cell line transformation on day 0 day15 and day 30 ×50



3 CNGB030108
Figure 3 The sequencing results of CNGB030108

3

EB EBV

B

A T

T B

2

Table 2 The verification results of immortalized lymphocyte cell lines

1	CNGB030075	c.392G>T
2	CNGB030078	c.871G>A
3	CNGB030079	c.871G>A
4	CNGB030081	c.95A>G
5	CNGB030082	c.95A>G
6	CNGB030084	c.95A>G
7	CNGB030085	c.1024C>T ; c.1388G>A
8	CNGB030086	c.1388G>A
9	CNGB030101	c.1388G>A
10	CNGB030102	c.1376G>T
11	CNGB030103	c.871G>A
12	CNGB030104	c.1388G>A ;
13	CNGB030105	c.1388G>A
14	CNGB030106	c.392G>T
15	CNGB030107	c.1376G>T
16	CNGB030108	c.1376G>T ; c.519C>T
17	CNGB030109	c.95A>G
18	CNGB030110	c.1360C>T
19	CNGB030111	c.1388G>A
20	CNGB030112	c.1388G>A ; c.519C>T
21	CNGB030113	c.1024C>T
22	CNGB030114	c.95A>G
23	CNGB030115	c.1376G>T
24	CNGB030116	c.95A>G
25	CNGB030117	c.1388G>A
26	CNGB030119	c.392G>T
27	CNGB030120	c.1388G>A ; c.392G>T

81370615

1. ICU 450000
2. 450000

P U s Y Bb07 /f P T M • T M T M i e A . s 01vU - # A D D É s Q @ 50b07 /f T M T M i e . . . s 02 ! a ` R 1 P p ' : ©

increased inflammatory factors. It is also a risk factor for the prognosis of patients with sepsis and cardiac dysfunction.

KEY WORDS Sepsis cardiac function miR 21 miR 155 Prognosis

1²

U ÖZ

1

2 P>0.05 CRP PCT cTnl BNP
 LVEF<50% <LVEF 50% <
 2.1 3 P<0.05 1
 3 BMI

Table 1 comparison of general data among 3 groups $\bar{x} \pm s$

	n=40	LVEF 50% n=38	LVEF<50% n=20	Z/F	P
/	23/17	22/16	12/8	0.036	0.982
BMI kg/m ²	42.39±9.59	45.12±10.92	40.39±11.87	1.432	0.244
CRP mg/L	22.93±5.82	23.14±6.14	22.46±5.67	0.087	0.917
PCT ng/mL	3.28±0.62	30.38±7.82	61.39±9.94	530.616	0.000
cTnl ng/mL	0.58±0.08	3.29±0.68	14.69±3.94	417.803	0.000
BNP ng/L	0.45±0.08	0.68±0.12	1.52±0.20	481.609	0.000
	32.93±7.95	63.29±10.29	132.29±21.29	417.546	0.000

2.2 3 miR 21 miR 155 IL 2 ICAM 1 LVEF<50%
 3 miR 21 miR 155 TNF α LVEF 50%
 P<0.05 2

Table 2 comparison of circulation miR 21 miR 155 and serum TNF α IL 2 ICAM 1 among 3 groups $\bar{x} \pm s$

	n	miR 21	miR 155	TNF α ng/L	IL 2 ng/L	ICAM 1 ng/mL
LVEF 50%	40	1.02±0.19	0.97±0.16	9.38±1.32	14.28±2.37	126.49±17.96
LVEF<50%	38	1.42±0.23	1.38±0.19	20.19±4.82	32.93±6.48	349.58±62.39
F	20	2.19±0.42	1.83±0.32	57.92±9.94	82.93±13.28	649.39±85.93
P		129.091	113.378	543.380	586.608	592.120
		0.000	0.000	0.000	0.000	0.000

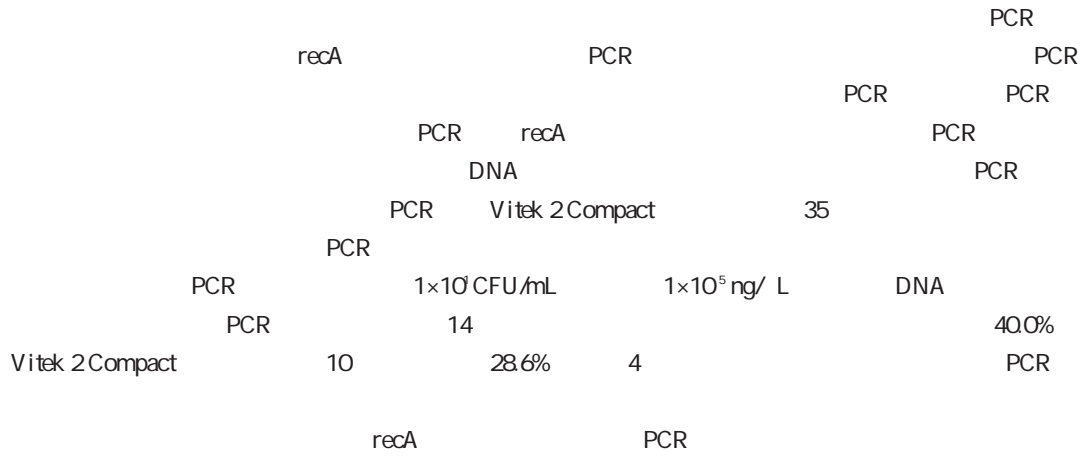
2.3 LVEF<50% miR 21 miR 155 2.4 LVEF<50%
 LVEF<50% miR 21 miR 155 LVEF<50% miR 21
 CRP PCT cTnl BNP TNF α IL 2 miR 155 TNF α IL 2 ICAM 1
 ICAM 1 P< P<
 0.05 3 0.05 4

Table 3 correlation between miR 21 miR 155 and serum index in LVEF <50% group

	miR 21		miR 155	
	r	P	r	P
CRP	0.273	<0.05	0.410	<0.05
PCT	0.306	<0.05	0.377	<0.05
cTnl	0.227	<0.05	0.342	<0.05
BNP	0.285	<0.05	0.266	<0.05
TNF α	0.329	<0.05	0.325	<0.05
IL 2	0.268	<0.05	0.367	<0.05
ICAM 1	0.402	<0.05	0.291	<0.05

2.5 LVEF<50%
 LVEF<50%
 miR 21 miR 155 CRP
 PCT cTnl BNP TNF α IL 2 ICAM 1
 logistics miR 21 miR 155
 PCT TNF α IL 2 ICAM 1
 LVEF<50%
 CRP BNP LVEF<50%
 5
 3

PCR

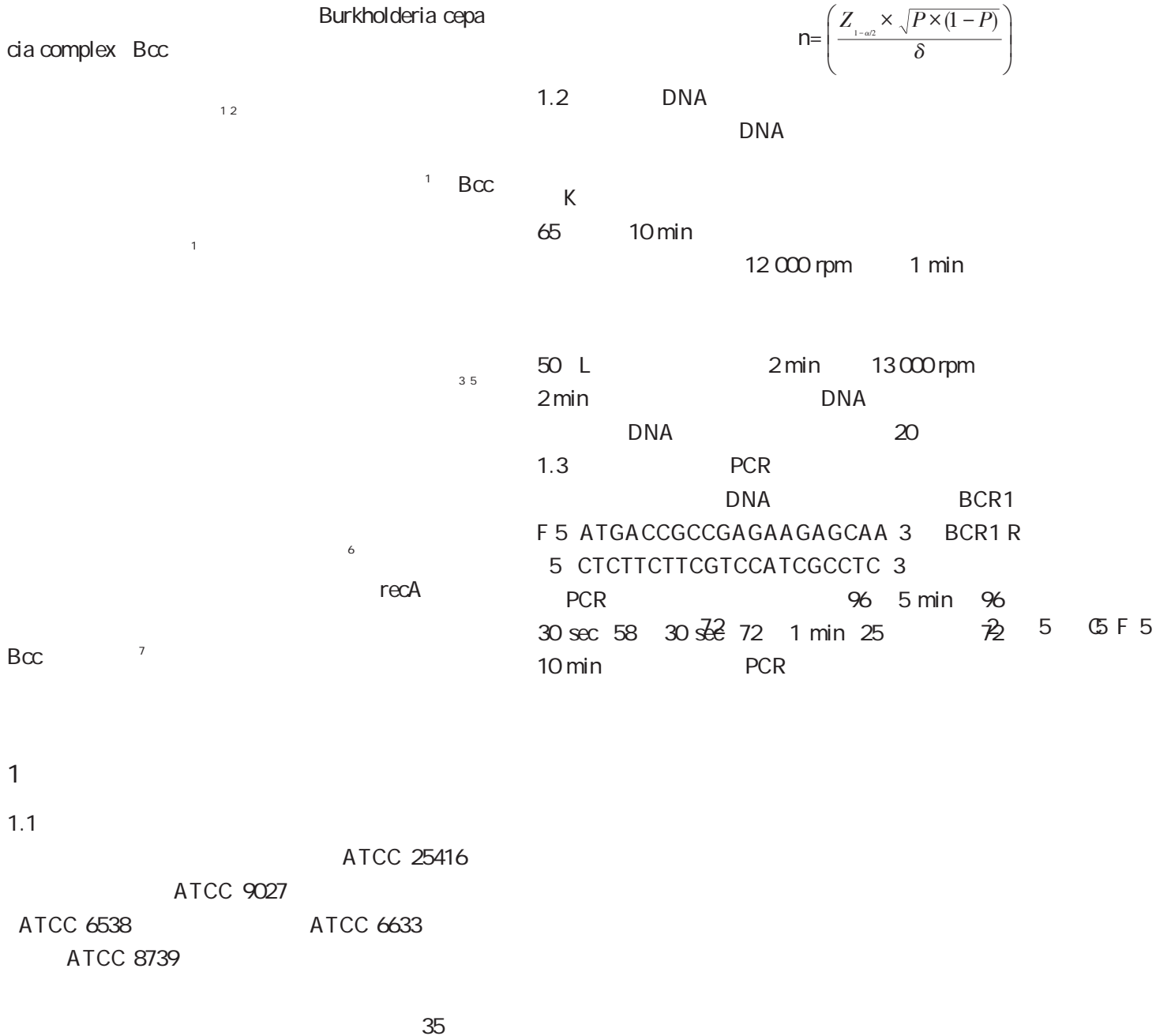


Establishment of nested fluorescent quantitative PCR for rapid detection of *Burkholderia cepacia*

1 c e° e

cating that the nested fluorescent quantitative PCR had more accurate detection performance. Conclusion Nested fluorescent quantitative PCR is an effective rapid and direct method for clinical detection of Burkholderia cepacia.

KEY WORDS Burkholderia cepacia RecA gene Nested fluorescent quantitative PCR Clinical detection



$Z_{1-\alpha/2}=1.96$ $P=0.9$

$\delta=0.1$
35

recA

ATCC 25416

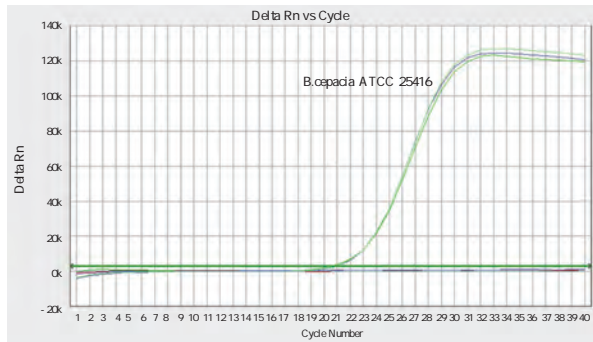
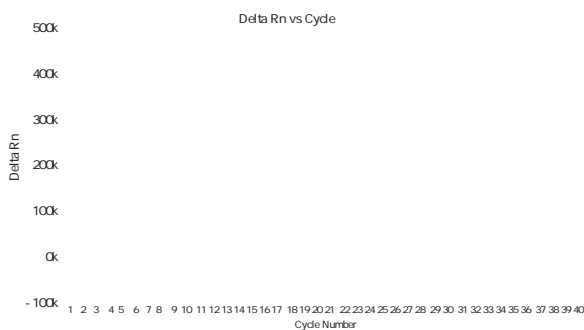


Figure 1 Amplification curves of nested quantitative PCR for different bacterial strains

2.2 PCR

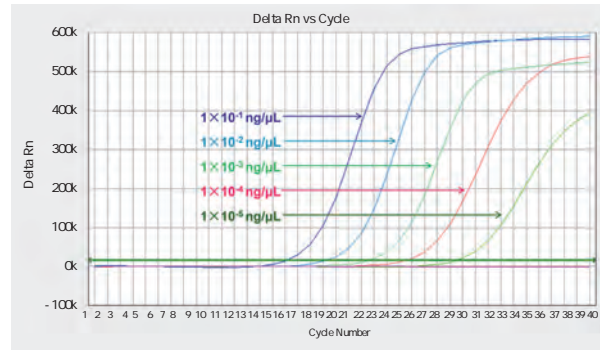
1×10^5 1×10^4 1×10^3 1×10^2
 1×10^1 1×10^0 CFU/mL
 PCR 1×10^0 CFU/mL
 1×10^1 CFU/mL
 1×10^3 1×10^4 1×10^5 1×10^6 ng/ L
 1×10^6 ng/ L
 10^5 ng/ L



2 PCR

Figure 2 Amplification curves of Burkholderia cepacia with different concentrations by nested quantitative PCR

PCR
B.cepacia



3 DNA PCR

Figure 3 Amplification curves of Burkholderia cepacia genomic DNA in different concentrations by nested quantitative PCR

2.3 PCR

35
 PCR Vitek 2 Compact
 Vitek 2 Compact 10
 4
 PCR
 Vitek 2 Compact
 14 Vitek 2 Compact
 4 PCR Vitek 2
 Compact
 $\chi^2=0.560$ $P=0.454$

3

16S rRNA 8 16S rRNA Bcc
 98%~100% Bcc
 8
 recA Bcc
 8 10 recA 8 recA
 Bcc

recA
Bcc
98.9% recA
98.9%
100%
recA
11 12 Bcc
recA
recA
recA
Jimenez ²⁰
PCR 16S rRNA
10 fg/ L
0.98
Wright ²¹ recA PCR
X Y !
X Y !

gyrB
13 hisA
442 bp hisA DNA
hisA Bcc
14
15 /
MALDI TOF MS
Furlan ¹⁶
Bcc
VITEK 2 MALDI TOF MS
16S rRNA recA
PCR Bcc recA PCR
Lambiase ¹⁷
MALDI TOF MS Bcc
Zakharova ¹⁸ β
PCR
Bcc
β
D β
Bcc
PCR
19 III
PCR
10 copies/ L

results of influenza A and B virus in oropharyngeal swab samples.

KEY WORDS Virus inactivation Quantitative real time polymerase chain reaction Influenza viruses Oropharyngeal swab

1 RNA

1.3 -20 1 mL

200 L

1.2 56

30 min

1.4 PCR

severe acute respiratory syndrome coronavirus 2 SARS CoV 2

RNA

ABI7500 PCR

50 15 min → 95 15 min →

94 15 s → 58 45 s 45

cycling threshold CT

PCR

2011

56 30 min

6.7

56 30 min 1.5

FAM

quantitative real time polymerase chain reaction qPCR

Ct 39.7

FAM

Ct 38.0

FAM

Ct >39.7

FAM

Ct >38.0

1.6

SPSS 26.0

GraphPad Prism

Version 8.0

$\bar{x} \pm s$

t

Bland Altman

$P < 0.05$

1

1.1

2020 1 31 2020 2 15

47 qPCR

21

26

n=27 Ct

n=16 26 Ct 33

n=4

26 33 < Ct 39

14

qPCR

1.2

ABI7500 PCR Thermofisher

qPCR

21

26

qPCR
 100% 56 30 min Ct
 P>0.05 1 2

1 qPCR

Table 1 The qPCR results of unheated and heat inactivation

Ct		qPCR			
32.52	32.83	0.31	30.36	28.72	-1.64
30.93	30.38	-0.55	25.60	26.73	1.13
30.26	36.64	6.38	28.31	25.58	-2.74
35.73	26.12	-9.61	23.02	23.81	0.79
26.55	20.79	-5.76	23.03	23.39	0.36
20.52	26.46	5.94	22.48	22.22	-0.26
27.74	31.06	3.33	20.80	21.67	0.87
24.05	23.32	-0.73	23.23	23.45	0.23
26.37	24.20	-2.18	20.88	21.46	0.58
28.18	27.05	-1.13	20.50	20.94	0.44
25.58	25.81	0.22	24.13	24.51	0.38
28.53	28.62	0.09	24.78	25.11	0.32
22.78	23.44	0.66	26.25	26.65	0.40
23.04	28.60	5.57	20.98	21.99	1.01
23.03	28.32	5.29	25.42	26.24	0.82
23.27	26.24	2.97	19.33	17.54	-1.79
19.56	19.10	-0.46	27.60	28.15	0.55
22.92	28.73	5.80	20.24	22.38	2.15
22.76	27.34	4.59	32.00	31.27	-0.73
37.46	38.17	0.71	26.59	25.15	-1.44
34.84	33.72	-1.13	26.11	26.66	0.55
			32.38	28.77	-3.60
			27.67	26.91	-0.76
			27.34	28.38	1.05
			27.64	28.26	0.62
			18.88	18.88	0

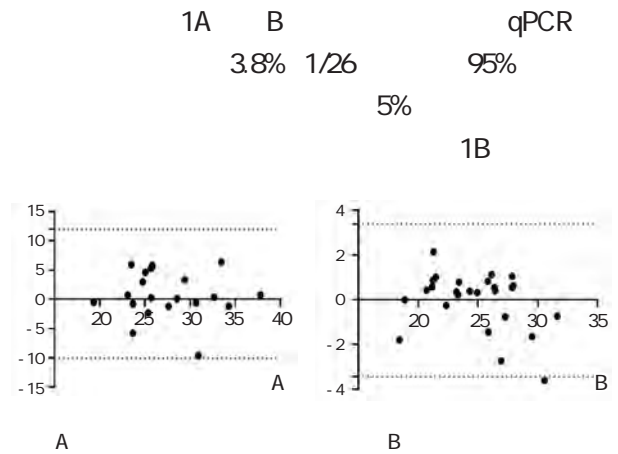
2 qPCR $\bar{x} \pm s$

Table 2 Comparison of the qPCR results between unheated and heat inactivation $\bar{x} \pm s$

n	t	P
Ct 21 26.98±5.07 27.95±4.76 -1.100	0.284	
Ct 26 24.83±3.77 24.80±3.32 0.108	0.915	

2.2 qPCR

qPCR 95%



1 Figure 1 A analysis of consistent results between unheated and heat inactivation

2.3 qPCR

14 qPCR

3

qPCR

89

10

11

12

13 SARS 56 60 min 56 30 min SARS 30 min 60 min

14 56 30 min 75%

15 qPCR

56
RNA
RNA

56 30 min

RNA

Ct

Ct

RNA

Ct

Ct

qPCR

16

56 30 min

qPCR

1
2
3
4
5
6
7
8
9
10
11
12
13
14
15
16

2011 S . 2020

J .

2001 5 1 60 62

Zhang N Wang LL Deng XQ et al. Recent advances in the detection of respiratory virus infection in humans J . J Med Virol 2020 92 4 408 417.

Xifeng Wu Yuanqing Ye. A public health perspective on preventing and controlling the spread of coronavirus disease 2019 J . China CDC Weekly 2020

S . 2020

. 2019

S . 2020

J . 2004

21 3 260 261.

J .

2019 23 14 2261 2268

J .

2017 34 2 166 171.

C I Bhagat M Lever A Prins J P Beilby. Effects of heat ing plasma at 56 for 30 min and at 60 for 60 min on routine biochemistry analytes J . Ann Clin Biochem 2000 37 802 804.

Chong YK Ng WY Chen PL Chloe M Mak. Effects of a plasma heating procedure for inactivation Ebola virus on common chemical pathology tests J . Hong Kong Med J 2015 21 3 201 207.

SARS

J . 2003 29 3 61 62

2019 PCR

J . 2020 43 DOI 10.3760/cmaj.issn.1009 9158.20200004.

J . ChinaXiv 202002.00034

2020

EB/OL . 2020 02 10 <https://mp.weixin.qq.com/s/e8JoY2n7pGaQ1vxN6PGp9g>.

2 UAER

hs CRP

1 2 1

hs CRP 2 T2DM CIMT C

T2DM 63 CIMT 2018 1 2019 12

CIMT 0.9-1.2 mm 23 CIMT >1.2 mm 22 3 CIMT 0.9 mm 18

BMI WHR SBP DBP TC TG

HDL C LDL C FPG SCr FINS

HbA1c 2h 2hPG C hs CRP UAER

CIMT hs CRP UAER 3 BMI WHR SBP DBP FINS SCr

P>0.05 3 HbA1c TC HDL C LDL C hs CRP UAER

P<0.05 FPG 2hPG TG P<0.05 T2DM

CIMT FPG 2hPG HbA1c TG TC LDL C hs CRP UAER P<0.05 HDL C

P=0.027 T2DM CIMT hs CRP UAER hs CRP UAER

T2DM AS

2 C

Correlation between carotid intima thickness and hs-CRP UAER in patients with type 2 diabetes mellitus

XIE Jun¹ SUN Yuanyuan² YU Qigui¹

1. Department of General Medicine The No.2 People's Hospital of Hefei Hefei Anhui China 230011

2. Department of Clinical Nutrition The No.2 Hospital of Hefei Hefei AnHui China 230011

ABSTRACT Objective To analyze the correlation between carotid medial intimal thickness CIMT and high sensitivity C reactive protein hs CRP and urine protein excretion rate UAER in patients with type 2 diabetes T2DM . Methods 63 T2DM patients admitted to our hospital from January 2018 to December 2019 were collected and the color Doppler ultrasound diagnostic instrument was used to detect CIMT. Based on CIMT grouping 18 patients in normal group CIMT 0.9 mm and 23 in thickened group CIMT 0.9-1.2 mm and 22 in plaque group CIMT >1.2 mm . The age sex T2DM course BMI WHR systolic blood pressure SBP diastolic blood pressure DBP total cholesterol TC triglyceride TG high density lipoprotein cholesterol HDL C Low density lipoprotein cholesterol LDL C fasting blood glucose FPG serum creatinine SCr fasting insulin FINS glycated hemoglobin HbA1c high sensitivity C reactive protein hs CRP and 2h blood glucose after meals 2hPG urinary protein excretion rate

2017

1704f0804042

1.

230011

2.

230011

E-mail ahmusyy@sina.com

UAER were compared and the correlation between CIMT and hs CRP and UAER was analyzed. Results There were no statistically significant differences in age gender BMI WHR SBP DBP FINS and SCr in the three groups $P>0.05$. The differences in the course of disease HbA1c TC HDL C LDL C hs CRP and UAER in the three groups were statistically significant $P<0.05$. FPG 2hPG and TG in the plaque and thickening group were significantly higher than those in the normal group $P<0.05$. CIMT was positively correlated with the course of disease FPG 2hPG HbA1c TG TC LDL C hs CRP and UAER in T2DM patients $P<0.05$ and negatively correlated with HDL C $P=0.027$. Conclusion CIMT and hs CRP are closely related to UAER in T2DM patients. The combined detection of hs CRP and UAER can predict the early assessment of macrovascular disease or AS in T2DM patients.

KEY WORDS 2 diabetes mellitus Carotid intima thickness Hypersensitive C reactive protein Urinary protein excretion rate Correlation

2 Type 2 Diabetes Mellitus
 T2DM T2DM
 1
 T2DM Athero 1.2
 sclerosis AS 1.2.1 CIMT
 2 T2DM LOGIQ500
 Carotid Intima MediaThickness CIMT GE
 AS 3
 4 T2DM
 C
 C reactive protein CRP AS
 T2DM CIMT
 CRP C
 Highsensitivity C reactive protein hs CRP
 Urinary albumin excretion rate UAER
 T2DM CIMT hs CRP UAER

1

1.1

	2018	1	2019	12
T2DM	63		53-72	
	63.81 ± 6.02	41	22	
	2		2017	
⁵	1-17		9.52 ± 4.17	
T2DM		⁵	3	

moglobin A 1c HbA 1c

C Highsensitivity C reactive protein
hs CRP 2 h
2 mL 2 h 2hPostprandial blood glu
cose 2hPG 3 h
Urinaro UŽU Đ @

2.2 T2DM CIMT
 T2DM CIMT FPG 2hPG
 HbA1c TG TC LDL C hs CRP UAER
 P<0.05 HDL C
 P<0.05 2

2 T2DM CIMT
 Table 2 T2DM Correlation analysis between patient CIMT and other factors

	r	P
FPG	0.196	0.039
2hPG	0.264	0.015
HbA1c	0.253	0.019
TG	0.297	<0.001
TC	0.246	0.018
HDL C	0.255	0.015
LDL C	-0.249	0.027
FINS	0.316	0.008
SCr	0.197	0.302
hs CRP	0.062	0.575
UAER	0.329	<0.001
	0.288	<0.001

2.3 Logistic
 T2DM CIMT >1.2 mm
 FPG 2hPG HbA1c TG TC
 HDL C LDL C FINS SCr hs CRP UAER
 Logistic
 HbA1 TC LDL C hs CRP UAER T2DM
 P<0.05 3

3 Logistic
 Table 3 Risk factors Logistic regression analysis of carotid plaque

	β	Wald	OR	95%CI	P
HbA1c	2.778	4.982	1.546	1.029-2.142	0.025
TC	2.661	4.831	1.438	0.985-2.021	0.023
LDL C	0.762	4.125	1.223	1.006-1.372	0.029
hs CRP	0.613	3.686	1.825	1.297-2.605	0.035
UAER	3.079	6.407	28.464	2.145-73.212	<0.001
	2.136	4.356	8.564	1.208-43.597	<0.001

3
 60%
 7
 8
 T2DM
 AS

AS
 T2DM
 9 T2DM AS

Jamshid 10
 CRP T2DM AS
 CRP T2DM
 AS
 CRP T2DM
 T2DM CIMT hs CRP
 T2DM AS
 12 T2DM
 13 CIMT 24 h
 UAER T2DM CIMT
 Logistic
 T2DM
 T2DM

UAER
 AS 14
 HbA1 TC LDL C T2DM
 T2DM
 CIMT 15

UAER T2DM CIMT hs CRP
 hs CRP UAER
 T2DM AS

1 Lee J Wan J Lee L et al. Study of the NLRP3 inflamma some component genes and downstream cytokines in patients with type 2 diabetes mellitus with carotid atherosclerosis J . Lipids Health Dis 2017 16 1 217.
 2 Liu CZ Zhong Q Huang YQ. Elevated Plasma miR 29a Levels Are Associated with Increased Carotid Intima Media Thickness in Atherosclerosis Patients J . Tohoku J Exp Med 2017 241 3 183-188.

3
 2019 38 6 617 619.
 4 CTRP12 J .
 2019 21 7 1048 1050.
 5 J . 2018 38 4 292 344.
 6 2018 J . 2019 19 1 1 44.
 7 .2 J .
 2017 25 7 481 492
 8 Hamamura M Mita T Osonoi Y et al. Relationships
 Among Conventional Cardiovascular Risk Factors and Life
 style Habits With Arterial Stiffness in Type 2 Diabetic Patients
 J . J Clin Med Res 2017 9 4 297 302
 9 Denimal D Monier S Brindisi MC et al. Impairment of the
 Ability of HDL From Patients With Metabolic Syndrome but
 Without Diabetes Mellitus to Activate eNOS Correction by

S1P Enrichment J . Arteriosclerosis 2017 37 5 804 811.
 10 Vafaeimanesh J Parham M Norouzi S et al. Insulin resis
 tance and coronary artery disease in non diabetic patients Is
 there any correlation J . Caspian J Intern Med 2018 9
 2 121 126.
 11 . C 2 J .
 2019 40 7 632 634.
 12 . C1q 2 J .
 2019 42 3 214 217.
 13 .2 J . 2019 23 5 932
 935.
 14 . J .
 2017 16 5 362 365.
 15 . J .
 2019 11 3 224 228.

1 J . 2019 29 6 35 38.
 2 J . 2019 28 4 494 497.
 3 miR
 155 J .
 2018 38 11 1545 1547.
 4 miRNA 21
 PCT J .
 2018 43 7 907 912
 5 /
 2018 J . 2018 38 9 741 756.
 6 Ehrman RR Sullivan AN Favot MJ et al. Pathophysiolo
 gy echocardiographic evaluation biomarker findings and
 prognostic implications of septic cardiomyopathy a review of
 the literature J . Crit Care 2018 22 1 112
 7 Kamad DR Saseedharan S. Myocardial Dysfunction in Sep
 sis and Septic Shock J . J Assoc Physicians India 2017 65
 12 11 12
 8 . miR 21 ox
 LDL J .
 2019 11 4 276 282 309.
 9 Sheng B Zhao L Zang X et al. miR 375 ameliorates sepsis
 by downregulating miR 21 level via inhibiting JAK2 STAT3
 signaling J . Biomed Pharmacother 2017 86 254 261.
 10 Marques Rocha JL Garcia Lacarte M Samblas M et al.

Regulatory roles of miR 155 and let 7b on the expression
 of inflammation related genes in THP 1 cells effects of fatty
 acids J . ~~Zhang~~ Marqueshw 309Zan_ 2017 86 4 Zar

OPG TNF α

GDM OPG TNF α /TNF α
 40 GDM
 40 OPG TNF α OPG TNF α
 BMI TG TC LDL C P>0.05
 FBG HDL C TG/TC TC/HDL C LDL C/HDL C AIP HOMA IR QUICKI
 P<0.05 GDM TNF α NGT OPG /TNF α r=- 0.68
 NGT P<0.05 /TNF α r=- 0.68
 P<0.05 r=- 0.39 P<0.05 r=0.69 P<0.05
 /TNF α GDM OPG
 /TNF α GDM OPG /TNF α
 GDM

Diagnostic analysis of serum OPG TNF - α and adiponectin in gestational diabetes mellitus

WEN Jie LIU Ping GUO Rui

Department of Obstetrics and Gynecology Affiliated Hospital of North China University of Technology Tangshan Hebei China 063000

ABSTRACT Objective To explore OPG TNF α adiponectin and adiponectin/TNF α ratio in the blood circulation of gestational diabetes mellitus GDM pregnant women and the relationship with metabolic syndrome biomarkers and clinical significance. Methods 40 women with GDM and 40 normal pregnant women were recruited in this study. The levels of serum OPG TNF α and total adiponectin were measured using enzyme linked immunosorbent assay ELISA . The correlation between OPG TNF α and adiponectin and the degree of GDM was analyzed. Results There was no statistically significant difference in gestational age BMI TG TC LDL C P>0.05 . The age of pregnant women FBG HDL C TG /TC TC /HDL C LDL C/HDL C AIP insulin HOMA IR and QUICKI were statistically significant between two groups P< 0.05 . The expression level of TNF α in the GDM group was higher than that in the control group. The ratio of OPG adiponectin and adiponectin /TNF α was significantly lower than that in the control group P<0.05 . Adiponectin/TNF α ratio was negatively correlated with insulin resistance r=- 0.68 P<0.05 . Triglycerides r=- 0.39 P<0.05 were positively correlated with insulin sensitivity r=0.69 P<0.05 . Multiple linear

20191162

063000

E-mial guchengchengpa@163.com

regression analysis showed that the adiponectin/TNF α ratio was independently related to insulin resistance. Binary logistic regression analysis indicated that GDM was positively correlated with OPG levels and negatively correlated with adiponectin/TNF α ratio. Conclusion the OPG level in the GDM group increased while the adiponectin/TNF α ratio decreased significantly. This ratio may be an effective biomarker for assessing pregnant women's high risk of insulin resistance and dyslipidemia as well as GDM diagnostic and treatment monitoring targets.

KEY WORDS Gestational diabetes mellitus Osteoprotein Tumor necrosis factor α Adiponectin Insulin resistance

Gestational diabetes mellitus

GDM

GDM ^{1 3} 1.2

GDM ⁴ GDM ⁷ 100 100g 250 mL

GDM GDM 30 4 10.3

osteoclastogenesis inhibi 5.6 nmol/L

tory factor OPG α nmol/L 8.6 nmol/L

TNF α adiponectin GDM

⁵ OPG 1.3

TNF α

AMP ⁶ 5 mL 3 000r/min 5 min

Thermo Multiskan FC

TNF α

Olympus AU400

GDM OPG TNF α FBG TC

TG HDL C

<10

normal glucose tolerance LDL C Friedewald ⁸

NGT GDM OPG TC/HDL C LDL C/HDL C TG/

TNF α /TNF α TC log TG/HDL C

AIP TINS ⁹

1 1.4

HOMA IR

1.1 HOMA IR= FPG \times FINS /225

2018 1 2018 12 ¹⁰ QUICKI

QUICKI=1/ logFINS U/mL +logFBG mg/dL

GDM GDM 40 24- ¹¹

28 NGT 1.5

SPSS 19.0

UŽD“ ©

2
2.1
BMI TG TC LDL C
P>0.05 FBG
HDL C TG/TC TC/HDL C LDL C/HDL C AIP
HOMA IR QUICKI
P<0.05 1

Table 1 Biochemical characteristics of gestational diabetes mellitus GDM and normal pregnant women $\bar{x} \pm s$

	NGT n=40	GDM n=40	t	P
BMI kg/m ²	27.25±1.18	27.66±1.17	1.560	>0.05
FBG mg/dL	78.45±1.29	100.83±1.54	70.458	<0.001
TG mg/dL	221.83±74	256.12±69.12	2.142	>0.01
TC mg/dL	242.67±30.18	225.84±39.88	2.128	>0.01
HDL C mg/dL	52.21±2.95	34.7±2.71	27.646	<0.001
LDL C mg/dL	146.1±27.84	139.92±20.11	1.138	>0.05
TG/TC	0.94±0.06	1.17±0.1	12.474	<0.001
TC/HDL C	5.32±0.54	7.88±0.65	19.160	<0.001
LDL C/HDL C	3.23±0.36	5.17±0.58	17.974	<0.001
AIP	0.63±0.04	0.87±0.04	26.833	<0.001
IU/mL	9.54±0.55	12.56±0.9	18.109	<0.001
HOMA IR	1.85±0.11	3.11±0.22	32.398	<0.001
QUICKI	0.36±0.01	0.33±0.01	13.416	<0.001

2.2 NGT GDM OPG TNF α

GDM TNF α NGT
OPG /TNF α
NGT NGT HOMA IR
/TNF α TNF α
QUICKI /TNF α
TNF α LDL C/HDL C
TG/TC 2

Table 2 OPG TNF α and adiponectin levels of gestational diabetes mellitus GDM and normal pregnant women $\bar{x} \pm s$

	n	OPG	Adiponectin g/mL	TNF α pg/mL	Adiponectin/TNF α ratio
NGT	40	2224.76±881.47	6.37±0.59	115.68±12.64	4.80±0.07
GDM	40	1148.15±700.13	4.50±0.38	225.08±27.35	4.31±0.05
t		6.049	16.853	22.964	36.026
P		<0.001	<0.001	<0.001	<0.001

2.3 OPG

HOMA IR TNF α TG
TG/TC AIP /TNF α
QUICKI TNF α TG TG/TC
AIP /TNF α

Table 3 Research and analysis of the correlation of clinical indicators

	HOMA IR		QUICKI	
	r	P	r	P
TNF α	0.38	0.001	-0.38	0.001
TG	0.30	0.006	-0.31	0.006
TG/TC	0.35	0.001	-0.35	0.001
AIP	0.36	0.001	-0.36	0.006
Adiponectin/TNF α ratio	-0.45	0.001	0.45	0.001

3

OPG

12

GDM OPG
Akinci GDM

OPG BMI
HOMA IR C
OPG
1 TNF α
OPG
GDM

13

14

OPG

OPG TNF α $\bar{x} \pm s$

		HOMA IR		2	Brogin Moreli J Cirino Ruocco A M Vernini J M et al. Interleukin 10 and tumor necrosis factor alpha in pregnancy aspects of interest in clinical obstetrics Z . 2012 2012 230742
		OPG		3	Yeral M I Ozgu Erdinc A S Uygur D et al. Prediction of gestational diabetes mellitus in the first trimester comparison of fasting plasma glucose two step and one step methods a prospective randomized controlled trial Z . 2014 46 512 518
	GDM	OPG		4	Chemerin 25 OH D3 visfatin J . 2019 11 6 503 507.
OPG		Logistic GDM		5	Vrachnis N Belitsos P Sifakis S et al. Role of adipokines and other inflammatory mediators in gestational diabetes mellitus and previous gestational diabetes mellitus Z . 2012 2012 549748
β		β	15	6	Xu J Hong Z Y Ping C Y et al. Maternal Circulating Concentrations of Tumor Necrosis Factor Alpha Leptin and Adiponectin in Gestational Diabetes Mellitus A Systematic Review and Meta Analysis J . Sci World J 2014 1 12
TNF α	GDM	López Tinoco ¹⁶		7	2014 J . 2014.
		GDM		8	Anna L Aleksandra R Iwona B et al. Serum Adiponectin and Leptin Concentrations in Relation to Body Fat Distribution Hematological Indices and Lipid Profile in Humans J . Int J Environ Res Public Health 12 9 11528 11548
TNF α		Liu ¹⁷		9	Akbas E M Timuroglu A Ozcicek A et al. Association of uric acid Atherogenic index of plasma and albuminuria in diabetes mellitus J . Int J Clin Experimental Med 2014 7 12 5737 5743
HOMA IR		TNF α		10	Vafaeimanesh J Bagherzadeh M Heidari A et al. Diabetic patients infected with helicobacter pylori have a higher Insulin Resistance Degree J . 2014 5 3 137 142
Aye ¹⁸		TNF α		11	Katz A Nambi S S Mather K et al. Quantitative Insulin Sensitivity Check Index A Simple Accurate Method for Assessing Insulin Sensitivity In Humansa *
		GDM			? 6 " # &
		TNF α IL10			
		¹⁹			
		/TNF α			
		/TNF α FBG TG			
		GDM			
OPG		TNF α			
/TNF α		OPG			
		TNF α			
		OPG			
		/TNF α			

1 Shobeiri S Abediankenari S Lashtoo Aghae B et al. Evaluation of soluble human leukocyte antigen G in peripheral blood of pregnant women with gestational diabetes mellitus Z . 2016 7 178 182

CRP sCD14 ST

CD14	sCD14 ST	2016	12	C	2019	3	CRP		
	164		CRP	sCD14 ST			logistic		
sCD14 ST					ROC	22	CRP		
							13.41		
							P<0.05		
T2 T3 T4		CRP	sCD14 ST						
		CRP	sCD14 ST						
P<0.05	logistic						CRP		
sCD14 ST				P<0.05	ROC		CRP sCD14 ST		
	AUC	0.712	0.804	0.918	71.02	79.55	87.22	72.27	77.48
85.96									
CRP	sCD14 ST			C		CD14			

Nosocomial infection factors and prediction of CRP and sCD14-ST in patients with rheumatoid arthritis

MENG Qingfang GUO Dongfang DANG Zheng LIU Zhe

Department of Rheumatology and immunology Zhumadian Central Hospital Zhumadian Henan China 463000

ABSTRACT Objective To study the risk factors of rheumatoid arthritis complicated with nosocomial infection and

creased first and then decreased while those without nosocomial infections continued to decline. The levels of CRP and sCD14 ST in patients with nosocomial infections were higher than those without nosocomial infections $P < 0.05$. Multivariate logistic regression analysis confirmed that diabetes mellitus invasive operation catheterization immunosuppressive agents hospitalization time and plasma CRP and sCD14 ST were risk factors for nosocomial infection in rheumatoid arthritis $P < 0.05$. ROC curve showed that CRP sCD14 ST and their combined detection AUC were 0.712 0.804 0.918 respectively sensitivity were 71.02% 79.55% 87.22% respectively specificity were 72.27% 77.48% 85.96% respectively. Conclusion There are various risk factors for rheumatoid arthritis complicated with nosocomial infection. Strengthening screening of plasma CRP and sCD14 ST levels are helpful for early detection early intervention and reduction of nosocomial infection rate.

KEY WORDS Rheumatoid arthritis Nosocomial infection Risk factors C reactive protein Soluble CD14 subtype Predictive value

109 22-85 3-24
 1.3-6.0 14
 19 8
 142 89
 53 7-38 d 11
 3 4
 1.3-2 5
 30.98
 10.76 6 7
 9.27 ~10.31 8
 1.2
 CRP sCD14 ST
 logistic
 9 10 Receiver operating characteristic curve ROC
 CRP sCD14 ST
 C C reactive protein CRP T1 T2 T0
 CD14 Soluble CD14 subtype T4 T3
 sCD14 ST 10 4-5 mL
 1 TGL 20MS
 1.1 3 000 /min 10-15 min
 CRP Siemens BN II
 2016 12 2019 3 sCD14 ST PATH
 164 55 FAST

2.3

1.3

SPSS 24.0
 $\bar{x} \pm s$
 χ^2
LSD t
n
logistic
ROC
CRP
sCD14 ST
Area under the
AUC<0.50
AUC=1.0
T0 T1
CRP sCD14 ST
P>0.05 T2 T3 T4
CRP sCD14 ST
T2 T3 T4
CRP
sCD14 ST
P<0.05
2
2.1
22 13.41 22
12 54.55%
7 31.82% 2 9.09%
1 4.55%
2.2
P<0.05 1

2.4

P<0.05 L logistic

		AUC			
CRP	25.10 mg/L	0.712	71.02	72.27	
sCD14 ST	801.80 pg/mL	0.804	79.55	77.48	
CRO	sCD14 ST	-	0.918	87.22	85.96

6 KRAJEWSK A WIODARCZYK M STOMPOR T. Osteoporosis and vascular calcification in rheumatoid arthritis the role of osteoprotegerin and sclerostin J . Pol Merkur Lekarski 2017 43 253 41 47.

7 Pagliarulo V Alba S Gallone MF et al. Diagnostic Accuracy of Hexaminolevulinic Acid in a Cohort of Patients Undergoing Radical Cystectomy J . J Endourol 2017 31 4 405 411.

8 BORTOLUZZI A FURINI F GENERALI E et al. One year in review 2018: novelties in the treatment of rheumatoid arthritis J . Clin Exp Rheumatol 2018 36 3 347 361.

9 Nazem K Motififard M Yousefian M. Variations in ESR and CRP in total knee arthroplasty and total hip arthroplasty in Iranian patients from 2009 to 2011 J . Adv Biomed Rese 2016 30 5 148 153.

10 J . 2018 24 30 61 64.

11 M . 4 . 2012 693 696.

12 J . 2018 25 15 2276 2278 @ Br UÅ

13 KIM SJ PARK JS LEE DW et al. Trichostatin A protects liver against septic injury through inhibiting Toll like receptor signaling J . Biomol Ther Seoul 2016 24 4 387 394.

14 . ESR CRP TKA J .

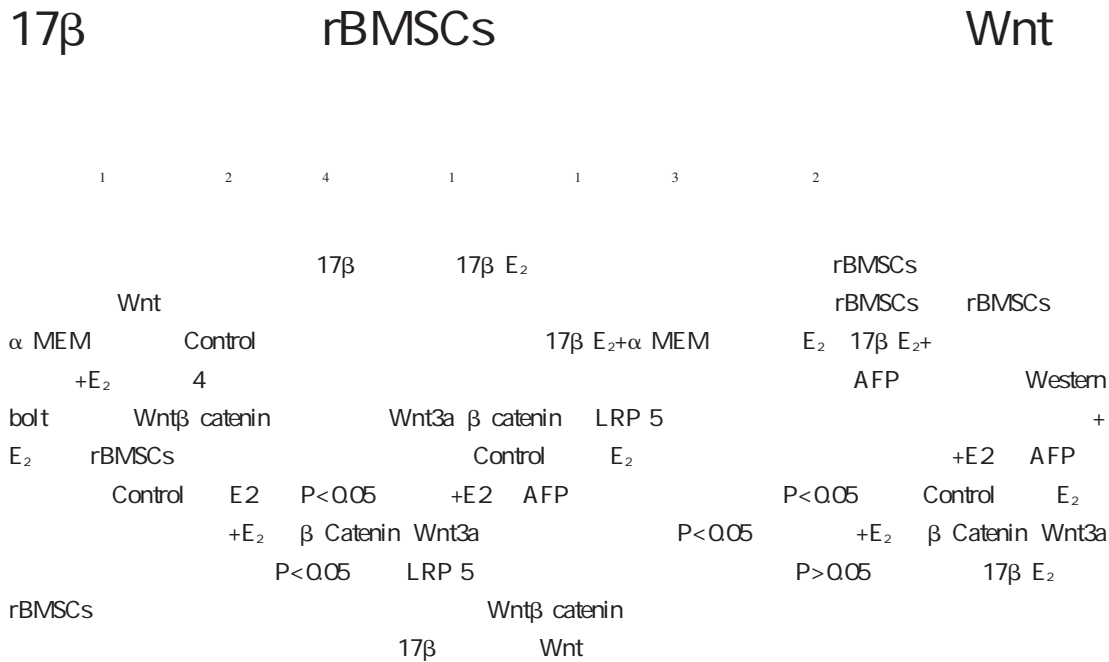
15 MARTÍNEZ FEITO A PLASENCIA RODRÍGUEZ C NAVARRO COMPÁN V et al. The effect of methotrexate versus other disease modifying anti rheumatic drugs on serum drug levels and clinical response in patients with rheumatoid arthritis treated with tumor necrosis factor inhibitors J . Clin Rheumatol 2019 38 3 949 954.

16 Glant T T Timea O Adrienn M et al. Characterization and Localization of Citrullinated Proteoglycan Aggrecan in Human Articular Cartilage J . PlosOne 2016 11 3 1 16.

17 J . 2017 17 4 713 716.

18 . C A CD64 2018 10 5 327 331.

19 JÄMSÄ J ALA KOKKO T HUOTARI V et al. Neutrophil CD64 (CBAc1) is a marker for active disease in rheumatoid arthritis J . Arthritis Rheum 2014 56 10 1641 1648.



Regulation of 17β -estradiol on the differentiation of hepatic progenitor cells and Wnt signaling pathway in rBMSCs

ZENG Lingfeng¹ HUANG Junyu² XIONG Yao⁴ ZHANG Zhidong¹ WANG Jinghao¹ HUANG Shuo³ WEI Hongcheng²

1. Department of pharmacy The first affiliated hospital of Jinan University Guangzhou Guangdong Chi na 510630 2. Department of gastroenterology The First Affiliated Hospital of Jinan University Guang zhou Guangdong China 510630 3. Departments of Radiology Xiehe Hospital Tongji Medical College Huazhong University of Science and Technology Wuhan Hubei China 430030 4. The fifth affiliated hos pital Guangzhou medical university Guangzhou Guangdong China 510700

ABSTRACT Objective To investigate the regulatory effect of 17β estradiol 17β E2 on the differ entiation of hepatic progeni tor cells of rat bone marrow mesenchymal stem cells rBMSCs and Wnt signaling pathway. Methods rBMSCs were obtained by whole bone marrow adherence method. The cells were divided into four groups α MEM medium control liver inducing medium classical and E2+α. MEM medium E2 E2 + hepatic inducing medium classical + E2 observed in morphology. The AFP concentration was measured using the luminescence immunoassay. The expression of Wnt signaling proteins included Wnt3a β

11619347

- 1. 510630
 - 2. 510630
 - 3. 430030
 - 4. 510700
- E-mail 33831827@qq.com E-mail twchc@jnu.edu.cn

catenin and LRP 5 was detected by Western blot. Results Morphologically rBMSCs in the classic and classic + E2 groups gradually showed liver progenitor like changes while the control group and E2 group showed no significant changes. The AFP concentration of classic group and classic + E2 group was significantly higher than that of the control group and E2 group $P < 0.05$. The AFP value of classic + E2 group was significantly higher than that of the classic group $P < 0.05$. Compared with the control group and the E2 group the expression levels of β Catenin and Wnt3a in the classic group and the classic + E2 group were significantly reduced $P < 0.05$ and the expression levels of β Catenin and Wnt3a in the classic + E2 group were significantly lower than that in the classic group $P < 0.05$. There was no statistically significant difference in the expression of LRP 5 $P > 0.05$. Conclusion 17β E2 can promote the differentiation of rBMSCs hepatic progenitor cells and the mechanism may be related to the regulation of Wnt/ β catenin signaling pathway.

KEY WORDS Bone mesenchymal stem cells 17β estradiol Wnt signaling pathway Differentiation of hepatic progenitor cells

artificial liver support system ALSS

CD45 legend β Catenin GAPDH CST CO₂

CD80 Tris HCL pH 8.3 Wnt3a WB Thermo Scientific3111

CD90 LRP 5 SW CJ IF

Bio Legend

1.2

Bone marrow mesenchymal stem cells BMSCs

Bio Rad680 SAria ScanDrop 100

BD FAC Boyue 17 4070

Tanon 1600 HE 120

3.6

BMSCs

1.3

1.3.1

row mesenchymal stem cells rBMSCs

P₃ P₅ rBMSCs 25 cm²

rBMSCs 37 5% CO₂

17 β 17 β estradiol 3 d 1 2

17 β E2 rBMSCs 4 α MEM

17 β E₂ Wnt Control 15% FBS

rBMSCs 10⁻⁶ mol/L 17 β E₂+ α MEM

1 E₂ 10⁻⁶ mol/L 17 β E₂+
+E₂

1.1 P₃ P₅ rBMSCs D Hanks

rBMSCs 2 9%

1.2 2 000 6 6

α MEM HyClone 10 200 L 37

D Hanks 5% CO₂ 1 6

PanEra CCK 8 100 L

0.25% Gibco 17 β 10 L CCK 8 25 h

CCK 8 Dojindo CD29 450 nm

OD OD

rBMSCs 1A rBMSCs S

1.3.2 2d 8d 1B rBMSCs

2000rpm 6min

D Hanks 3 300 L G₀/G₁ # &

1.5mL 700 L

4 D Hanks

2 500 L 1 600rpm 10

min 200 L PI

15min

1.3.3 rBMSCs

1 × 10⁶ cells/

mL CD29 CD45 CD80

CD90 37 30min

1.3.4 rBMSCs

1.4.1 60%

D Hanks

3 95% 10min

3 0.1% Tris HCL

O 37 45min 60min

Tris HCL 60%

O

1.3.5 rBMSCsAFP

1.4.1 1.4.2 3 6 10

4 300 L

AFP

1.3.6 Wnt

1.4.1 1.4.2

1 4

99 10min

β Catenin Wnt3a

LRP 5 4 37 2h

1.3.7

SPSS 13.0

$\bar{x} \pm s$

Bon

ferroni P<0.05

2

2.1 rBMSCs

rBMSCs

2.5 rBMSCs

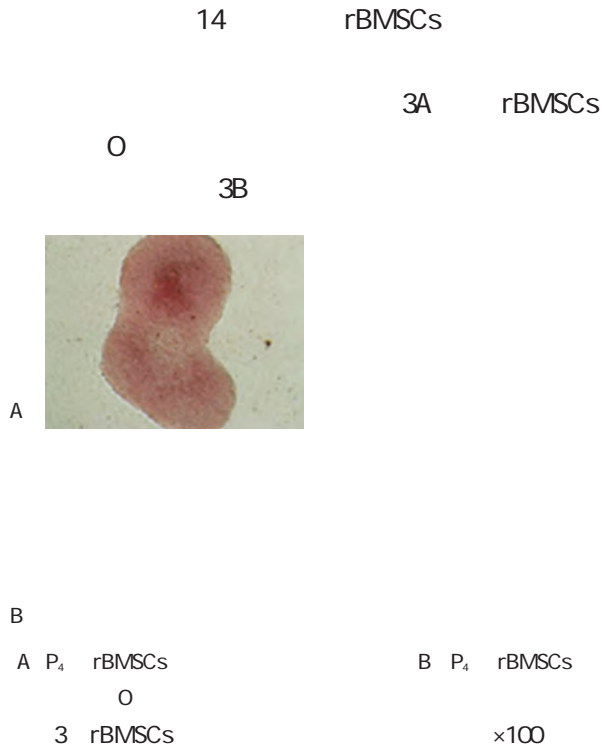


Figure 3 Identification of differentiation potency of rBMSCs from P₄ generation ×100

2.7 rBMSCs

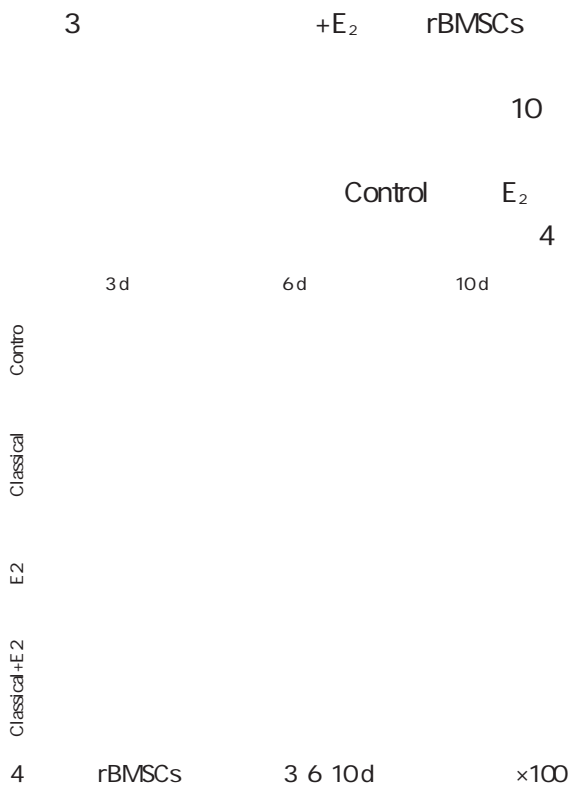


Figure 4 Cell morphology after 3 6 and 10 days of rBMSCs induction in each group ×100

2.8 rBMSCsAFP

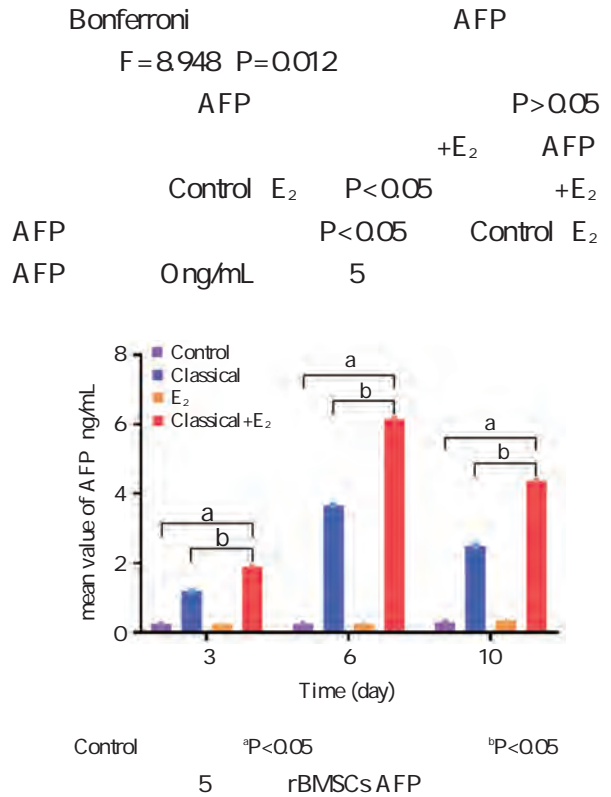
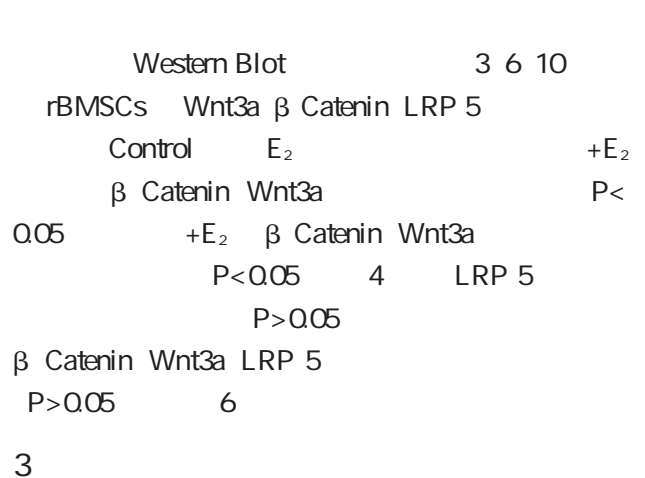


Figure 5 Average AFP of rBMSCs in each group

2.9 rBMSCs



BMSCs

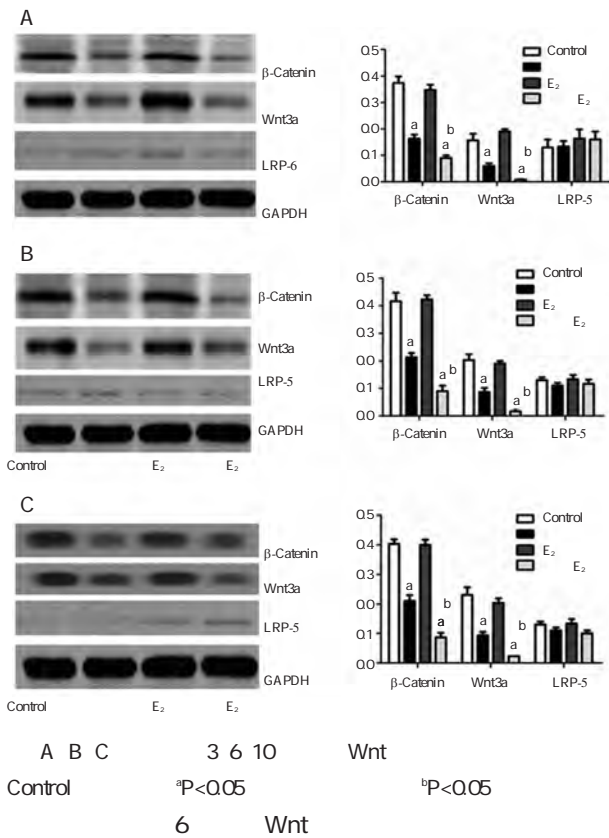
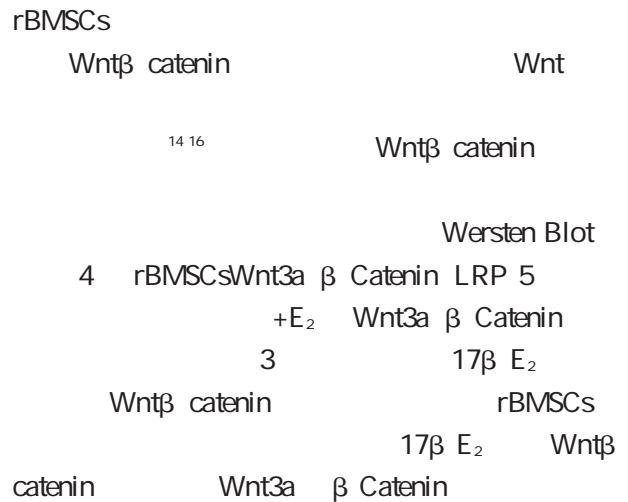
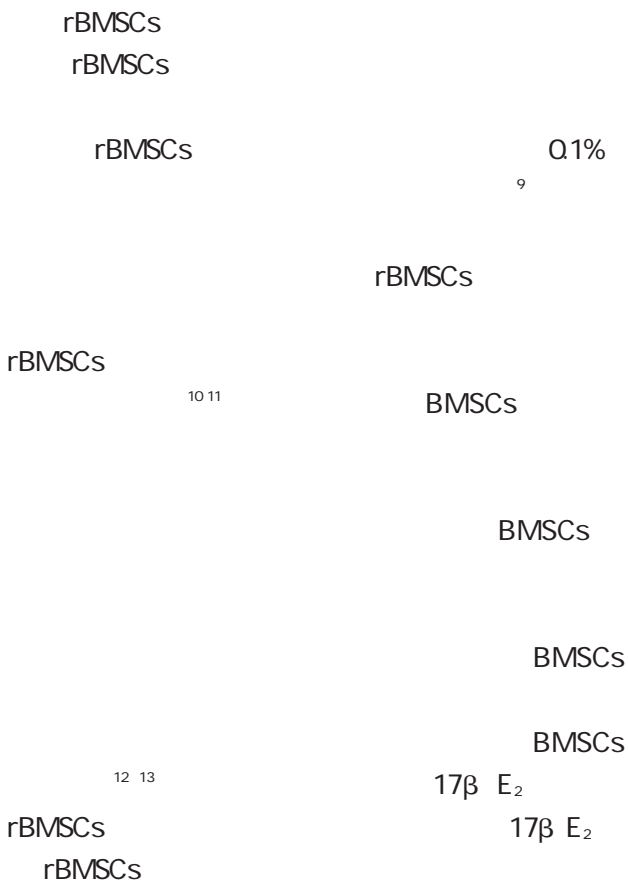
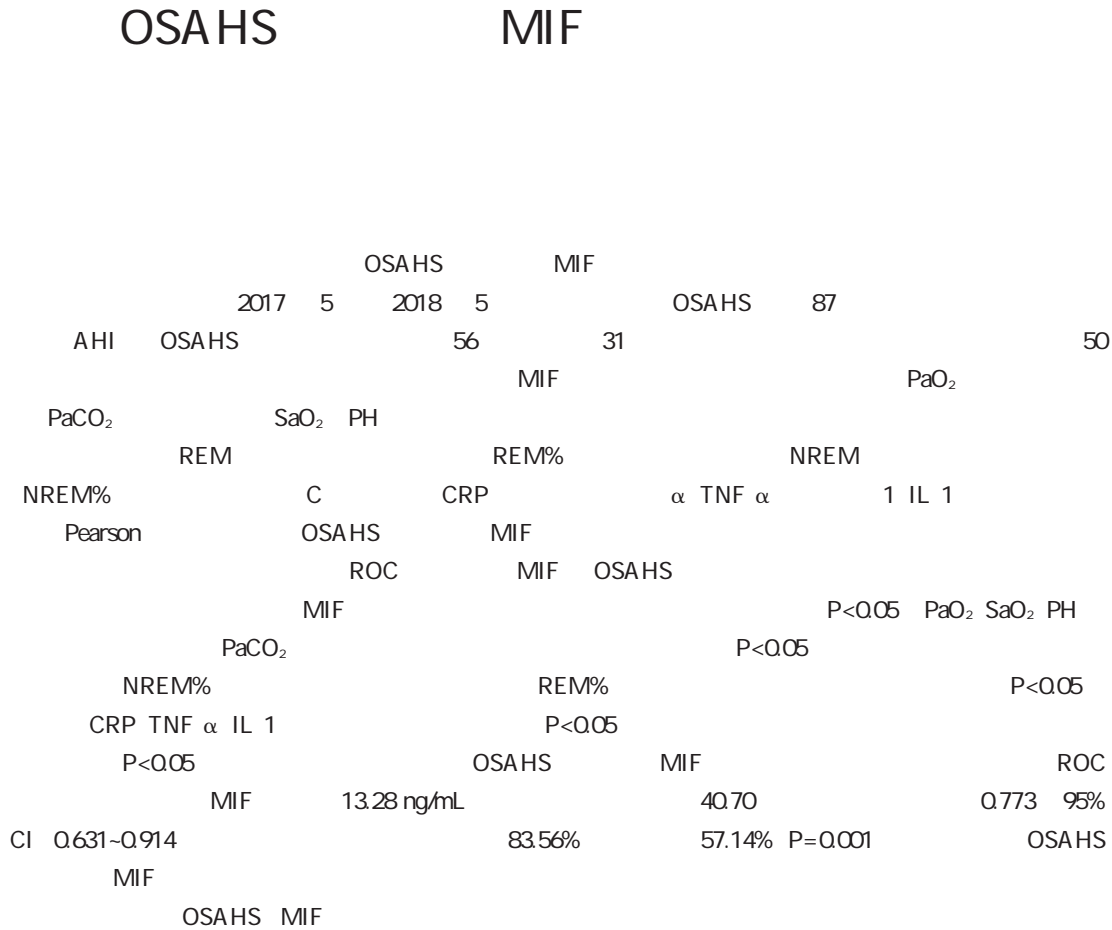


Figure 6 Expression of Wnt signaling protein in each group



- 1 Struecker B Raschzok N Sauer I M. Liver support strategies cutting edge technologies J . Nat Rev Gastroenterol Hepatol 2014 11 3 166 176.
- 2 Ciezowska M Pluta K. Clinical applications of liver support systems J . Postepy Biochem 2019 65 3 193 201.
- 3 Zhang B Zhang C G Ji L H et al. Estrogen receptor β selective agonist ameliorates liver cirrhosis in rats by inhibiting the activation and proliferation of hepatic stellate cells J . J Gastroenterol Hepatol 2018 33 3 747 755.
- 4 Besse Patin A Leveille M Oropeza D et al. Estrogen Signals Through Peroxisome Proliferator Activated Receptor gamma Coactivator 1alpha to Reduce Oxidative Damage As associated With Diet Induced Fatty Liver Disease J . Gastroenterology 2017 152 1 243 256.
- 5 Galmes Pascual B M Martinez Cignoni M R Moran Costoya A et al. 17β estradiol ameliorates lipotoxicity induced hepatic mitochondrial oxidative stress and insulin resistance J . Free Radic Biol Med 2020 150 148 160.
- 6 Zhang B Ji L H Zhang C G et al. Gender differences in vascular reactivity of mesenteric arterioles in portal hypertensive and non portal hypertensive rats J . World J Gastroenterol 2019 25 39 5953 5960.
- 7 Lee C W Chen Y F Wu H H et al. Historical Perspectives and Advances in Mesenchymal Stem Cell Research for the Treatment of Liver Diseases J . Gastroenterology 2018 154 1 46 56.
- 8 Gramignoli R Tahan V Dorko K et al. New potential cell source for hepatocyte transplantation discarded livers from metabolic disease liver transplants J . Stem Cell Res 2013 11 1 563 573.
- 9 Lou G Chen Z Zheng M et al. Mesenchymal stem cell derived exosomes as a new therapeutic strategy for liver diseases J . Exp Mol Med 2017 49 6 e346.



Estimated value of serum MIF level in assessing hypoxia sleep disorder and vascular endothelial injury in adult OSAHS patients

HUANG Yiwei ZHANG Hao LI Lingzhen

Department of Neurology Zhumadian Central Hospital Zhumadian Henan China 463000

ABSTRACT Objective To investigate the correlation between serum macrophage migration inhibiting factor MIF level and severity of in adult OSAHS patients and its predictive value to long term risk of cerebral infarction in patients. Methods 87 cases of adult OSAHS patients in our hospital during May 2017 to May 2018 were divided into mild to moderate group n=56 severe group n=31 according to apnea hypopnea index AHI . The differences in serum MIF arterial blood gas indicators Blood oxygen partial pressure

cytokines C reactive protein CRP tumor necrosis factor alpha TNF alpha Interleukin 1 IL 1 were compared among the subjects in each group. Pearson test was used to evaluate the correlation between serum MIF level and hypoxia sleep disorder and vascular endothelial injury in adult OSAHS patients. The ROC curve was used to analyze the predictive value of MIF for long term cerebral infarction in OSAHS patients. Results Serum MIF level of mild to moderate group severe group were higher than those in normal control group PaO₂ SaO₂ and PH levels were lower than normal control group PaCO₂ level was higher than that in normal control group Sleep latency total time of awakening number of awakening and NREM% were greater than those in normal control group while total sleep time and REM% were smaller than those in normal control group serum levels of CRP TNF α IL 1 were higher than those in normal control group level of NO was lower than that of normal control group P<0.05 . Changes of above indexes in severe group were all greater than those in mild and moderate group P<0.05 . Correlation analysis showed that serum MIF level of adult OSAHS patients was directly correlated with the severity of disease. ROC curve showed that when serum MIF level was 13.28 ng/mL the maximum yoden index was 40.70 and the area under the curve was 0.773 95% CI 0.631-0.914 . The sensitivity and specificity of predicting the occurrence of cerebral infarction were 83.56% and 57.14% P=0.001. Conclusion Serum MIF level of adult OSAHS patients increases abnormally which has certain value in reflecting the severity of disease.

KEY WORDS OSAHS MIF Arterial blood gases Sleep structure Endothelial injury Inflammatory response Cerebral infarction

Obstruc 2011 4 OSAHS
 tive sleep apnea hypopnea syndrome OSAHS 18-79 OSAHS

1 2

OSAHS

Macrophage migration inhibitor MIF
 3

Apnea hypopnea Index AHI OSAHS
 5 h AHI<30 h 56
 AHI 30 31

OSAHS 1.2 MIF
 MIF OSAHS 3 8 00am
 OSAHS MIF 3.0mL 37 2h
 OSAHS HBS 1101 BioRad
 1 HumanMIF ELISA Kit MIF
 1.3
 3 8 00am
 20mL GEM3000
 OSAHS 87
 AHI OSAHS 56
 31 50 CO₂ Oxygen partial pressure PaO₂
 Partial pressure of carbon dioxide Pa
 Oxygen saturation SaO₂ PH
 21-59 44.76±
 7.65 28 22 Alice4

Rapid eye movemenent

REM REM% $\bar{x} \pm s$ LSD t n
 Non Rapid Eye Movement NREM
 NREM% % χ^2
 HBS 1101 BioRad Pearson MIF
 C Receiver operating char
 C reactive protein CRP Human CRP ELISA acteristic curve ROC P<0.05
 Kit α Tumor necrosis fac
 tor α TNF α Human TNF α ELISA Kit 2
 1 Interleukin 1 IL 1 Human IL 1 2.1 MIF
 ELISA Kit 1.4 MIF
 MIF
 P<0.05 PaO₂
 2019 10 31 SaO₂ PH PaCO₂
 1.5 SPSS 20.0 P<0.05 1

Table 1 Comparison of serum MIF and arterial blood gas index levels between the 3 groups $\bar{x} \pm s$

	n=50	n=56	n=31	F/ χ^2	P
/	28/22	34/22	22/9	1.822	0.402
	44.76±7.65	44.83±8.29	45.10±8.32	0.652	0.516
	24.50±3.74	24.87±3.49	24.76±3.52	0.782	0.436
MIF	8.59±0.97	11.51±0.76	13.73±0.98	16.454	0.000
PaO ₂	98.63±1.23	92.20±5.81	83.64±9.52	7.725	0.000
PaCO ₂	38.46±5.10	44.80±6.37	50.72±7.34	9.470	0.000
SaO ₂	98.77±1.20	94.65±3.42	85.84±9.20	10.711	0.000
PH	7.39±0.11	7.28±0.18	7.13±0.24	8.295	0.000

2.2 REM% P<0.05
 NREM% 2

Table 2 Comparison of sleep structure parameters between 3 groups $\bar{x} \pm s$

	n	min	min	min	REM%	NREM%	
	50	30.15±4.28	439.74±73.13	57.12±8.59	5.46±0.68	22.38±2.75	73.10±8.65
	56	43.84±5.61	380.31±45.82	79.66±9.21	8.20±0.92	19.45±2.17	82.64±9.53
	31	57.96±8.22	311.49±37.24	93.74±11.85	9.76±1.14	14.02±1.83	87.92±9.70
F		15.914	10.920	15.549	12.845	15.372	8.055
P		0.000	0.000	0.000	0.000	0.000	0.000

2.3

3 3 $\bar{x} \pm s$
 Table 3 Comparison of serum inflammatory cytokine levels
 between 3 groups $\bar{x} \pm s$

	n	CRP mg/L	TNF α (pg/mL)	IL 1 (pg/mL)
	50	1.05±0.23	3.46±0.48	2.81±0.35
	56	4.28±0.59	9.21±1.52	5.03±0.57
	31	10.64±2.12	17.58±2.63	9.74±1.13
F		29.022	35.634	34.385
P		0.000	0.000	0.000

2.4

OSAHS MIF PaO₂ SaO₂ PH
 PaCO₂
 NREM%
 REM% CRP TNF α
 IL 1 P<0.05 4 3
 OSAHS
 \$ t \cdot`

2.6 ROC

87 OSAHS
 14 MIF 13.28 ng/mL
 40.70 0.773
 95%CI 0.631-0.914
 83.56% 57.14% P=0.001
 1

PCT NT proBNP

XZY XZY;:O 9t:O Ñ Ū5 qP 9 9p50 t U •)

XZYF2017-22

102600

E-mail shijiu546754@163.com

NT pro BNP

P<0.05 3

3 ARDS PCT NT pro BNP

$\bar{x} \pm s$

Table 3 Comparison of serum PCT and NT-pro BNP levels in patients with ARDS with different prognosis $\bar{x} \pm s$

	n	PCT (ng/mL)	NT pro BNP (ng/L)
	84	6.6±1.9	1576.3±163.5
	12	10.3±2.8	4722.1±405.2
t		4.434	26.586
P		0.001	0.000

2.5 PCT NT pro BNP ARDS

ROC

ROC PCT NT pro BNP

AUC 0.847 95% CI 0.795-0.900

0.729 95% CI 0.657-0.802 0.932 95% CI 0.899-0.965

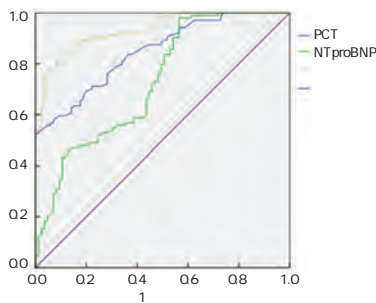
PCT 6.3 ng/mL

0.835 0.759 NT pro BNP 2794.5 ng/L

0.729 0.721

0.906 0.913

1



1 PCT NT pro BNP ARDS

ROC

Figure 1 ROC curve of PCT and NT pro BNP for prognosis diagnosis of ARDS patients

3

ARDS

ARDS

ARDS 8

ALI 6 7

ARDS

ARDS

ARDS

AR

DS

HR MAP CVP

ARDS

9

PCT 116

C PCT

PCT PCT PCT

10 11

PCT PCT

BNP

NT pro BNP NT pro BNP BNP

12 NT pro BNP ARDS

13 NT pro BNP

ARDS 14

BNP

15 IL 6 TNF α

BNP

NT pro BNP

PCT NT pro BNP ARDS

ARDS

1 Hendrickson CM Matthay MA. Potential Value of Biomarker Signatures in Sepsis and Acute Respiratory Distress Syn 477

4

9

4 HE4 9 CXCL9 LN 80
2016 1 ~2018 1 82 LN
SLE LN HE4 CXCL9 6
ROC HE4 CXCL9
1
6 HE4 CXCL9 Logistic LN ROC
HE4 CXCL9 HE4 CXCL9
P<0.05 4)& \$9\$- i)& UoCXCL 0)&

122102310013

453000

E-mail 15637359221@163.com

CL9 in the study group were higher than those in the control group $P < 0.05$. The ROC curve analysis showed that the combined AUC of serum HE4 and CXCL9 was 0.773 which was greater than HE4 0.670 and CXCL9 0.613 when the cutoff value of HE4 > 160.07 U/mL and the cutoff value of CXCL9 > 218.93 pg/mL the sensitivity was 76.83% and the specificity was 76.25% the serum HE4 and CXCL9 levels were higher than those with good prognosis after 6 months of treatment $P < 0.05$. Logistic regression analysis showed that SLE DAI score OR=2.820 serum HE4 OR=1.283 and CXCL9 OR=2.141 levels were important factors affecting the prognosis of LN $P < 0.05$ the ROC curve analysis showed that CXCL9 predicted a poor prognosis AUC of 0.670 after treatment for 6 months which was greater than HE4 0.667 when the cutoff value was > 191.88 the sensitivity was 60.00% and the specificity was 76.12%. Conclusion Serum HE4 and CXCL9 are highly expressed in LN. Combined detection has good diagnostic value and is an important prognostic factor. It can be used as a predictor of poor prognosis.

KEY WORDS Lupus nephritis Chemokine ligand 9 Human epididymis protein 4 Composite renal endpoint

Lupus nephritis LN
Systemic lupus erythematosus SLE

12 LN

3 SLE

9

4 SLE

4 Human epi

5 LN

HE4 CXCL9 LN

1

1.1

LN	2016	1	~2018	1	82
20-63			12		70
			35.31±7.33		
	126.30±35.27		mol/L		9.22±
2.05 mmol/L		80			
SLE	LN				11
69	21-64				36.48

eGFR 50% >218.93 pg/mL 76.83%
 1.4 76.25% 2
 2.3
 SPSS 24.0 1
 $\bar{x} \pm s$ t n % χ^2 15 2 8
 Logistic LN eGFR 50%
 ROC HE4 CXCL9 LN
 P<0.05 P>0.05 SLE
 SLEDAI P<0.05
 2 3

2.1 HE4 CXCL9
 HE4 CXCL9
 P<0.05 1
 1 HE4 CXCL9 $\bar{x} \pm s$
 Table 1 Comparison of serum HE4 and CXCL9 levels in two groups at admission $\bar{x} \pm s$

n	HE4 U/mL	CXCL9 pg/mL
82	184.35±62.24	234.46±42.09
80	126.27±58.82	207.11±38.20
t	6.101	4.328
P	<0.001	<0.001

3 $\bar{x} \pm s$
 Table 3 Comparison of General information of patients with different prognosis $\bar{x} \pm s$

	n=67	n=15	t/ χ^2	P
	35.14±7.06	36.09±6.57	0.477	0.635
	1.60±0.49	1.74±0.61	0.955	0.342
/	10/57	2/13	0.061	0.805
SLEDAI	12.80±2.33	17.16±2.51	6.461	0.001

2.2 HE4 CXCL9 HE4 CXCL9
 ROC HE4 CXCL9 P>0.05 6
 AUC 0.773 HE4 0.670 CXCL9 HE4 CXCL9 P<0.05
 0.613 HE4 >160.07 U/mL CXCL9 4

2 ROC
 Table 2 ROC analysis results

	AUC	95%CI	Z	P		%	%
HE4	0.670	0.588-0.753	4.044	<0.001	>162.08 U/mL	45.12	81.25
CXCL9	0.613	0.526-0.700	2.559	0.011	>221.07 pg/mL	75.61	43.75
	0.773	0.697-0.848	7.092	<0.001	HE4>160.07 U/mL CXCL9>218.93 pg/mL	76.83	76.25

4 6 HE4 CXCL9 $\bar{x} \pm s$
 Table 4 Serum HE4 and CXCL9 levels at admission to patients with different prognosis at 6 months after treatment $\bar{x} \pm s$

	n	HE4 U/mL		CXCL9 pg/mL	
		4	6	6	6
	15	193.39±35.49	137.58±27.25	247.73±38.84	201.85±33.51
	67	182.32±31.26	116.19±24.17	231.49±34.77	174.31±28.26
t		1.210	3.027	1.601	3.297
P		0.230	0.05	0.113	0.05

3 Wang Z Wang Y Zhu R et al. Long Term Survival and Death Causes of Systemic Lupus Erythematosus in China J . Medicine Baltimore 2015 94 17 e794.

4 CXCL9 CXCL10 CXCL11 J . 2015 29 2 125 128.

5 ProGRP HE4 J . 2017 24 10 50 52.

6 Hahn BH McMahon MA Wilkinson A et al. American College of Rheumatology guidelines for screening treatment and management of lupus nephritis J . Arthritis Care Res Hoboken 2012 64 6 797 808.

7 Mok CC Kwok RC Yip PS. Effect of renal disease on the standardized mortality ratio and life expectancy of patients with systemic lupus erythematosus J . Arthritis Rheum 2013 65 8 2154 2160.

8 J . 2019 34 5 401 404.

9 HE4 J . 2019 27 6 196 199.

10 . T CA125 HE4 J . 2019 27 3 119 121.

11 HE4 CEA NSE J . 2018 15 1 109 112.

12 Dong C Liu P Li C. Value of HE4 Combined with Cancer Antigen 125 in the Diagnosis of Endometrial Cancer J . Pakistan J Med Sci 2017 33 4 1013 1017.

13 HE4 J . 2019 26 1 45 48.

14 J . 2017 27 11 78 80.

15 IL 15 J . 2019 35 5 439 443.

16 Kuo P Tuong Z K Teoh S M et al. HPV 16E7 Induced Hyperplasia Promotes CXCL9/10 Expression and Induces CXCR3+ T cell Migration to Skin J . J Invest Dermatol 2018 138 6 1348 1359.

17 Tajfirouz D West DM Yin XT et al. CXCL9 compensates for the absence of CXCL10 during recurrent Herpetic stromal keratitis J . Virology 2017 63 506 7 13.

18 CXCL9/10/11 D . 2016.

drome in Children and Adults J . Crit care med 2020 48 3 428 430.

2 ARDS J . 2017 46 15 2146 2149.

3 Li H Wang D Wei W et al. The Predictive Value of Coefficient of PCT × BG for Anastomotic Leak in Esophageal Carcinoma Patients With ARDS After Esophagectomy J . J Intensive Care Med 2019 34 7 572 577.

4 C J . 2015 35 9 2464 2465.

5 Ranieri VM Rubenfeld GD Thompson BT et al. Acute respiratory distress syndrome the Berlin Definition J . JAMA 2012 307 23 2526 2533.

6 Bein T Weber Carstens S Apfelbacher C et al. The quality of acute intensive care and the incidence of critical events have an impact on health related quality of life in survivors of the acute respiratory distress syndrome a nationwide prospective multicenter observational study J . German medical science 2020 8 1 277.

7 Chambers ED White A Vang A et al. Blockade of equilibrative nucleoside transporter 1/2 protects against Pseudomonas aeruginosa induced acute lung injury and NLRP3 inflammasome activation J . FASEB J 2020 34 1 1516 1531.

8 J . 2017 28 06 783 786.

9 J . 2015 18 16 1931 1935.

10 PCT sTM TNF α J . 2020 40 5 984 986.

11 ARDS EVLWI PCT J . 2020 30 2 189 193.

12 . NT proBNP J . 2016 8 3 178 181.

13 J . 2018 39 4 560 565.

14 J . 2019 35 11 1813 1815.

15 . Pro BNP J . 2018 11 7 643 645.

1.4 RT PCR mRNA

Survivin 2

TRIzol

2.1 Survivin

Survivin

RNA cDNA PCR

0.00% Survivin

GAPDH 2^{ct}

Survivin

1.5

SPSS 20.00

n

Survivin

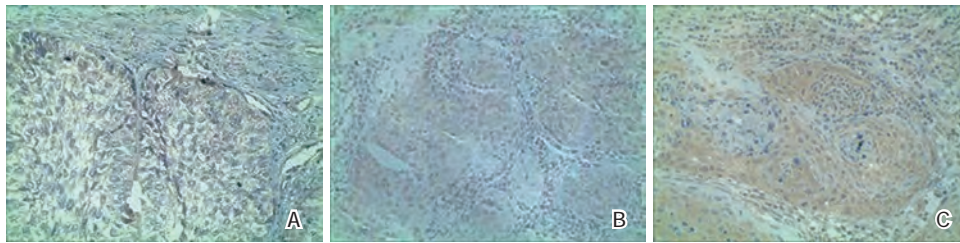
$\bar{x} \pm s$

t

P<0.05

P<0.05

1



A

- B

+ C

++ D

+++

1 Survivin

x40

Figure 1 The expression of Survivin in different tissues

x40

2.2 Survivin mRNA

HPV

RT PCR

Survivin mRNA

4.46±0.97

13

1.17±0.42

1.29±0.51

P<0.05 Sur

14

Survivin mRNA

P>0.05

2.3

Survivin

FIGO

15 16

Survivin

Survivin mRNA

17

FIGO

Survivin

Survivin mRNA

Sur

18 19

Surv

0.05

Survivin

20 21

P>0.05

1

Survivin

3

Survivin

4. Zumbärgel F K, Machtens D A, Curth U et al. Survivin does not influence the anti-apoptotic action of XIAP on caspase 9. *J. Biochem Biophys Res Commun*. 2017; 482(4): 530-535.
5. Guo L, Huang C, et al. .

LP a OPN IRF 4

DHVD a LP a OPN
 4 IRF 4 120 DHVD
 115 LP a OPN IRF 4 mRNA DHVD
 DHVD 3 LP a OPN IRF 4 mRNA
 LVEF CI
 LP a OPN IRF 4 mRNA
 F=47.427 66.514 36.432 P<0.05 LP a
 OPN IRF 4 mRNA DHVD P<0.05 LP a DHVD
 AUC 0.802 70.00% 86.09% 3 LP
 a OPN IRF 4 mRNA LVEF CI P<0.05
 LP a OPN LVEF CI IRF 4 mRNA LVEF CI
 P<0.05 DHVD LP a OPN IRF 4 mRNA DHVD
 DHVD
 a 4

Expressions and clinical significance of serum LP a OPN IRF-4 in patients with degenerative heart valve disease

WANG Junhua CUI Qintao HAN Peili LIU Xiaochen

Department of cardiovascular surgery The First affiliated hospital of xinxiang medical college Weihui Henan China 453100

ABSTRACT Objective To investigate the expression of serum lipoprotein a LP a osteopontin OPN interferon regulatory factor 4 IRF 4 in patients with degenerative heart valve disease DHVD and its clinical significance. Methods 120 patients with DHVD in our hospital were selected as the study group and 115 healthy people who were examined during the same period were used as the control group. The serum LP a OPN IRF 4 mRNA levels were compared between the two groups. The influencing factors of the incidence of DHVD and the diagnostic value of serum indicators for DHVD were analyzed. The levels of serum LP a OPN IRF 4 mRNA and cardiac function indexes left ventricular ejection fraction LVEF cardiac index CI of patients with different therapeutic effects after 3 months of treatment were compared. The correlation between serum indexes and cardiac function indexes was evaluated. Results The serum LP a OPN IRF 4 mRNA levels have significant difference in the patients with multi valvular disease and with single valvular disease and healthy people F=47.427 66.514 36.432 P<0.05 . Coronary heart disease smoking

17A320017

453100

E-mail doctorjh1981@163.com

history high blood pressure serum LP a OPN and IRF 4 mRNA are important influencing factors for the onset of DHVD P<0.05 . Coronary heart disease smoking history hypertension serum LP a OPN IRF 4 mRNA are important influencing factors of DHVD P<0.05 . Among the various serum indexes the area under the curve AUC for diagnosis of DHVD by LP a is the largest 0.802 the sensitivity of the cutoff value is 70.00% and the specificity is 86.09%. After the treatment for 3 months the serum LP a and OPN levels of the effective patients were lower than those of the effective and ineffective patients and the IRF 4 mRNA levels and LVEF CI were higher than those of the effective and ineffective P<0.05 . The serum LP a and OPN had negative correlation with LVEF and CI. Interestingly the IRF 4 mRNA had positive correlation with LVEF and CI P<0.05 . Conclusion The abnormal expression of serum LP a OPN and IRF 4 mRNA in DHVD patients is an important influencing factor of DHVD and has high application value in the diagnosis and evaluation of DHVD.

KEY WORDS Degenerative heart valve disease Lipoprotein a Osteopontin Interferon regulatory factor 4 Cardiac function Diagnosis

Degenerative heart valve disease DHVD

1.2 DHVD 1.2.1

1.2.1 3 000 r/min 5 mL 3 mL 10 min

4.5 LP a OPN

Lipoprotein a LP a Osteopontin 2 mL Trizol IRF 4

OPN 4 Interferon regulatory factor 4 IRF 4

6.8 DHVD LP a OPN IRF 4 DHVD

10

1 1

1.1 120 DHVD 38 60

2016 1 2018 12 120 3

DHVD 22 1.2.3

P>0.05 DHVD LP a OPN IRF 4 mRNA LP

9 DHVD a OPN IRF 4 mRNA DHVD 3 LP a

OPN IRF 4 mRNA 3

3 Left ventricular ejection fraction LVEF Cardiac index CI LP a OPN IRF 4 LVEF CI

1.3

SPSS 22.0

n

%

χ^2

$x \pm s$

t

Logistic

Pearson

Receiver oper

ating characteristic ROC

P<0.05

2

2.1

LBP HSP70 DcR3

1 2 1

ARDS 30d

92 ARDS 64

28 LBP HSP70 DcR3 SOFA

II APACHE II 7

LBP DcR3 HSP70 SOFA APACHE II P<

Q05 7 P<Q05 LBP DcR3 SOFA

APACHE II HSP70 SOFA APACHE II P<Q05 7 HSP70AUC

Q.830 > 7 LBP Q.806 > 7 DcR3 Q.766 LBP HSP70 DcR3

P<Q05 LBP HSP70 DcR3 ARDS

ARDS

70 3 ROC

The value of serum LBP HSP70 DcR3 levels in predicting the outcome of patients with acute respiratory distress syndrome

MA Lingling¹ YANG Qiuwei² KONG Bianduo¹

1. Department of respiratory medicine Luoyang first people s hospital Luoyang Henan China 471000

2. Department of endocrinology Luoyang first people s hospital Luoyang Henan China 471000

ABSTRACT Objective To investigate the value of serum lipopolysaccharide binding protein LBP heat shock protein 70 HSP70 and trap receptor 3 DcR3 levels in predicting the outcome of patients with acute respiratory distress syndrome ARDS . Methods 92 patients with ARDS admitted to our hospital from May 2017 to May 2019 were recruited as the research object. According to the prognosis of 30 days 64 surviving patients were selected as the survival group and 28 patients with all cause death were the death group. The serum levels of LBP HSP70 DcR3 sequential organ failure assessment sofa acute physiology and chronic health II APACHE II were compared between the two groups. Results The serum LBP and DcR3 levels were higher in the death group on the day of admission and the 7th day after admission than those in the survival group. HSP70 level was lower than that in the survival group. SOFA and APACHE II scores were higher than in the survival group P<0.05 . The difference in the survival group and the seventh day after admission was significant compared to the death group P<0.05 . The Serum LBP and DcR3 levels were positively correlated with SOFA and APACHE II scores and HSP70 was negatively corre

20182017x

1. 471000

2. 471000

E-mail 18623753239@163.com

lated with SOFA and APACHE II scores $P < 0.05$. Seventh day after admission HSP70 AUC 0.830 > LBP 0.806 > DcR3 0.766. There were significant differences in the survival curves of serum LBP HSP70 and DcR3 between the high risk groups and the low risk groups $P < 0.05$. Conclusion Serum LBP HSP70 and DcR3 levels are closely related to the severity of ARDS patients and are expected to be the main predictors of ARDS prognosis.

KEY WORDS Acute respiratory distress syndrome Lipopolysaccharide binding protein Heat shock protein 70 Trap receptor 3 ROC Lung injury

	Acute respiratory dis		1.3						
tress syndrome ARDS				3 mL		12 min	3 000 r/		
46.0% ¹	ARDS	35.0% ~	min						
		ARDS	DcR3 HSP70 LBP						
	Lipopolysacchoride Binding Pro		1.4						
tein LBP	Toll	4 Toll like receptor				LBP HSP70 DcR3			
TLR 4		³	SOFA APACHE II			SOFA			
70 Heat shock proteins 70 HSP70									6
		3 Decoy receptor3	APACHE II			1~4			
DcR3						71	>17		
			LBP HSP70 DcR3			SOFA APACHE II			
	⁴	LBP HSP70				ARDS			
DcR3	ARDS		LBP HSP70 DcR3			ARDS			
		ARDS				LBP HSP70 DcR3			
1			1.5						
1.1				SPSS 22.0					
	2017	5	2019	5	92	$\bar{x} \pm s$	t	n	
ARDS				30 d		%	χ^2	Logistic	
	64				28		Pearson		
						ROC			
						Kaplan Meier KM			
$P > 0.05$						Log Rank	$P < 0.05$		
1.2						2			
X		ARDS	⁵			2.1			
								BMI	
mmHg	200 mmHg				18		$P > 0.05$	1	
						2.2	LBP HSP70 DcR3		
							7	LBP DcR3	
							HSP70	$P < 0.05$	
							7		
							$P < 0.05$	2	

1 n %

Table 1 Comparison of 2 groups of general data n %

	n=64	n=28	t/ χ^2	P
/	35/29	16/12	0.048	0.827
BMI kg/m ²	60.70±7.09	60.28±7.27	0.260	0.796
	20.92±1.86	21.14±2.05	0.506	0.614
	53 82.81	23 82.14	0.049	0.825
	5 7.81	2 7.14	0.100	0.752
	3 4.69	2 7.14	0.001	0.983
	3 4.69	1 3.57	0.097	0.754
ng/mL	7.40±1.08	6.83±1.86	1.847	0.068
	40/24	16/12	3.058	0.080

2 LBP HSP70 DcR3 $\bar{x} \pm s$

Table 2 Comparison of serum LBP HSP70 and DcR3 levels between 2 groups $\bar{x} \pm s$

	n	LBP g/mL	HSP70 g/L	DcR3 ng/mL
	28	121.90±32.27	1.02±0.31	3.16±0.62
	64	93.37±29.06	1.33±0.34	2.59±0.58
t		4.189	4.130	4.247
P		<0.001	<0.001	<0.001
	28	102.05±34.00	1.17±0.42	3.04±1.01
	64	67.44±22.46	1.85±0.69	1.83±0.60
7 t		5.774	4.829	7.149
P		<0.001	<0.001	<0.001
	28	19.85±3.23	0.15±0.06	0.12±0.04
	64	25.93±5.10	0.52±0.21	0.76±0.25
7 t		5.809	9.136	13.431
P		<0.001	<0.001	<0.001

2.3 SOFA APACHE II

7 SOFA APACHE II

P<0.05

7

P<0.05 3

2.4 LBP HSP70 DcR3 SOFA

APACHE II

Pearson

SOFA APACHE II

SOFA APACHE II

4

4 LBP HSP70 DcR3 SOFA APACHE II

Table 4 Correlation of serum LBP HSP70 DcR3 levels with sofa and Apache II scores

	LBP		HSP70		DcR3	
	r	P	r	P	r	P
SOFA	0.471	<0.001	0.446	<0.001	0.486	<0.001
7	0.583	<0.001	-0.529	<0.001	0.537	<0.001
APACHE II	0.503	<0.001	-0.512	<0.001	0.611	<0.001
7	0.621	<0.001	-0.635	<0.001	0.702	<0.001

2.5 ARDS

ARDS

MODS

DcR3 SOFA APACHE II

Logistic

MODS

DcR3 SOFA APACHE II

P<0.05 5

2.6 LBP HSP70 DcR3 ARDS

ROC

7

LBP HSP70 DcR3 ARDS

7 HSP70 AUC 0.830 > 7

LBP 0.806 > 7 DcR3 0.766

6 1

3 SOFA APACHE II $\bar{x} \pm s$

Table 3 Comparison of sofa and Apache II scores between 2 groups $\bar{x} \pm s$

	n	SOFA			APACHE II		
		7	7	7	7	7	7
	28	8.69±1.41	8.03±2.67	0.66±0.23	18.10±1.73	17.06±4.75	1.04±0.96
	64	7.37±1.35	5.39±1.80	1.98±0.30	16.96±1.40	12.34±3.22	4.62±1.13
t		4.258	5.550	20.744	3.340	5.562	14.605
P		<0.001	<0.001	<0.001	0.001	<0.001	<0.001

5 ARDS

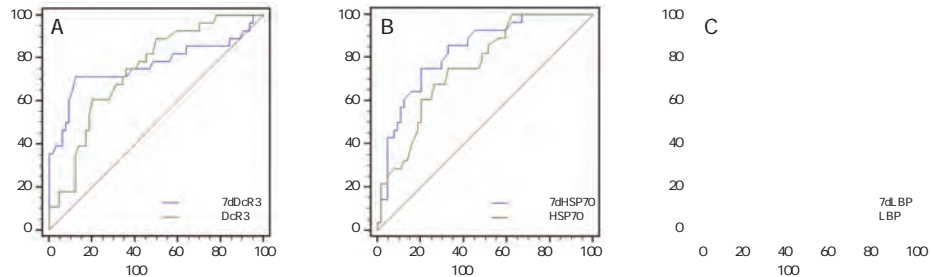
Table 5 Prognostic factors of death in patients with ARDS

	β	SE	Wald/ χ^2	OR	95%CI	P
MODS	1.553	0.420	13.670	4.725	2.711-8.235	<0.001
	1.426	0.517	7.605	7.105	2.437-7.105	<0.001
LBP	0.990	0.381	6.749	5.063	1.430-5.063	<0.001
HSP70	-0.615	0.273	5.082	0.907	0.322-0.907	0.013
DcR3	1.282	0.409	9.831	6.004	2.165-6.004	<0.001
SOFA	1.180	0.426	7.666	5.179	2.043-5.179	<0.001
APACHE II	0.973	0.312	9.723	4.081	1.715-4.081	<0.001

6 ROC

Table 6 ROC analysis results

	AUC	95%CI	Z		%	%	P
LBP	0.686	0.581-0.779	3.281	>100.30	78.57	59.38	0.001
HSP70	0.760	0.659-0.843	0.843	1.29	75.00	67.19	<0.001
DcR3	0.744	0.643-0.830	4.616	>3.02	60.71	79.69	<0.001
7 LBP	0.806	0.710-0.881	5.379	>92.28	67.86	90.62	<0.001
7 HSP70	0.830	0.737-0.900	7.413	1.45	75.00	79.69	<0.001
7 DcR3	0.766	0.667-0.848	4.095	>2.46	71.43	87.50	<0.001



A DcR3 ARDS ROC B HSP70 ARDS ROC C LBP ARDS ROC
1 ROC

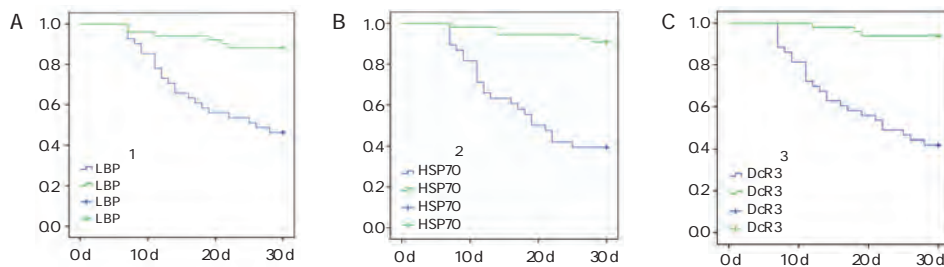
Figure 1 ROC curve

2.7

LBP HSP70 DcR3

= 0 = 1 ROC
KM

$\chi^2_1=19.438$ $\chi^2_2=31.134$ $\chi^2_3=$
30.894 P<0.001 2



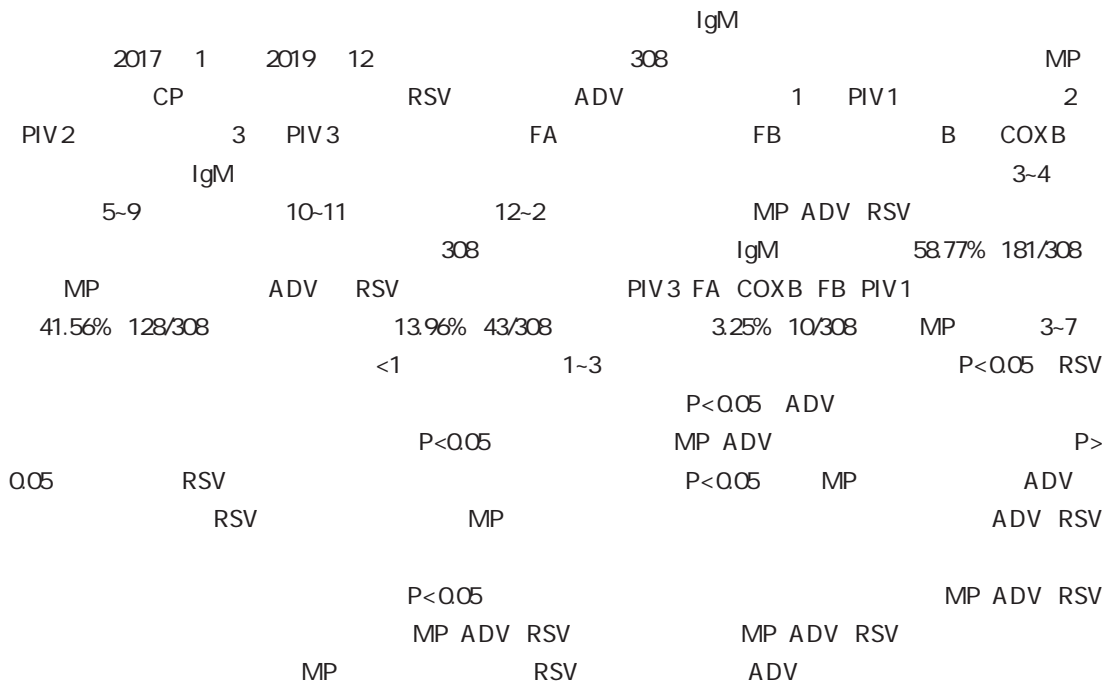
A LBP B HSP70 C DcR3

2 LBP HSP70 DcR3

Figure 2 Survival curve LBP HSP70 DcR3

3				ARDS	
	ARDS			DcR3	
				M2	
				ICAM 1 IL 8	
				Pearson	DcR3
				SOFA APACHE II	
^{6,7}	LBP I		LBP	DcR3	ARDS
	5-10 g/mL		24 h	DcR3	ARDS
	200 g/mL				
LPS	A			LBP HSP70 DcR3	
	^{8,9}		ARDS	ARDS	ARDS
			7d LBP		ARDS
LPS			ARDS		
	α TNF α		NF κ B		
			6		
1	ICAM 1		^{10,11}	1	Li H Zhou X Tan H et al. Neutrophil extracellular traps contribute to the pathogenesis of acid aspiration induced ALI/ARDS J . Oncotarget 2017 9 2 1772-1784.
	HSP70			2	
^{12,13}			¹⁴	3	J . 2016 22 6 487-491.
HSP70					
	TNF α IL 1				J . 2016 13 20 2916
				4	2918
HSP70			7		J . DcR3
	ARDS		HSP70	5	J . 2016 16 6 409-411.
			ARDS		
			HSP70		J .
					2016 96 6 404-424.
				6	Peretti M Hervochon R Loi M et al. Predictors of post pneumonectomy respiratory failure and ARDS usefulness of normalized pulmonary artery diameter J . Intensive Care Med 2018 44 8 1357-1359.
TNF α			HSP70	7	
¹⁵			7		
	HSP70		ARDS		/ J .
					2016 21 1 15-21.
DcR3	33 kD			8	THP21
FasL					MCP 1 IL 6 J .
FasL/DcR3				9	2012 4 4 258-261.
					/
			¹⁶		J . 2015 21
¹⁷			21	12	1943-1946.
	ARDS		ARDS	10	
	DcR3				J . 2015
DcR3					33 7 512-516.
Cox	ARDS			11	
30 d	DcR3 2.7 ng/mL		ARDS		CD14 LBP J .
					2019 24 6 1030-1033
					496

IgM



Detection characteristics and epidemiological trend analysis of different pathogenic antigens and IgM antibodies in children with severe pneumonia

TAO Shan

Department of Special Needs Xiamen Children s Hospital Xiamen Fujian China 361006

ABSTRACT Objective To explore the detection characteristics and epidemic trend of IgM antibody anti different pathogens in children with severe pneumonia. Methods A total of 308 children with severe pneumonia admitted to Xiamen Children s Hospital from January 2017 to December 2019 were collected. Mycoplasma pneumoniae MP Chlamydia pneumoniae CP respiratory syncytial virus RSV and Virus ADV parainfluenza virus type 1 PIV1 parainfluenza virus type 2 PIV2 parainfluenza virus type 3 PIV3 influenza A virus FA influenza B virus FB Kosa Detection of multiple pathogenic

3502Z20174016

361006

E-mail mubanpe27204@163.com

antigens such as parvovirus B19, COXs antigens and IgM antibodies were detected by immunofluorescence. According to the climatic characteristics of Xiamen, the average temperature classification method is used to divide spring (March to April), summer (May to September), autumn (10 to November) and winter (12 to February). Seasonal distribution characteristics of MP, ADV and RSV infections were observed. The children with severe pneumonia and their complications were investigated. Results: The positive rate of pathogenic IgM antibodies in 308 children with severe pneumonia was 58.77% (181/308), among which MP infection accounted for the highest proportion, followed by ADV and RSV infection, and others included PIV3, FA, COXs, FB, PIV1. The single infection rate was 41.56% (128/308), the double infection rate was 13.96% (43/308), and the multiple infection rate was 3.25% (10/308). Among MP infections, the infection rate is the highest between 3 and 7 years old (preschool age), which is significantly higher than <1 year (infancy) and 1 to 3 years (infancy); the difference is statistically significant ($P < 0.05$). Infants with RSV infection in early childhood are significantly higher than preschool age; the difference is statistically significant ($P < 0.05$). ADV infection in middle school and early childhood is significantly higher than infancy; the difference is statistically significant ($P < 0.05$). The infection rates of MP and ADV in male and female children were not statistically significant ($P > 0.05$). The RSV infection rates in male children were significantly higher than that in females, and the difference was statistically significant ($P < 0.05$). MP infection is the highest in summer, ADV infection is higher in spring and summer, and RSV infection is the highest in summer. Children with MP infection have higher rates of respiratory failure and myocardial damage complications. Various complications of children with ADV and RSV infection are also frequent. Children with multiple infections have complications such as respiratory failure, pleural effusion, myocardial damage, and abnormal liver function, significantly higher than that of a single pathogen ($P < 0.05$). Conclusion: The pathogens detected in children with severe pneumonia in our hospital are mainly MP, ADV and RSV infections, and the risk of double infection is high. Summer is the high risk season for MP, ADV and RSV infection. MP, ADV, RSV infection is related to the season.

imP# RSV ted in R

Respiratory syncytial virus pneumonia RSV

Adenovirus ADV 1 Parainflu

enza virus type 1 PIV1 2 Parain

fluenza virus type 2 PIV2 3

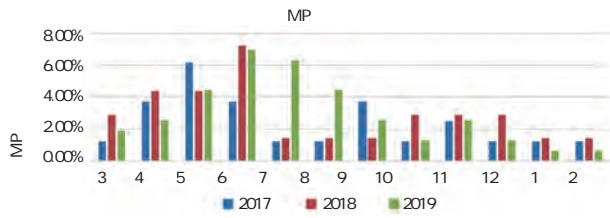
Parainfluenza virus type 3 PIV3

influenza A FA influenza B

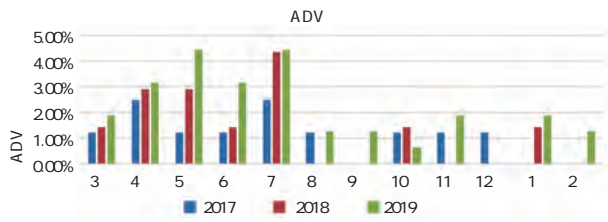
FB B Coxsackie b virus COXB

IgM 0 U•?•hÑ=2h0Û "h%T ÷pD@e DWNtp,8yEAp7 0'UG4 © 10)Aÿ 7 + „h %6%Ä

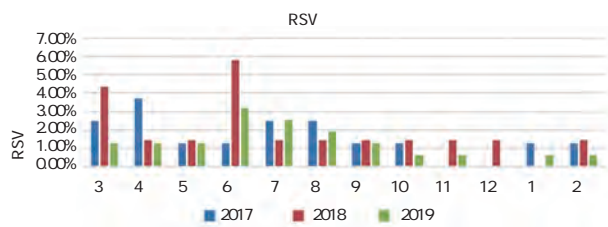
EUROStar III Plus



1 MP
Figure 1 Severe pneumonia MP infection in different seasons



2 ADV
Figure 2 Severe Pneumonia ADV Infection in Different Season



3 RSV
Figure 3 Severe pneumonia RSV infection in different seasons

2.5

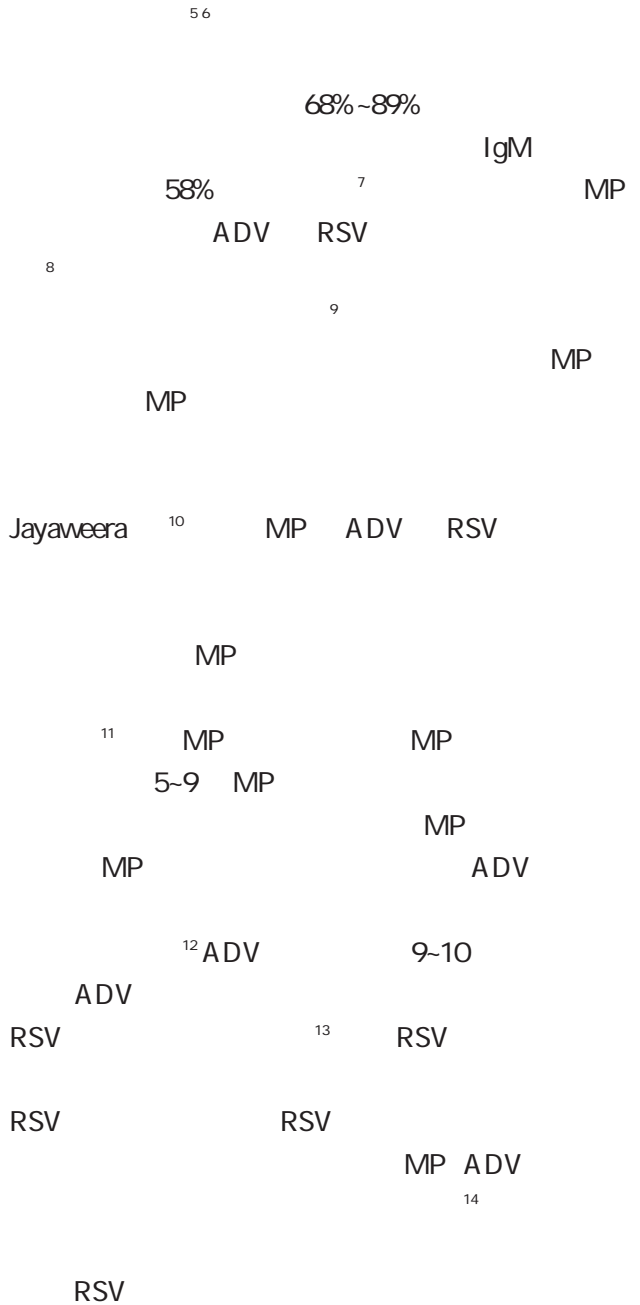
RSV

P<0.05

4

	n	
MP	103	0
ADV	62	
RSV	55	
	10	
χ^2		
P		

3



SAA sTREM 1 CRP/PAB SP

CRP / PAB A SAA 1 sTREM 1 C
SP 82 80
21 61 1 3 5 7 d
SAA sTREM 1 SAA sTREM 1 CRP/PAB
ROC 3
SAA sTREM 1 CRP/PAB 3
3d SAA sTREM 1 CRP/PAB V SAA #) B 3 # 4@ sTREM 1 3 4

" a@ P
7X

20170521

050031

E-mail hnzzz200@yeah.net

levels of SAA sTREM 1 and CRP/PAB in patients with severe infection and mild infection were compared and the relationship between the three and the degree of infection was analyzed. Results The serum SAA sTREM 1 CRP/PAB ratio reached a peak at 3 days postoperatively in the infected group and was higher than the uninfected group at 3 5 7 days postoperatively P<0.05 serum SAA was positively correlated with sTREM 1 and CRP/PAB ratio at the third days after surgery and sTREM 1 was positively correlated with CRP/PAB ratio P<0.01 the area under the ROC curve of serum SAA sTREM 1 CRP/PAB combined diagnosis of pulmonary infection after surgery was 0.876 serum SAA sTREM 1 and CRP/PAB ratios in patients with severe infection were higher than those in patients with mild infection at the third day after surgery P<0.05 serum SAA sTREM 1 and CRP/PAB ratios were positively correlated with the degree of infection P<0.05 . Conclusion The level of serum SAA sTREM 1 and the ratio of CRP/PAB were increased in SP patients with pulmonary infection after upper abdominal general anesthesia and it is closely related to the severity of infection and has a high diagnostic value in postoperative pulmonary infections which can provide theoretical basis for clinical diagnosis and disease evaluation.

KEY WORDS Amyloid A C reactive protein Prealbumin Schizophrenia Pulmonary infection

Schizophrenia SP	46.01±5.77	18-21 kg/m ²
SP	20.96±0.91 kg/m ²	SP
SP		
SP		
SP	1.2	
SP	1.2.1	
SP	A	6-8 mL/kg
Serum amyloid A SAA	ViewT 8	Bene
1 Soluble triggering receptor expressed on myeloid cells 1 sTREM 1	A 2000xp	Aspect
	tral index BIS	Bispec
	kg	10 min 1.0 g/
	H 12070534	
45	0.4 g·kg ⁻¹ ·h ⁻¹	
C C reactive protein CRP	0.05 mg/kg	3-5 g/kg
6	1.5-2.5 mg/kg	0.15 mg/kg
CRP/PAB	1-2L/min	8-10 mL/kg
SP	1 2	10-15 /min
	P _{ET} CO ₂ 35-40mmHg	
1	2-6 mg·kg ⁻¹ ·h ⁻¹	0.1-0.3 g·kg ⁻¹ ·h ⁻¹
1.1		1%~3%
	0.1 mg·kg ⁻¹ ·h ⁻¹	
2016 7		
7		
2019 7		
SP 82	BIS 40-55	
	1.2.2	
21		
61		
45	min	2 mL 15
35		SAA PAB
31-61		

sTREM 1 P>

0.05 1

1.3

1 3 5 7 d SAA
sTREM 1 CRP/PAB 3 d

Table 1 Comparison of basic in 2 groups n % $\bar{x} \pm s$

SAA sTREM 1 CRP/PAB
3 d SAA sTREM 1 CRP/PAB
SAA sTREM 1 CRP/PAB

	n=21	n=61	χ^2/t	P
	40.31±5.33	41.10±5.16	0.600	0.550
/	12/9	34/27	0.013	0.911
			0.010	0.919
	13 61.90	37 60.66		
	8 38.10	24 39.34		

sTREM 1 CRP/PAB

1.4

SPSS 22.0 n
% χ^2 $\bar{x} \pm s$
t Pearson 3

	h	min		
kg/m ²	21.46±1.33	20.96±1.22	1.583	0.117
	2.49±0.46	2.53±0.50	0.322	0.748
	133.12±31.64	129.87±29.55	0.427	0.671

d SAA sTREM 1 CRP/PAB
P<0.05

2.2 SAA sTREM 1 CRP/PAB
1 d SAA sTREM 1 CRP/PAB
P>0.05

2

3 d SAA sTREM 1 CRP/PAB

2.1

3 5 7 d P<0.05

2

Table 2 Serum SAA sTREM 1 and CRP/PAB ratios $\bar{x} \pm s$

	n	1 d	3 d	5 d	7 d
SAA mg/L	21	35.42±6.28	64.11±21.37	51.04±15.24	40.78±10.07
	61	37.27±8.41	40.06±13.30	24.07±7.69	13.71±4.10
t		0.922	5.899	10.533	17.366
P		0.359	<0.001	<0.001	<0.001
sTREM 1 ng/mL	21	206.29±57.41	267.53±60.04	218.49±50.71	170.56±41.25
	61	202.44±52.09	210.14±53.30	174.06±38.46	132.02±29.14
t		0.285	4.120	4.195	4.674
P		0.777	<0.001	<0.001	<0.001
CRP/PAB	21	0.10±0.04	0.30±0.10	0.23±0.07	0.15±0.04
	61	0.09±0.03	0.12±0.04	0.07±0.02	0.04±0.01
t		1.206	11.696	16.194	19.949
P		0.232	<0.001	<0.001	<0.001

2.3 3 d SAA sTREM 1 CRP/PAB

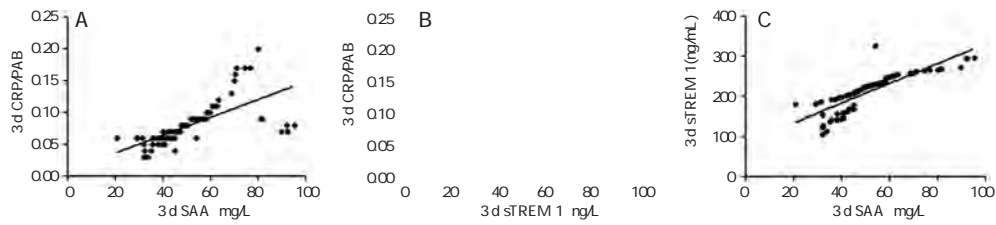
2.4 3 d SAA sTREM 1 CRP/PAB

Pearson 3 d SAA $r_1=0.845$
 $r_2=0.671$ sTREM 1 CRP/PAB

SAA sTREM 1 CRP/PAB
AUC 0.876 SAA 0.768

sTREM 1 $r=0.784$ CRP/PAB P<
0.01 1

sTREM 1 0.701 CRP/PAB 0.786 P<0.01 3
2



A SAA CRP/PAB B sTREM 1 CRP/PAB C SAA sTREM 1
1 3d SAA sTREM 1 CRP/PAB

Figure 1 Correlation between serum SAA sTREM 1 and CRP/PAB ratios at 3 days after surgery

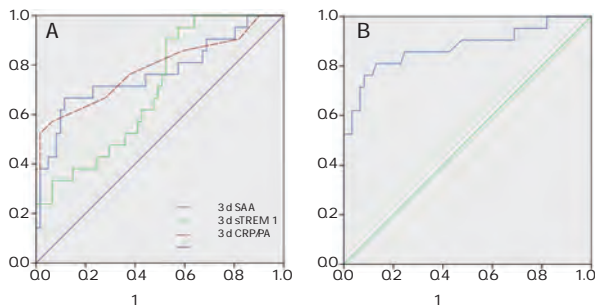
3
Table 3 Diagnostic value

	AUC	95%CI	%	%
SAA	0.768	0.662-0.854	>58.4	66.67
sTREM 1	0.701	0.590-0.797	>210.3	90.48
CRP/PAB	0.786	0.682-0.869	>0.1	52.38
	0.876	0.785-0.939	-	76.19

4
SAA sTREM 1 CRP/PAB
 $\bar{x} \pm s$

Table 4 Comparison of serum SAA sTREM 1 CRP/PAB ratios in patients with different infection $\bar{x} \pm s$

	n=8	n=13	t	P
SAA mg/L	73.96±17.03	58.05±13.29	2.396	0.027
sTREM 1 ng/mL	288.85±40.16	254.41±31.22	2.204	0.040
CRP/PAB	0.35±0.07	0.27±0.04	3.355	0.003



A SAA sTREM 1 CRP/PAB ROC
B SAA sTREM 1 CRP/PAB ROC

2 ROC
Figure 2 ROC curve

2.5 SAA sTREM 1
CRP/PAB

3 d

8

1 d

SAA

13 SAA sTREM 1
CRP/PAB

P<0.05 4

SAA

SAA mRNA

T

2.6 SAA sTREM 1 CRP/PAB

IL 17 IL 23

13

SAA

Spearman

SAA r=0.512

sTREM 1 r=0.0473 CRP/PAB r=0.608

P<

3 d

SAA

0.05

SAA N
ty lipoprotein HDL
A2l ApoA2l

High densi

HDL
SAA/HDL

Cells 1 TREM 1 Dampens Proinflammatory Cytokine Se
cretion by Lamina Propria Cells from Patients with IBD J .
Inflamm Bowel Dis 2016 22 8 1803 1811.

6

CRP/ALB

J .

2016

SAA ¹⁴

23 6 630 632

SAA

7

Korean Neuropsychiatric Association. Korean Guidelines for
the Pharmacological Treatment of Social Anxiety Disorder
Initial Treatment Strategies

¹⁵

SAA

23

sTREM 1 TREM 1

^{16 17}

sTREM 1

PAB

CRP

SAA sTREM 1 CRP/

PAB

SP

SAA sTREM 1

CRP/PAB

1 Cloutier M Aigbogun MS Guerin A et al. The Economic
Burden of Schizophrenia in the United States in 2013 J . J
Clin Psychiatry 2016 77 6 764 771.

2 J . MECT
2019 41 2 118 120

3 J .
2019 39 3 268
271.

4 A J .
2019 25 4 466 470

5 Brynjolfsson SF Magnusson MK Kong PL et al. An Anti
body Against Triggering Receptor Expressed on Myeloid

TSP 1 PDGF

1 2

1 TSP 1 PDGF
 2017 3 2019 2 65 ICH
 Rankin n=37
 Logistic
 90 d 5 n=23
 NIHSS P<0.05
 Logistic OR=1.275 95%CI 1.052-1.545 OR=1.551 95%CI 1.219-
 1.974 OR=1.368 95%CI 1.124-1.664 NIHSS OR=2.537 95%CI 1.109-5.802
 TSP 1 OR=2.659 95%CI 1.202-5.881 PDGF OR=3.086 95%CI 1.324-7.197 6
 P<0.05 ROC TSP 1 121.23 ng/mL
 78.26% 78.38% AUC 0.877 95%CI 0.782-0.971 PDGF
 369.34 ng/L 73.91% 70.27% AUC 0.778 95%CI 0.638-0.918
 0.881-1.000 86.96% 67.57% AUC 0.943 95%CI
 NIHSS TSP 1 PDGF
 TSP 1 PDGF
 1

Clinical value of serum TSP-1 and PDGF in evaluating short-term prognosis in patients with intracerebral hemorrhage

GAO Yangyang¹ LI Jieng²

1. Department of Neurology Bayannaer Hospital Bayannaer Inner Mongolia China 015000

2. Department of Neurology Bayannaer Hospital Bayannaer Inner Mongolia 015000

ABSTRACT Objective To study the clinical value of serum TSP 1 and PDGF in evaluating short term prognosis in patients with intracerebral hemorrhage. Methods 65 cases of patients with intracerebral hemorrhage ICH from March 2017 to February 2019 in our hospital were retrospectively analyzed. After 90 days of follow up 5 patients withdrew from the study because of their personal reasons. The patients were divided into favorable outcome group n=37 and unfavorable outcome group n=23 depending on modified Rankin scale scores. The basic information and treatment of patients in the two groups were compared using single factor analysis and the significantly different single factors were analyzed by non conditional logistic regression analysis. Finally the dangerous factors for poor prognosis were established. Results There were significant differences in body mass index hypertension hematoma volume NIHSS score pulmonary

201608A036

1. 015000

2. 015000

E-mail laxiong954@163.com

infection broken ventricle and fasting blood glucose between the two groups. Logistic regression analysis show that hypertension OR=1.275 95%CI 1.052-1.545 fasting blood glucose OR=1.551 95%CI 1.219-1.974 hematoma volume OR=1.368 95% CI 1.124-1.664 NIHSS score OR=2.537 95% CI 1.109-5.802 TSP 1 OR=2.659 95% CI 1.202-5.881 and PDGF OR=3.086 95% CI 1.324-7.197 are independent prognostic factors of intracerebral hemorrhage. $H^2 = 0.52$ $I^2 = 91.52$ in blood

1.6

SPSS 25.0

$x \pm s$ t n % χ^2 Logistic P<

0.05

2

2.1

NIHSS

P<0.05

1

2.2

TSP 1

PDGF

TSP 1 PDGF

P<0.05

2

2.3

Logistic

90d

Logistic

Logistic

NIHSS

TSP 1

PDGF 6

P<0.05

3

2.4

TSP 1

PDGF

X

1

Y

ROC

1

ROC

TSP 1

121.23 ng/

mL PDGF

369.34 ng/L

3

ICH

9

ICH

#

8 1

2

TSP 1 PDGF $\bar{x} \pm s$

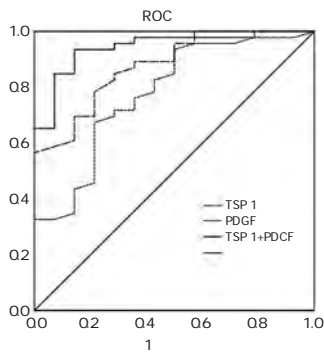
Table 2 Comparison of serum TSP 1 PDGF value between the 2 groups $\bar{x} \pm s$

	n	TSP 1 ng/mL	PDGF ng/L
	37	102.47±18.65	341.34±32.59
	23	165.34±10.76	421.32±52.60
t		16.548	8.205
P		<0.001	<0.001

3 Logistic

Table 3 Result of logistic regression

	B	S.E	Wald	P	OR	95%CI
	0.243	0.098	6.148	0.013	1.275	1.052-1.545
	0.439	0.123	12.739	<0.001	1.551	1.219-1.974
	0.313	0.100	9.797	0.002	1.368	1.124-1.664
NIHSS	0.931	0.422	4.867	0.027	2.537	1.109-5.802
TSP 1	0.978	0.405	5.831	0.016	2.659	1.202-5.881
PDGF	1.127	0.432	6.806	0.009	3.086	1.324-7.197
	-0.564	0.121	21.726	<0.001	-	-



1 Logistic ROC

Figure 1 ROC curve of the prediction model based on Logistic regression analysis

Logistics

NIHSS ICH

14

15

16

ICH

NIHSS

ICH

ICH

17

TSP 1

18

ICH TSP 1

19

PDGF

α

PDGF

PDGF

20

ICH

ICH

NIHSS TSP 1 PDGF

PDGF

TSP 1

1 Li W Jin C Vaidya A et al. Blood pressure trajectories and the risk of intracerebral hemorrhage and cerebral infarction J .Hypertension 2017 70 3 508 514.

2 Hung LC Sung SF Hsieh CY et al. Erratum to Validation of a novel claims based stroke severity index in patients with intracerebral hemorrhage J Epidemiol 27 1 2017 24 29 J . J Epidemiol 2017 27 9 451 453.

3 MMP 9 TIMP 1 J . 2017 17 3 373 375.

4 Kim DH Lim H Lee D et al. Thrombospondin 1 secreted by human umbilical cord blood derived mesenchymal stem cells rescues neurons from synaptic dysfunction in Alzheimer s disease model J . Sci Rep 2018 8 1 354.

5 Roswall P Bocci M Bartoschek M et al. Microenvironmental control of breast cancer subtype elicited through paracrine platelet derived growth factor CC signaling J . Nature Medicine 2018 24 4 463 473.

6

2014 J .
 2015 48 6 435 444.
 7 Georgievski Brkic B Savic M Nikolic D et al. Evaluation of functional outcome measured by modified Rankin scale in rtPA treated patients with acute ischemic stroke J . Arch Ital Biol 2016 154 4 125 132
 8 Kwah LK Diong J. National Institutes of Health Stroke Scale NIHSS J . J Physiother 2014 60 1 61.
 9 J .
 2015 17 2 214 215.
 10 Giakoumettis D Alexiou GA Vrachatis DA et al. Anti thrombotic treatment management in patients with intracerebral hemorrhage reversal and restart J . Curr Pharm Des 2017 23 9 1392 14 5.
 11 Spina S Marzorati C Vargiolu A et al. Intracerebral hemorrhage in Intensive Care Unit early prognostication fallacies A single center retrospective study J . Minerva Anestesiol 2018 84 5 572 581.
 12 TSP1/2 MMP2/9 J .
 2017 42 12 1649 1652
 13 Cates CC Arias AD Wong LSN et al. Regression/Eradication of gliomas in mice by a systemically deliverable ATF5 dominant negative peptide J . Oncotarget 2016 7 11

12718 12730.
 14 Roh D Sun CH Schmidt JM et al. Primary intracerebral hemorrhage a closer look at hypertension and cerebral amyloid angiopathy J . Neurocrit Care 2018 29 1 77 83.
 15 J .
 2019 11 3 224 228.
 16 J .
 2018 31 5 328 331.
 17 NIHSS
 J . 2019 25 5 755 759.
 18 Zhang J Li CL Zheng YN et al. Inhibition of angiogenesis by arsenic trioxide via TSP 1 TGF β1 CTGF VEGF functional module in rheumatoid arthritis J . Oncotarget 2017 8 43 73529 73546.
 19 Yang AL Zhou HJ Lin Y et al. Thrombin promotes the expression of thrombospondin 1 and 2 in a rat model of intracerebral hemorrhage J . J Neurol Sci 2012 323 1 141 146.
 20 Burchell SR Tang J Zhang JH. Hematoma expansion following intracerebral hemorrhage mechanisms targeting the coagulation cascade and platelet activation J . Curr Drug Targets 2017 18 12 1329 1344.

486

LP a OPN IRF 4 mRNA
 DHVD DHVD
 DHVD
 1 Chandrasekhar J Dangas G Mehran R. Valvular Heart Disease in Women Differential Remodeling and Response to New Therapies J . Curr Treat Options Cardiovasc Med 2017 19 9 74.
 2 Xu ZJ Pan J Zhou Q et al. Analysis of the prevalence and risk factors of preoperative angiography confirmed coronary artery stenosis in patients with degenerative valvular heart disease J . Zhonghua Xin Xue Guan Bing Za Zhi 2017 45 4 837 842.
 3 J . 2018 2 1 129 130.
 4 J .
 2017 45 10 837 842
 5 Caldeira D David C Costa J et al. Non vitamin K antagonist oral anticoagulants in patients with atrial fibrillation and valvular heart disease systematic review and meta analysis J . Eur

Heart J Cardiovasc Pharmacother 2018 4 2 111 118
 6 B J .
 2016 31 5 459 462
 7 a A2 J .
 2016 32 4 46 50
 8 J . 2019 23 4 646 650.
 9 2014 J .
 2015 4 3 8 11.
 10 J .
 2017 14 11 4 7.
 11 a J . 2019 19 5 698 701.
 12 Danny T. M. Leung Pak Leong Lim Tak Hong Cheung et al. Osteopontin Fragments with Intact Thrombin Sensitive Site Circulate in Cervical Cancer Patients J . Plos One 2016 11 8 e0160412
 13 mRNA J . Th9 2019
 40 8 18 22.
 14 J . 4
 2016 22
 5 392 397.

TNF α PCT IL 1 β

1 2 2

PCT 1 β IL 1 β α TNF α
80 2015 1 2017 12
160
TNF α PCT IL 1 β 3
1 TNF α PCT IL 1 β
P>0.05 1 3 5 TNF α PCT IL 1 β P<0.05 β R ϕ

201806115

1. 473000
2. 473000

E-mail 545089160@qq.com

TNF α PCT IL 1 β 1 5 1 3 5 TNF α PCT IL 1 β
 1 3 5
 TNF α PCT IL 1 β P<
 P>0.05 0.05 1

Table 1 Comparison of dynamic trends of serum TNF α PCT IL 1 β in two groups of women $\bar{x} \pm s$

	TNF α ng/mL			PCT g/mL			IL 1 β pg/mL		
	1	3	5	1	3d	5	1	3	5
	1.55 \pm 0.32	2.67 \pm 0.69	3.04 \pm 0.55	0.81 \pm 0.27	2.23 \pm 0.69	2.52 \pm 0.77	0.81 \pm 0.27	2.23 \pm 0.69	2.52 \pm 0.77
	1.48 \pm 0.29	1.50 \pm 0.31	1.44 \pm 0.38	0.78 \pm 0.24	0.63 \pm 0.20	0.47 \pm 0.15	0.78 \pm 0.24	0.63 \pm 0.20	0.47 \pm 0.15
t	1.702	18.125	26.334	0.875	27.184	32.528	0.875	27.184	32.528
P	0.090	0.000	0.000	0.382	0.000	0.000	0.382	0.000	0.000

2.2 3 TNF α PCT IL 1 β 7
 ROC 3 TNF α PCT IL 1 β 5%
 PCT TNF α IL 1 β 8
 AUC 0.888
 0.766 0.751 1.26 g/
 mL 2.00 ng/mL 2.51 pg/mL P<0.05 1 C 6
 C

40%
9

Tumor Necrosis Factor TNF

TNF α TNF β

TNF α

TNF α

PCT

PCT

PCT

3

β hCG

β hCG P
 2018 1 2019 10 81
 MOT 79 β hCG P MOT
 VAS FT4 FT3 TSH
 β hCG P VAS MOT β hCG P
 P<0.05 FT3 FT4
 VAS TSH MOT P<0.05 β hCG
 TSH MOT FT3 FT4 VAS P<0.05 P
 TSH MOT FT3 FT4 VAS P<0.05
 β hCG P P<0.05 β hCG P
 MOT
 β

Correlation of serum β - hCG and progesterone expression with thyroid function and motilin in patients with hyperemesis gravidarum

LI Feng LU Haifeng CUI Bingyi QIN Chunyi

Clinical laboratory Tangshan hospital of traditional Chinese medicine Tangshan Hebei China 063000

ABSTRACT Objective To investigate the expression of serum β human chorionic gonadotropin β hCG and progesterone P in patients with hyperemesis gravidarum and the correlation with thyroid function and motilin MOT . Methods From January 2018 to October 2019 81 pregnant women with severe vomiting in hospital were selected as the study group and 79 normal pregnant women were selected as the control group. The serum β hCG P MOT levels hyperemesis gravidarum VAS score thyroid function free thyroxine FT4 free triiodothyronine FT3 and thyroid stimulating hormone TSH were measured and compared between the two groups. The correlations of serum β hCG and P levels with VAS score and thyroid function and MOT were analyzed. Results The serum β hCG level in the study group was higher than that in the control group and the serum P level was lower than that in the control group P<0.05 . Serum FT3 and FT4 levels and VAS scores in the study group were higher than those in the control group and serum TSH and MOT levels were lower than those in the control group P<0.05 . There was a significant negative correlation between serum β hCG levels and serum TSH and MOT levels and a significant positive correlation with se

2018322

063000

E-mail hblf147258@163.com

2

2.1

P>0.05

2.2

β hCG P

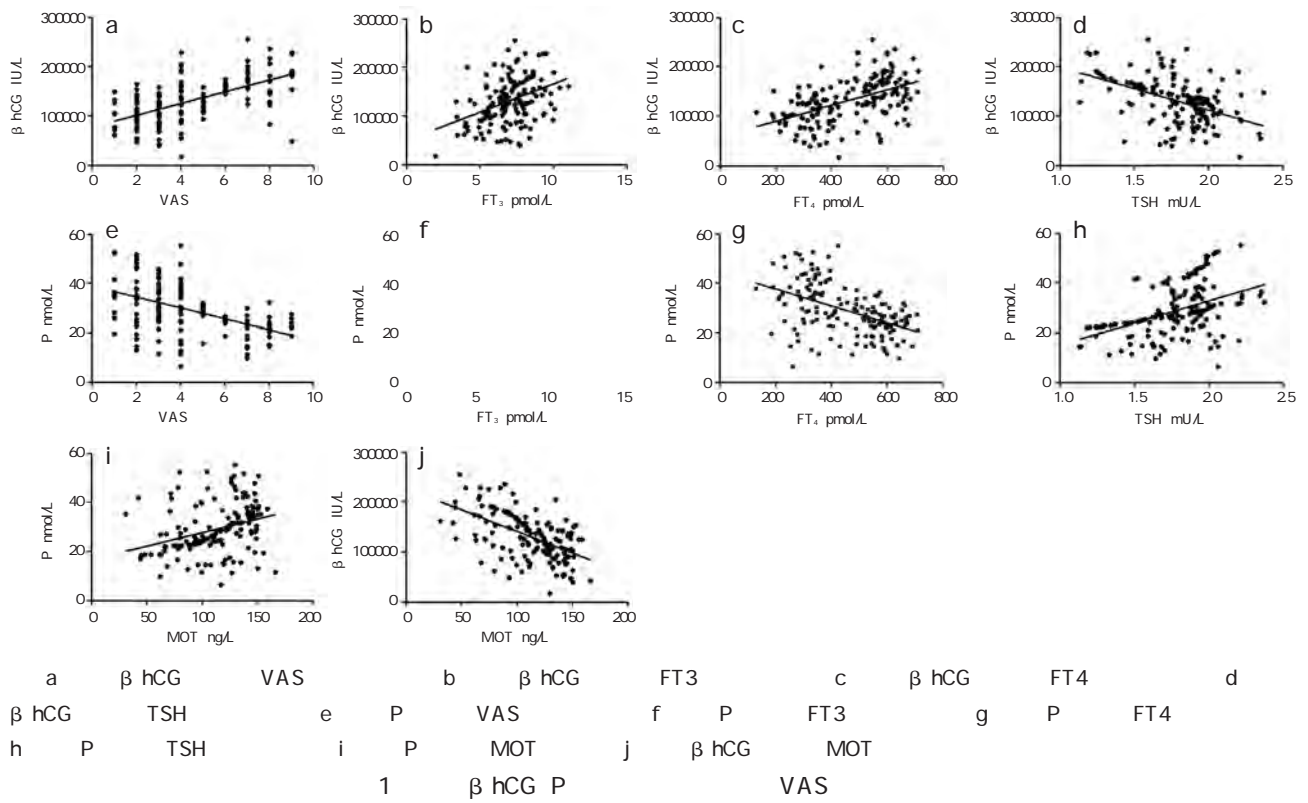


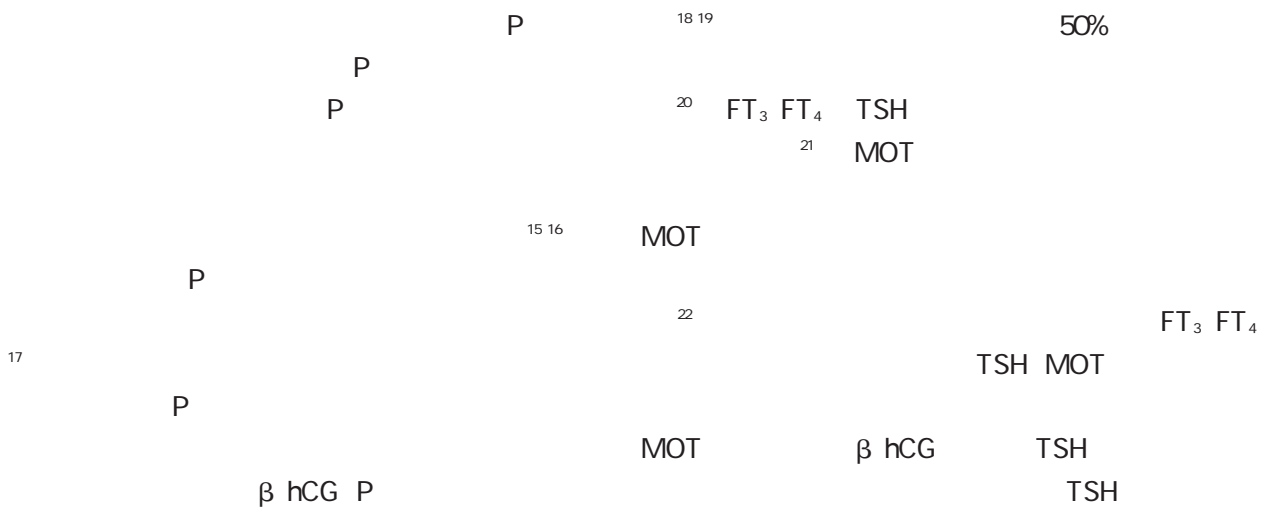
Figure 1 Correlation of serum β hCG P levels with thyroid function and VAS score

Table 4 Relationship between serum β hCG P and hyperemesis gravidarum

	β	S.E.	Wald/ χ^2	OR	95%CI	P
β hCG	1.291	0.462	7.807	3.636	1.278-10.344	<0.001
P	1.169	0.454	6.633	3.220	1.071-9.679	<0.001

β hCG

β hCG P



FT₄
22 23
β hCG
FT₃ FT₄
TSH MOT

24 25
β hCG P
MOT TSH FT₃ FT₄
β hCG P

β hCG P
MOT

1 Fejzo MS Myhre R Colodro Conde L et al. Hyperemesis gravidarum associated with RYR2 genetic analysis of hyperemesis gravidarum reveals association with intracellular calcium release channel RYR2 J . Mol Cell Endocrinol 2017 439 1 308 316.

2 2015 J . 2015 50
11 801 804.

3 Patel BG Rudnicki M Yu J et al. Progesterone resistance in endometriosis origins consequences and interventions J . Acta Obstet Gynecol Scand 2017 96 6 623 632.

4 J .
2018 26 6 67 69.

5 Boelig RC Barton S Saccone G et al. Interventions for treating hyperemesis gravidarum J . Cochrane Database Syst Rev 2016 5 5 CD010607.

6 J . 2015 7 2
57 59.

7 Kos D Raeymaekers J Remoortel AV. Electronic visual analogue scales for pain fatigue anxiety and quality of life in people with multiple sclerosis using smartphone and tablet a reliability and feasibility study J . Clin Rehabil 2017 31 9 1215 1225.

8 β
J . 2018 39 17 2021 2023.

9 Günaydın B Özek A Özterlemez NT et al. Unique Liver Disease of Pregnancy Requiring Anaesthesia Support A Case with Severe Hyperemesis Gravidarum J . Turk J Anaesthesiol Reanim 2017 45 4 234 236.

10 O Donnell A Mcparlin C Robson SC et al. Treatments for hyperemesis gravidarum and nausea and vomiting in pregnancy a systematic review and economic assessment J . Health Technol Assess 2016 20 74 13 268.

11 β
J .
2018 10 5 307 314 346.

12 J .
2017 23 2 126 129.

13 Beyazit F1 Öztürk FH Pek E et al. Evaluation of the hematologic system as a marker of subclinical inflammation in hyperemesis gravidarum A case control study J . Ginekol Pol 2017 88 6 315 319.

14 J . 2018 37 1 51 55.

15 HCG E₂ P CA125
J .
2019 27 8 1051 1054.

16 β CA199
J .
2018 17 14 1553 1556.

17 Oktem O Akin N Bildik G et al. FSH Stimulation promotes progesterone synthesis and output from human granulosa cells without luteinization J . Hum Reprod 2017 32 3 643 652.

18 J . 2019 34 8 574 577.

19 Stagnaro Green A. Second trimester levothyroxine treatment for subclinical hypothyroidism or hypothyroxinaemia of pregnancy does not improve cognitive outcomes of children J . Evid Based Med 2017 22 4 149.

20 J .
2018 16 18 37 39.

21 J . 2016 25 6
411 414.

22 J . 2019 38 9
170 173.

23 hCG
J . 2017 12 19 65 66.

24 O Donnell A Mcparlin C Robson SC et al. Treatments for hyperemesis gravidarum and nausea and vomiting in pregnancy a systematic review and economic assessment J . Health Technol Assess 2016 20 74 1392 1401.

25 J . 2016 26 24 17 17.

CysC α1 MG β2 MG

C CysC α1 α1 MG β2 β2 MG
 COPD 2013 1
 2016 8 206 COPD SPO2 64 86
 56 50 4 CysC α1 MG β2 MG Scr
 BUN ROC CysC α1 MG β2 MG COPD COPD
 Pearson CysC BUN α1 MG β2 MG Scr COPD
 CysC α1 MG β2 MG COPD Scr BUN P>0.05
 Cys C P<0.05 α1 MG β2 MG
 P<0.05 CysC α1 MG β2 MG P<0.05
 ROC CysC α1 MG β2 MG COPD 0.810 0.743 0.812 0.915
 0.936 1.74 mg/L 12.22 mg/L 2.34 mg/L 0.806 0.726 0.794 0.903
 0.795 0.705 0.782 0.903 CysC α1 MG β2 MG 0.864 0.832 0.812
 1.62 mg/L 12.08 mg/L 2.58 mg/L 0.824 0.816 0.808 0.914
 0.786 0.774 0.762 0.903 CysC α1 MG β2 MG COPD
 C α1 β2

The detection and significance of CysC α1-MG β2-MG of early kidney injure in patients with chronic obstructive pulmonary disease

LI Haiyan

Dongying New District Hospital Dongying Shandong China 257000

ABSTRACT Objective To investigate the detection value of serum cystatin C CysC α1 microglobulin α1 MG and β2 microglobulin β2 MG in chronic obstructive pulmonary disease COPD and correlation of the early stage of hypoxia kidney injury. Methods A total of 206 elderly patients with COPD from January 2013 to August 2016 in our hospital were selected as the study object. Based on the blood gas analysis they were divided into COPD with mild moderate and severe hypoxia groups. A total of 50 healthy people were selected as control group. The CysC α1 MG β2 MG Scr levels were detected and compared for analysis. The ROC curve was used to analyze the diagnostic value of CysC α1 MG and β2 MG on COPD and COPD combined with renal injury. Pearson correlation analysis was used to analyze the correlation between CysC BUN α1 MG and β2 MG and Scr. Results Compared with control group CysC α1

MG β2 MG levels in COPD group significantly increased and the Scr levels had no statistical significance on the difference with the control group $P > 0.05$. CysC level in mild moderate and severe hypoxia group were significantly higher than that in control group and the differences had no statistical significance $P < 0.05$ α1 MG β2 MG levels in moderate and severe hypoxia group were significantly higher than that in control group

$P < 0.05$ Comparison 0.05/α `T, r, s # E @ signd werd d the in 1 the MG in—

€ ð•U,,ð• dJ G T•Y

AUC COPD P<0.05 2.2 4 CysC α1 MG β2 MG Scr BUN CysC P>0.05 1 α1 MG β2 MG P<0.05 2.1 COPD CysC α1 MG β2 MG CysC α1 MG β2 MG Scr BUN P<0.05 COPD CysC α1 MG β2 MG Scr BUN P<0.05 CysC P<0.05 2

Table 1 Comparison of related indicators between the 2 groups $\bar{x} \pm s$

	n	Scr mol/L	BUN mmol/L	CysC mg/L	α1 MG mg/L	β2 MG mg/L
COPD	50	76.01±15.76	5.84±1.43	1.14±0.22	8.84±1.56	1.64±0.26
t	206	83.36±34.39	6.43±3.12	1.69±0.53	13.63±4.35	2.63±1.15
P		1.318	1.562	4.472	5.124	4.115
		0.231	0.128	0.013	0.004	0.021

Table 2 Comparison of related indicators between the 4 groups $\bar{x} \pm s$

	n	Scr mol/L	BUN mmol/L	CysC mg/L	α1 MG mg/L	β2 MG mg/L
	50	76.01±15.76	5.84±1.43	1.14±0.22	8.84±1.56	1.64±0.26
	64	80.58±17.43	6.36±1.61	1.37±0.41 ^a	9.54±1.85	1.93±1.35
	86	86.56±19.23	6.73±1.98	1.64±0.72 ^{ab}	12.24±1.81 ^a	2.64±1.81 ^a
	86	93.38±21.73	7.04±2.09	1.98±1.23 ^{abc}	17.42±2.79 ^{ab}	3.72±2.79 ^{ab}
F		9.677	6.379	7.240	8.660	9.275
P		0.000	0.001	0.000	0.000	0.000

2.3 CysC α1 MG β2 MG COPD ROC
 ROC CysC COPD
 0.810 1.74 mg/L
 COPD 0.806
 0.795 α1 MG 0.743
 12.22 mg/L COPD
 0.726 0.705 β2 MG
 0.812 2.34 mg/L
 COPD 0.794
 0.782 3 0.915
 0.903 0.897 1

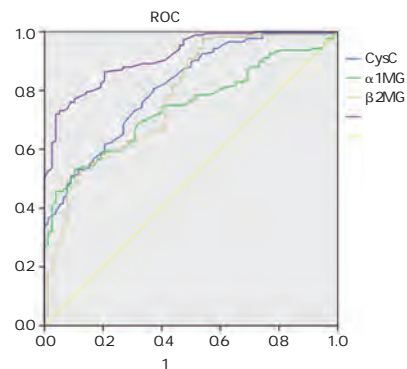


Figure 1 ROC curves of CysC α1 MG β2 MG for COPD prediction

2.4 CysC α1 MG β2 MG BUN Scr
 Pearson CysC r=0.672 P=0.011
 α1 MG r=0.415 P=0.031 β2 MG r=0.550 P=0.029
 BUN r=0.023 P=0.436 COPD
 Scr P<0.05 0.856 1.62 mg/L COPD
 0.824 0.786 α1 MG

2.5 CysC α1 MG β2 MG COPD
 ROC
 ROC CysC
 1.62 mg/L COPD
 0.824 0.786 α1 MG

AML
p53

COX 2 VEGF

			AML		2 COX 2		
		VEGF p53			2014	1	2019
1	80	AML		40			
		COX 2 VEGF p53					
		n=48	n=32		COX 2 VEGF p53		
		CNSL			ROC	COX 2 VEGF p53	
AML			COX 2 VEGF p53				
		P<0.05	COX 2 VEGF p53				
		P<0.05			IgA IgG IgM		
		P<0.05			CD3+ CD4+ CD8+ CD4+/CD8+		
			P<0.05		COX 2 VEGF p53		
		P<0.05		AML	COX 2 VEGF p53		
		P<0.05		AML			
	P<0.05	ROC	COX 2 VEGF p53		CNSL		
AUC	0.836	95% CI 0.776-0.896	0.802	95% CI 0.730-0.873	0.716	95% CI 0.639-	
0.793	0.905	95% CI 0.863-0.947	COX 2 VEGF p53		AML		
			2		p53		

Expressions of COX-2 VEGF and p53 in elderly AML patients treated with decitabine and their prognosis

WANG Zhanfang ZHANG Fangfang YANG Hai CHEN Chaohua

Department of Hematology the First People's Hospital of Pingdingshan Pingdingshan Henan China 467000

ABSTRACT Objective To investigate the expression of serum cyclooxygenase 2 COX 2 vascular endothelial growth factor VEGF and p53 protein in elderly patients with acute myeloid leukemia AML treated with decitabine and their prognostic value. Methods 80 patients with AML admitted to our hospital from January 2014 to January 2019 were selected as the study group and 40 healthy people who underwent physical examination in our hospital were selected as the control group. The levels of COX 2 VEGF p53 protein humoral immunity and cellular immunity in the study group before and after treatment and the control group were compared and the correlation of indexes were also analyzed. According to the patients

HGF-20165021358

467000

E-mail musijiu2535898@163.com

after treatment they were divided into complete remission group n=48 and incomplete remission group n=32 . The levels of COX 2 VEGF p53 protein in the two groups were analyzed. The incidence of central nervous system leukemia CNSL between the two groups was compared. The predictive value of COX 2 VEGF and p53 protein in the prognosis of AML was analyzed using the receiver operating characteristic curve ROC . Results The levels of COX 2 VEGF and p53 proteins in the study group were significantly higher than those in the control group and the difference was statistically significant P<0.05 . However after treatment the levels of COX 2 VEGF and p53 protein in the study group were significantly lower than those before treatment. The difference was statistically significant P<0.05 . After treatment the levels of humoral immune indicators IgA IgG and IgM in the study group were significantly lower than before treatment P<0.05 . After treatment the cell immune indicators of CD3+ CD4+ CD8+ and CD4+ /CD8+ in the study group were significant lower than before treatment P<0.05 . Correlation analysis indicates that there is a significant positive correlation between COX 2 VEGF and p53 proteins P<0.05 . The difference in COX 2 VEGF and p53 protein levels between AML patients in complete remission group and incomplete remission group was statistically significant P<0.05 . The difference in median survival between AML patients in complete remission group and incomplete remission group was statistically significant P<0.05 . ROC curve results showed that the area under the curve AUC of COX 2 VEGF p53 protein and combined detection in CNSL diagnosis were 0.836 95%CI 0.776-0.896 0.802 95%CI 0.730-0.873 0.716 95%CI 0.639-0.793 and 0.905 95%CI 0.863-0.947 . Conclusion The levels of serum COX 2 VEGF and p53 are of great significance for the clinical treatment effect and prognosis evaluation of elderly AML patients.

KEY WORDS Acute myeloid leukemia Old age Cyclooxygenase 2 Vascular endothelial growth factor p53 protein

acute myeloid leukemia

AML / 6 COX 2 VEGF p53
AML 1 65 AML
AML 10
AML 1
+ + 1.1
Ara c+ACR+G CSF CAG 2014 1 2019 1 80
DNA AML AML 49 31
60-76 68.8±2.4 M1 8 M2
14 M4 18 M5 31 M6 9
2 CAG 40
24 16 60-78 68.3±
COX 2 2 Cyclooxygenase 2 25 P>0.05
3
vascular endothelial growth fac AML 7
tor VEGF 60 AML MICM
VEGF M1 M2 M4 M5 M6
45 P53
p53

1.2 AML 15mg/m² d d1 d5
20mg/d d1 d4
m² q12h d1 d14
150 g q12h d1 d14
>20×10⁹/L

CAG 10mg/

CD3+ CD4+ CD8+
1.3.3

T
CD4+/CD8+

1~5

central nervous system leukemia CNSL
CNSL

2016⁸

1.3 1.3.1 COX 2 VEGF p53

5 mL
30 min 3 000 r/min 15 min
enzyme linked
immunosorbent assay ELISA COX 2 VEGF
p53

5 mL
receiver operator characteristic curve ROC
COX 2 VEGF p53 CNSL
P<0.05

2

AML 14 d 5 mL 2.1

COX 2 VEGF p53

1.3.2

14 d
IgA IgG IgM

P<0.05

P<0.05

CyFlow Partec 1

1 $\bar{x} \pm s$

Table 1 Changes of serum indicators in the 2 groups $\bar{x} \pm s$

	n=80		n=40	t	P
COX 2 ng/L	53.2±6.1	31.0±3.1	30.3±3.2 ^a	29.019	0.000
VEGF pg/mL	158.8±35.7	72.2±7.5	70.7±6.9 ^a	21.233	0.000
p53 ng/L	211.5±33.8	108.3±13.7	106.7±14.9 ^a	25.309	0.000
IgA g/L	2.3±0.9	1.5±0.7	-	4.276	0.000
IgG g/L	11.7±1.9	9.1±1.6	-	9.362	0.000
IgM g/L	1.0±0.2	0.7±0.2	-	9.487	0.000
CD3+ %	54.2±6.6	38.7±4.5	-	17.355	0.000
CD4+ %	34.2±4.3	28.8±3.2	-	9.011	0.000
CD8+ %	29.0±2.7	20.9±2.6	-	19.328	0.000
CD4+/CD8+	1.2±0.3	0.9±0.2	-	7.442	0.000

^aP<0.05

2.2 COX 2 VEGF p53 P<0.05

Table 2 Correlation analysis of COX 2 VEGF and p53 proteins with various indicators

	COX 2		VEGF		p53	
	r	P	r	P	r	P
COX 2	-	-	0.583	0.000	0.612	0.000
VEGF	0.501	0.000	-	-	-	0.000
p53	0.559	0.000	0.537	0.000	-	-

2.3 AML COX 2 VEGF Overall Survival OS P<0.05 AML OS P<

Table 3 Comparison of various indicators in different treatment outcomes of elderly AML patients $\bar{x} \pm s$

	n	COX 2 ng/L	VEGF pg/mL	p53 ng/L	OS
	48	31.5±4.4	70.3±7.7	102.3±10.4	12.6±2.7
	32	44.1±5.3	166.9±20.8	198.7±10.8	5.9±1.6
t		11.555	25.148	39.997	13.914
P		0.000	0.000	0.000	0.000

2.4 COX 2 VEGF p53 CNSL ROC 3
 ROC COX 2 VEGF p53
 CNSL AUC
 0.836 95%CI 0.776-0.896 0.802 95%CI
 0.730-0.873 0.716 95%CI 0.639-0.793 0.905
 95%CI 0.863-0.947 1

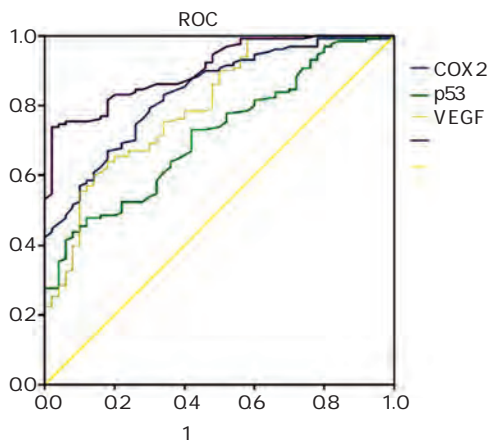


Figure 1 COX 2 VEGF and p53 predict ROC curves of CNSL

AML CAG
 GO S
 DNA DNA
 AML 9
 10
 11
 12 COX 2
 COX 2
 COX 2
 DNA

13¹⁴ COX 2
 VEGF
 AML J . Cancer Res 2019 79 6 1165 1177.

4 Jabari M Allahbakhshian FM Salari S et al. Hypoxia Inducible Factor1 A HIF1 α and Vascular Endothelial Growth Factor A VEGF A Expression in De Novo AML Patients J . Asian Pac J Cancer P. 2019 20 3 705 710.

5
 15 ALL AML CLL
 VEGF
 VEGF J . 2018 38 24 5936

6
 VEGF VEGF
 5938.

7
 p53 p53
 DNA
 p53 J . P P53
 2017 35 2

8
 16¹⁷ CAG AML COX 2
 VEGF p53
 VEGF p53
 AML COX 2
 AML
 AML
 COX 2 VEGF p53 OS
 COX 2 VEGF p53
 AML ROC
 COX 2 VEGF p53 CNSL
 AUC 3 COX 2
 VEGF p53 AML
 CNSL
 COX 2 VEGF p53
 AML
 AML
 CAG
 2019 39 20 4931 4934.

9
 10
 11
 12
 13
 15
 16
 17

2017 37 23 5858 5860.

Levine AJ. The p53 protein plays a central role in the mechanism of action of epigenetic drugs that alter the methylation of cytosine residues in DNA J . Oncotarget 2017 8 5 7228 7230.

Pan R Ruvolo V Mu Hong et al. Synthetic Lethality of Combined Bcl 2 Inhibition and p53 Activation in AML Mechanisms and Superior Antileukemic Efficacy J . Cancer cell 2017 32 6 748 760.

2019 39 22 5475

5480

/

J . 2019 27 2

390 395.

Carter BZ Mak PY Wang X et al. An ARC regulated IL1 β /Cox 2/PGE2 β catenin/ARC circuit controls leukemia microenvironment interactions and confers drug resistance in

CD40 CD40L BAFF ITP

1 2 1 1 1 1 1 1

CD40 CD40L BAFF ITP

ITP 80 100

CD40 CD40L BAFF

2 CD40 CD40L BAFF

CD40 CD40L BAFF CD40 CD40L

BAFF P<0.05 CD40 CD40L

BAFF P<0.05 ITP CD40 CD40L BAFF

r<0 P<0.05 ROC CD40 CD40L BAFF ITP

AUC>0.7 P<0.05 ITP CD40 CD40L ITP

CD40 CD40L BAFF ITP

The predictive value of peripheral blood CD40 CD40L expression and serum BAFF level on the efficacy of patients with immune thrombocytopenic purpura

YIN Fenglei¹ YIN Juan² ZHAO Fang¹ ZHANG Rui¹ LIU Jing¹ ZHANG Wei¹ LI Shuchen¹ WANG Juan¹

1. Department of Hematology Cangzhou Central Hospital Cangzhou Hebei China 061000 2. Operating Room of Cangzhou People s Hospital Cangzhou Hebei China 061000

ABSTRACT Objective To investigate the predictive value of peripheral blood CD40 CD40L expression and serum BAFF level in the treatment of immune thrombocytopenic purpura ITP patients. Methods 80 patients with ITP admitted to our hospital were recruited as the observation group. 100 healthy people who underwent physical examination in our hospital were selected as the control group. Peripheral blood CD40 CD40L expression and serum BAFF level were observed in both groups. The patients were divided into two groups according to the results of efficacy judgment. The expression of CD40 CD40L and serum BAFF in peripheral blood from the two groups were compared. Results The expression of CD40 CD40L and serum BAFF in the peripheral blood in the observation group were significantly higher than those in the control group P<0.05 . The expression of CD40 CD40L and serum BAFF in peripheral blood of patients with non re

1. 172302129 061000
2. 061000

E-mail wang_juan01@126.com

sponse group were significantly higher than those in response group $P < 0.05$. The expression of CD40, CD40L and serum BAFF in peripheral blood of patients with ITP were negatively correlated with curative effect $r < 0$, $P < 0.05$. ROC curve analysis results show that the peripheral blood CD40, CD40L and BAFF have high predictive value for ITP efficacy, all $AUC > 0.7$, $P < 0.05$. Conclusion: The peripheral blood CD40 and CD40L in patients with ITP have a high predictive value for the efficacy of ITP patients.

KEY WORDS: Bone marrow CD40, CD40L, Serum BAFF level, ITP, Curative effect

idiopathic thrombocytopenic purpura (ITP)

1.2

CD40, CD40L

4 mL

CD40 FITC, CD40L PE

10 L, R&G

PBS

Attune NxT

10 000

BAFF, 2 mL

3 000 r/min, 15 min, 0.8 mL

BAFF

Sigma

100 × 10⁹ L

30 × 10⁹ L

2, 30 × 10⁹ L

1, 2, 2

1.1

2017, 12, 2019, 3

ITP, 80

100

44, 36, 23-58, 42.23 ± 6.11

BMI, 21-29 kg/m², 26.58 ± 3.05 kg/m²

m², 55, 45, 21-59

42.22 ± 6.31, Body Mass Index, ITP, P < 0.05

dex BMI, 20-28 kg/m², 26.33 ± 2.88 kg/m²

5

2

2.1, 2, CD40, CD40L

BAFF

CD40, CD40L

BAFF

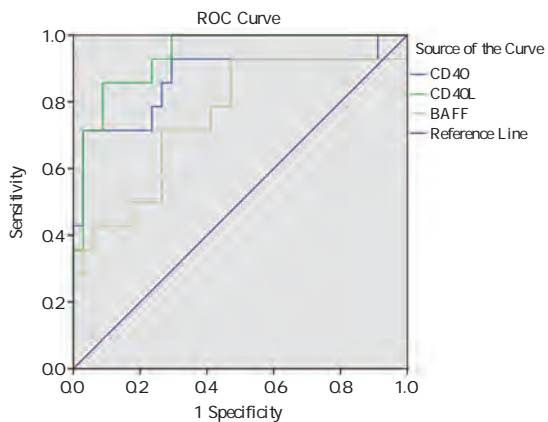
BMI, P > 0.05, P < 0.05, 1

	1	2	CD40	CD40L	BAFF	2.2	CD40	CD40L
			$\bar{x} \pm s$					
Table 1 Comparison of CD40 CD40L expression and serum BAFF levels in peripheral blood of 2 groups of patients $\bar{x} \pm s$								
			CD40	CD40L	BAFF ng/L			
			7.31±2.07	3.24±1.06	603.17±112.38	2.3	ITP	
			12.92±3.05	6.09±1.70	716.44±137.48	BAFF		
t			6.721	5.947	2.936	ITP	CD40	CD40L
P			0.000	0.000	0.005		r	-0.691
						-0.713	-0.652	P<0.05

	2	CD40	CD40L	BAFF	$\bar{x} \pm s$
Table 2 Comparison of CD40 CD40L expression and serum BAFF levels in peripheral blood of patients with different curative effects in the observation groups $\bar{x} \pm s$					
	n	CD40	CD40L	BAFF ng/L	
	56	11.63±3.73	5.61±1.14	683.08±111.88	
	24	15.92±5.09	6.88±1.25	804.07±117.65	
t		2.127	2.237	2.155	
P		0.045	0.034	0.040	

2.4 ROC

ROC	CD40	ITP	3
cutoff	12.28 %	AUC 0.892	30% ITP
83.16%	92.06%	CD40L	
ITP	cutoff	6.08% AUC 0.784	6.7
	81.75%	90.25% BAFF ITP	ITP
	cutoff	745.02 ng/L AUC	T B
0.708	81.02%	90.14%	ITP ITP
1			



1 ROC
Figure 1 ROC analysis chart

8 13 ITP CD40
CD40L CD40L

T CD40 5

CD40L

ITP B ITP

B BAFF 9

ITP

BAFF ITP

14 15

ITP CD40 CD40L

BAFF

CD40 CD40L BAFF

ITP

1 Iwasa T Nakamura K Ihara E et al. The Effective Treatment with Cyclosporine of a Ulcerative Colitis Patient with Concurrent Idiopathic Thrombocytopenic Purpura Who Subsequently Developed Spontaneous Pneumomediastinum J . Intern Med 2017 56 11 1331 1337.

2 Nakao H Ishiguro A Ikoma N et al. Acquired idiopathic thrombotic thrombocytopenic purpura successfully treated with intravenous immunoglobulin and glucocorticoid A case report J . Medicine 2017 96 14 e6547.

3 Shimazu Y Uchiyama T Mizumoto C et al. Concurrent Autoimmune Neutropenia and Idiopathic Thrombocytopenic Purpura Associated with IgG4 related Disease J . Intern Med 2018 57 13 1911 1916.

4 Khoury HJ Collins RH Blum W et al. Immune responses and long term disease recurrence status after telomerase based dendritic cell immunotherapy in patients with acute myeloid leukemia J . Cancer 2017 123 16 3061 3072.

J .

2011 3 214 216.

6 Takase K Kada A Iwasaki H et al. High dose Dexamethasone Therapy as the Initial Treatment for Idiopathic Thrombocytopenic Purpura Protocol for a Multicenter Open Label Single Arm Trial J . Acta Med Okayama 2018 72 2 197 201.

7 Ichimata S Kobayashi M Honda K et al. Acquired amegakaryocytic thrombocytopenia previously diagnosed as idiopathic thrombocytopenic purpura in a patient with hepatitis C virus infection J . World J Gastroenterol 2017 23 35 6540 6545.

8 Segna D Dufour JF. Other Extrahepatic Manifestations of Hepatitis C Virus Infection Pulmonary Idiopathic Thrombocytopenic Purpura Nondiabetes Endocrine Disorders J . Clin Liver Dis 2017 21 3 607 629.

9 Ackv DN Annichinobizzacchi JM Maximo CA et al. Patterns of care and burden of chronic idiopathic thrombocytopenic purpura in Brazil J . J Medical Econ 2017 20 8 1.

10 Aref S Elghonemy MS Elaziz SA et al. Impact of serum immunoglobulins level and IL 18 promoter gene polymorphism among Egyptian patients with idiopathic thrombocytopenic purpura J . Hematology 2017 22 2 99 104.

11 Chen J Li JH Zhao SJ et al. Clinical significance of costimulatory molecules CD40/CD40L and CD134/CD134L in coronary heart disease A case control study J . Medicine 2017 96 32 e7634.

12 Chen JM Guo J Wei CD et al. The association of CD40 polymorphisms with CD40 serum levels and risk of systemic lupus erythematosus J . BMC Genetics 2015 16 1 121.

13 Petramala L Iacobellis G Carnevale R et al. Enhanced Soluble Serum CD40L and Serum P-Selectin Levels in Primary Aldosteronism J . Horm Metab Res 2016 48 07 440 445.

14 Lin XF Ten XL Tang XB et al. Serum soluble CD40 ligand levels after acute intracerebral hemorrhage J . Acta Neur Scand 2016 133 3 192 201.

15 Elizondo D Andargie T Kubhar D et al. CD40-CD40L crosstalk drives fascin expression in dendritic cells for efficient antigen presentation to CD4+ T cells J . Int Immunol 2017 29 3 121 131.

1

1

1

1

2

3

1

1 SPRCC

SPRCC 1
HE

SPRCC

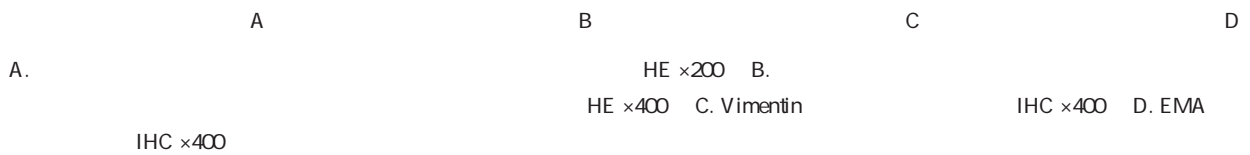
EnVision

ð

-
1. 272111
 2. 272111
 3. 256610

E-mail 461940072@qq.com

papillary renal cell carcinoma
 2016 12 5
 ma PRCC
 50% 3.7×3.6×2.1 cm
 solid variant of papillary renal cell carcinoma
 SPRCC
 PRCC 1 2.2 4×3×2 cm
 1
 10% HE
 CKpan CK7 CK8/18
 CK19 P504S CD10 EMA PAX 8 Vimentin
 RCC WT 1 CK20 CD57 Syn CD56 CgA WHO/ISUP 1 2
 CD117 Desmin SMA Myogenin S 100 E cadherin Ki 67 1A B 1C D 1
 2 2.3 39
 2.1 73 CT



1 SPRCC
 Figure 1 Histological characteristics and immunophenotype of SPRCC

1
 Table 1 The clinical datas and immunohistochemical results of SPRCC

73	4×3×2 cm	CKpan CK7 CK8/18 CK19 P504S CD10 EMA PAX 8 Vimentin Ki 67	RCC WT 1 CK20 CD57 Syn CD56 CgA CD117 Desmin SMA Myogenin S 100 E cadherin
----	----------	---	--

3

3.1

3.2.1 SPRCC

2

metanephric adenoma

5

80%~90%
PRCC

11

15cm

2

PRCC

I

II

I

3

II

12

I

CK

CK

II

4

PRCC

Vimentin

CKpan CD57

WT 1 EMA P504S

12 13

50%

5

SPRCC

PRCC

Cadherin17

CDH17

81%

SPRCC

14

3.2.2 SPRCC

renal oncocytoma

6

2016

60-70

WHO

WHO/SUP

4

SPRCC

WHO/SUP1 2

7

CK 8/

18 CK19 EMA CK7 CD10 P504S PAX 8

Vimentin CK20 RCC WT 1 CD57

S 100 CD117

8 9

SPRCC

39

SPRCC

10

3.2

SPRCC

SPRCC

15

COPD
IL 17 ACTA

CysC VEGF

1 1 2 3

A ACTA 2019 3 n=146

3 224

C CysC COPD 86

VEGF 3

17 IL 17 2016 n=78

CysC VEGF IL 17

APACHE II P<Q05 VEGF CysC IL 17 ACTA

3 CysC VEGF IL 17 ACTA

P<Q05 CysC IL 17 ACTA APACHE II VEGF

P<Q05 VEGF APACHE II CysC IL 17 ACTA APACHE II

P<Q05 CysC VEGF IL 17 ACTA COPD

AUC 0.864 92.86% 70.00% CysC VEGF IL 17

ACTA COPD

COPD C 17 A

Changes of serum CysC VEGF IL-17 and ACTA levels in elderly patients with COPD and severe respiratory failure

CAO Tingting¹ WAN Jun¹ FENG Yonghai² CHU Heying³

1. Department of general medicine the Fifth Affiliated Hospital of Zhengzhou University Zhengzhou Henan China 450052 2. Department of respiratory medicine the Fifth Affiliated Hospital of Zhengzhou University Zhengzhou Henan China 450052 3. Department of respiratory medicine the First Affiliated Hospital of Zhengzhou University Zhengzhou Henan China 450052

ABSTRACT Objective To investigate the changes of serum CysC VEGF IL-17 and ACTA levels in elderly patients with COPD and severe respiratory failure.

19A320065

- 1. 450052
- 2. 450052
- 3. 450052

E-mail chuheyings@163.com

tion group and analyzed the diagnostic value of serum indicators for elderly COPD with severe respiratory failure and the correlation between serum indicators and the correlation between serum indicators and APACHE II score and the prognostic value were analyzed. Results The levels of serum CysC VEGF IL 17 and ACTA in the three groups were statistically significant $P<0.05$ VEGF was negatively correlated with CysC IL 17 and ACTA levels and CysC IL 17 and ACTA levels were positively correlated $P<0.05$ the serum levels of CysC IL 17 ACTA and APACHE II score were higher in dead patients than in surviving patients and VEGF levels were lower than in surviving patients $P<0.05$ VEGF level was negatively correlated with APACHE II score and CysC IL 17 and ACTA levels were positively correlated with APACHE II score $P<0.05$ the combined serum levels of CysC VEGF IL 17 and ACTA in predicting the prognosis of COPD with severe respiratory failure in elderly patients 0.864 was greater than that of a single serum indicator with a sensitivity of 92.86% and a specificity of 70.00%. Conclusion Serum CysC VEGF IL 17 and ACTA levels are abnormally expressed in elderly patients with COPD and severe respiratory failure and are closely related to the disease and the combined detection is expected to be an effective method for diagnosis and prognosis of elderly COPD with severe respiratory failure.

KEY WORDS Cystatin C Vascular endothelial growth factor Interleukin 17 Activin A Chronic obstructive pulmonary disease Respiratory failure

Chronic obstructive pulmonary disease COPD
 Cystatin C CysC
 Vascular endothelial growth factor VEGF
 Interleukin 17 IL 17
 Activin A AC

TA
 CysC VEGF IL 17 ACTA
 IL 17 ACTA
 COPD

COPD
 COPD
 COPD
 COPD

2016 3 2019 3 224
 n=78 n=146
 86
 P>0.05 1

n % $\bar{x} \pm s$

Table 1 Comparison of general data between the 2 groups n % $\bar{x} \pm s$

	n=78	n=146	n=86	F/ χ^2	P
/	45/33	84/62	49/37	0.010	0.995
	65.97±2.15	66.19±1.74	65.80±1.83	1.218	0.297
COPD	9.89±1.22	10.02±1.13	9.72±1.30	1.693	0.186
kg/m ²	22.79±2.20	23.15±2.08	22.94±2.13	0.779	0.460
	20 25.64	37 25.34	21 24.42		
	13 16.67	24 16.44	14 16.28	0.019	1.000
	8 10.26	14 9.59	8 9.30		

COPD⁵

<60mmHg >

50mmHg >60 1.2

3 CysC VEGF IL 17 ACTA

6 CysC VEGF IL 17 ACTA

II APACHE II 71

1.2 APACHEII CysC VEGF IL 17 ACTA APA

1.2.1 CHEII CysC VEGF IL 17

3mL 12min 3000r/min ACTA COPD

- 70 Bio Bad 1.5

CysC VEGF IL 17 ACTA SPSS 22.0

$\bar{x} \pm s$ t n %

50 L 50 L 37 50 L

30min Pearson χ^2 ROC P<0.05

5 50 L 37 30min 2

5 37 10min 2.1 3 CysC VEGF IL 17 ACTA

50 L 15min 3 CysC VEGF IL 17 ACTA

450nm OD 3 CysC VEGF IL 17 ACTA

1.2.2 P<0.05 CysC IL 17 VEGF

ACTA > > 2

< <

Table 2 Comparison of serum CysC VEGF IL 17 and Acta levels between the 2 groups $\bar{x} \pm s$

	n	CysC ng/mL	VEGF mg/L	IL 17 ng/L	ACTA ng/L
	78	151.23±30.24 ^a	323.43±54.12 ^b	65.14±18.52 ^b	45.69±8.24 ^b
	146	130.47±24.58 ^b	387.64±69.12 ^a	44.87±15.76 ^b	36.51±6.25 ^a
	86	102.41±20.37	451.63±67.29	18.31±12.84	25.74±6.13
F		79.021	79.267	182.984	178.781
P		0.001	0.001	0.001	0.001

^aP<0.05

^bP<0.05

2.2 APACHE II VEGF

VEGF CysC IL 17 ACTA P<0.05 3

CysC IL 17 ACTA 2.4 APACHEII

IL 17 ACTA P<0.05 1 VEGF r=- 0.349 APACHE II

2.3 APACHEII CysC r=0.836 IL 17 r=

28 50 0.654 ACTA r=0.675 APACHE II

CysC IL 17 ACTA P<0.05

VEGF mg/L

450	100
400	80
350	60
300	40
250	20
200	

14-3-3ζ

1 2 2

14-3-3 14-3-3 protein family

14-3-3

14-3-3ζ 14-3-3

14-3-3ζ 14-3-3ζ

14-3-3ζ

14-3-3ζ and breast cancer

DONG Zhengyuan¹ YANG Qingling² CHEN Changjie²

1. Key Laboratory of Cancer Transforming Medicine in Anhui Province Bengbu Medical College Bengbu Anhui China 233000 2. Department of Biochemistry & Molecular Biology Bengbu Medical College Bengbu Anhui China 233000

ABSTRACT The 14-3-3 protein family is a kind of acidic and highly conserved small molecule proteins widely exists in eukaryotic cells. The 14-3-3 protein has no obvious catalytic activity and mainly interacts with other proteins to regulate the target protein. 14-3-3ζ is one of the important members of the 14-3-3 protein family. Recently we found that 14-3-3ζ is a novel target for the cancer therapy. In this review we focus on the current progress on breast cancer resistance recurrence and metastasis and discuss the potential of 14-3-3ζ serviced as an effective therapeutic target for breast cancer in patient whose tumors overexpress 14-3-3ζ.

KEY WORDS 14-3-3ζ protein Breast cancer

14-3-3ζ

14-3-3ζ

¹ 14-3-3ζ

^{2,3} 14-3-3ζ

KJ2019ZD28 2017H110

Byyex1926

1. 233000
2. 233000

E-mail tochenchangjie@163.com

¹⁸ Bergamaschi A ¹⁹
14 3 3ζ
14 3 3ζ microRNA 451
miR 451 14 3 3ζ
SERMs
Liu ZR ²⁰ miR 451a
MCF 7 LCC 2
miR 451a 14 3 3ζ 14 3 3ζ
14 3 3ζ miR 451a
14 3 3ζ
14 3 3ζ

FOXM 1
²¹ 14 3 3ζ

2.3 14 3 3ζ

14 3 3ζ
²² 14 3 3ζ
70% -75%
45% ²³ 14 3 3ζ
14 3 3ζ
14 3 3ζ
B 1 CDC25B birc5
²⁴
14 3 3ζ
Li Y

- 1 . 14 3 3ζ
J . 2017 31 6 543-547.
- 2 . 14 3 3 zeta
J . 2017
47 3 192-196.
- 3 Luo Z Yang X Ma LT et al. 14 3 3 zeta Positive Cells Show More Tumorigenic Characters in Human Glioblastoma J . Turk Neurosurgery 2016 26 6 813-817.
- 4 Hong L Chen W Xing A et al. Inhibition of Tyrosine 3-Monooxygenase / Tryptophan 5-Monooxygenase Activation Protein Zeta-YWHAZ Overcomes Drug Resistance and Tumorigenicity in Ovarian Cancer J . Cell Physiol Biochem 2018 49 53-64.
- 5 Matta A Siu KW. 14 3 3 zeta as novel molecular target for cancer therapy J . Expert Opin Ther Targets 2012 16 515-523.
- 6 Zhao GY Ding JY Lu CL et al. The overexpression of 14 3 3 ζ and Hsp27 promotes non-small cell lung cancer progression J . Cancer 2014 120 5 652-663.
- 7 Shi J Ye J Fei H et al. YWHAZ promotes ovarian cancer metastasis by modulating glycolysis J . Oncol Rep 2019 41 1101-1112.
- 8 . 14 3 3 theta
J . 2015 15 27
5221-5224.
- 9 Zhao JF Zhao Q Hu H et al. The ASH1-miR-375-YWHAZ Signaling Axis Regulates Tumor Properties in Hepatocellular Carcinoma J . Mol Ther Nucleic Acids 2018 11 538-553.
- 10 Slinin Y Greer N Ishani A et al. Timing of dialysis initiation duration and frequency of hemodialysis sessions and membrane flux: a systematic review for a KDOQI clinical practice guideline J . Am J Kidney Dis 2015 66 823-836.
- 11 Ayers D. Influence of microRNAs and Long Non-Coding RNAs in Cancer Chemoresistance J . Genes Basel 2017 8 95.
- 12 Danes CG Wyzomierski SL Lu J et al. 14 3 3 zeta down regulates p53 in mammary epithelial cells and confers luminal filling J . Cancer Res 2008 68 1760-1767.
- 13 Rehman SK Li SH Wyzomierski SL et al. 14 3 3 ζ orchestrates mammary tumor onset and progression via miR-221-mediated cell proliferation J . Cancer Res 2014 74 363-373.
- 14 Ten Dijke P. 14 3 3 ζ turns TGF-β to the dark side J . Cancer Cell 2015 27 151-153.
- 15 Xu J Acharya S Sahin O et al. 14 3 3 ζ turns TGF-β's function from tumor suppressor to metastasis promoter in breast cancer by contextual changes of Smad partners from p53 to Gli2 J . Cancer Cell 2015 27 177-192.
- 16 Morrison CD. Tipping the balance between good and evil ab-errant 14 3 3 ζ expression drives oncogenic TGF-β signaling in metastatic breast cancers J . Breast Cancer Res 2015 17 92.
- 17 Suen KM Lin CC Seiler C et al. Phosphorylation of threonine residues on Shc promotes ligand binding and mediates crosstalk between MAPK and Akt x J
Zhen M e b Z a d k Cancer Cell
2017
1 Suen \$) Tipping on

" 4EÑE166F0\$Q2@USQ4[PióE('Cq61UœQ-LY !# \ ‡• H• %XD

-
1. HZ 2019 100
563003
 2. 563003
- E-mail 864925019@qq.com

MYC¹⁵ MYCN SHH Group4 MB
 1.4 Group 4 Group3 TP53
 Group 4 MB SHH³¹
 35%⁷ 5 75%¹¹ MB
 Group 4
 /
 EOMES LIM GTR MB
 1α LMX1A²⁸ 35%~40% Thompson NTR GTR
 Group 4
 KDM6A α Group4 MB NTR
 SNCAIP MYCN³² GTR
 CDK6 Northcott PRDM6 GTR
 4
 PRDM6 SNCAIP 600kb SNCAIP
 Group 4²⁶ 2.3
 ERBB4 SRC Group 4²⁹ MB
 17q Group 4 MB
 Group 4α Group 4y CDK6 MB
 8p 7q Group
 4β SNCAIP PRDM6³⁰
 2
 MB
 WNT MB 100%
 24 Gy 18Gy
 12.8% MB
 33 XRT
 PRT XRT
 /
 2.1 3 2.4^{34 35}
 MB
 3
 1.5 cm² MB
 4 >90%
 75%~90% 50%~75% SHH PCT1
 <50% Group 4 11 MB G SMO SHH
 WNT 17 Group 4 MB MYC
 Group3 Group 4 MB MYC
 Group3 SHH
 SMO SHH³⁶ SMO
 Robinson Vismo

- gates for molecular subgroups of medulloblastoma J . AJNR Am J Neuroradiol 2014 35 1263 1269.
- 18 Garrè Maria Luisa Cama Armando Bagnasco Francesca et al. Medulloblastoma variants age dependent occurrence and relation to Gorlin syndrome a new clinical perspective J . Clin Cancer Res 2009 15 2463 2471.
- 19 Deshpande Ishan Liang Jiahao Hedeem Danielle et al. Smoothened stimulation by membrane sterols drives Hedgehog pathway activity J . Nature 2019 571 284 288.
- 20 Orr Brent A Clay Michael R Pinto Emilia M et al. An update on the central nervous system manifestations of Li Fraumeni syndrome J . Acta Neuropathol 2020 139 14 689 701.
- 21 Begemann Matthias Waszak Sebastian M Robinson Giles W et al. GPR161 Germline Mutations Predispose to Pediatric Medulloblastoma J . J Clin Oncol 2020 38 1 43 50.
- 22 Suzuki Hiromichi Kumar Sachin A Shuai Shimin et al. Recurrent noncoding U1 snRNA mutations drive cryptic splicing in SHH medulloblastoma J . Nature 2019 574 707 711.
- 23 Spliceosomal RNA Mutations May Drive Medulloblastoma and Other Cancers J . Cancer Discov 2019 9 1644.
- 24 Kool Marcel Korshunov Andrey Remke Marc et al. Molecular subgroups of medulloblastoma an international meta analysis of transcriptome genetic aberrations and clinical data of WNT SHH Group 3 and Group 4 medulloblastomas J . Acta Neuropathol 2012 123 473 484.
- 25 Rickman David S Schulte Johannes H Eilers Martin The Expanding World of N MYC Driven Tumors J . Cancer Discov 2018 8 150 163.
- 26 Northcott Paul A Buchhalter Ivo Morrissy A Sorana et al. The whole genome landscape of medulloblastoma subtypes J . Nature 2017 547 311 317.
- 27 Shih David J H Northcott Paul A Remke Marc et al. Cytogenetic prognostication within medulloblastoma subgroups J . J Clin Oncol 2014 32 886 896.
- 28 Lin Charles Y Erkek Serap Tong Yiai et al. Active medulloblastoma enhancers reveal subgroup specific cellular origins J . Nature 2016 530 57 62.
- 29 Forget Antoine Martignetti Loredana Puget Stéphanie et al. Aberrant ERBB4 SRC Signaling as a Hallmark of Group 4 Medulloblastoma Revealed by Integrative Phosphoproteomic Profiling J . Cancer Cell 2018 34 379 395.e7.
- 30 Cavalli Florence M G Remke Marc Rampasek Ladislav et al. Intertumoral Heterogeneity within Medulloblastoma Subgroups J . Cancer Cell 2017 31 737 754.e6.
- 31 Ramaswamy Vijay Remke Marc Bouffet Eric et al. Risk stratification of childhood medulloblastoma in the molecular era the current consensus J . Acta Neuropathol 2016 131 821 831.
- 32 Thompson Eric M Hielscher Thomas Bouffet Eric et al. Prognostic value of medulloblastoma extent of resection after accounting for molecular subgroup a retrospective integrated clinical and molecular analysis J . Lancet Oncol 2016 17 484 495.
- 33 Al Wassia Rolina K Ghassal Noor M Naga Adly et al. Optimization of Craniospinal Irradiation for Pediatric Medulloblastoma Using VMAT and IMRT J . J Pediatr Hematol. Oncol 2015 37 e405 11.
- 34 Kahalley Lisa S Peterson Rachel Ris M Douglas et al. Superior Intellectual Outcomes After Proton Radiotherapy Compared With Photon Radiotherapy for Pediatric Medulloblastoma J . J Clin Oncol 2020 38 5 454 461.
- 35 Das Manjulika Intelligence outcomes after proton versus photon therapy J . Lancet Oncol 2020 38 5 454 461.
- 36 Neve Anuja Migliavacca Jessica Capdeville Charles et al. Crosstalk between SHH and FGFR Signaling Pathways Controls Tissue Invasion in Medulloblastoma J . Cancers Basel 2019 11 pii:E1985.doi:10.3391cancers11121985.
- 37 Robinson Giles W Orr Brent A Wu Gang et al. Vismodegib Exerts Targeted Efficacy Against Recurrent Sonic Hedgehog Subgroup Medulloblastoma Results From Phase II Pediatric Brain Tumor Consortium Studies PBTC 025B and PBTC 032 J . J Clin Oncol 2015 33 2646 2654.
- 38 Goranci Buzhala Gladiola Gabriel Elke Mariappan Aruljothi et al. Losers of Primary Cilia Gain the Benefit of Survival J . Cancer Discov 2017 7 1374 1375.
- 39 Zhao Xuesong Pak Ekaterina Ornell Kimberly J et al. A Transposon Screen Identifies Loss of Primary Cilia as a Mechanism of Resistance to SMO Inhibitors J . Cancer Discov 2017 7 1436 1449.
- 40 Eckerdt Frank Clymer Jessica Bell Jonathan B et al. Pharmacological mTOR targeting enhances the antineoplastic effects of selective PI3K α inhibition in medulloblastoma J . Sci Rep 2019 9 12822.
- 41 Altshuler C Haley K Dhall G et al. Decreased morbidity and mortality of autologous hematopoietic transplants for children with malignant central nervous system tumors the Head Start trials 1991 2009 J . Bone Marrow Transplant 2016 51 945 948.
- 42 Koo Jane Silverman Stacy Nuechterlein Brandon et al. Safety and feasibility of outpatient autologous stem cell transplantation in pediatric patients with primary central nervous system tumors J . Bone Marrow Transplant 2019 42 Koo Janro5 p 51

